AtlantTIC
Research Center for
Information & Communication Technologies

Universidade Vigo



Detection of Image Resampling and Video Encoding Footprints for Forensic Applications

David Vázquez-Padín

January 18, 2016

Advisor: Fernando Pérez-González

Outline

1 Introduction
- Motivation
- Structure

2 Forensic Analysis of Resampled Signals
- Problem Description
- Resampling Process Description
- Proposed Techniques

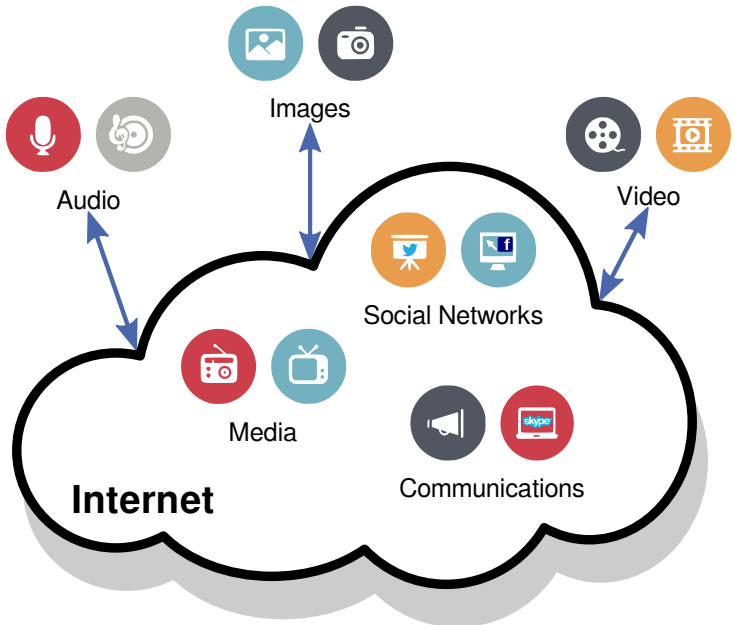
3 Forensic Analysis of Video Sequences
- Problem Description
- Basics on Video Coding
- Proposed Techniques

4 Conclusions
- Future Work

1. Introduction

Motivation

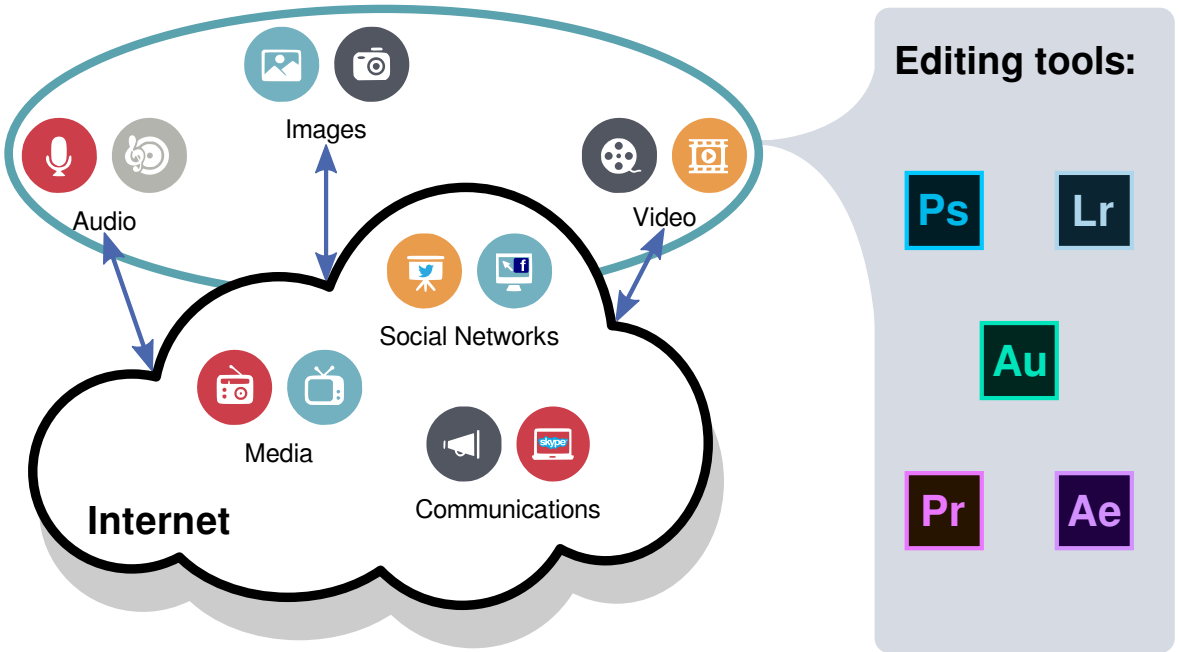
Multimedia contents have become a vehicle for communication:



1. Massive use → valuable asset.

Motivation

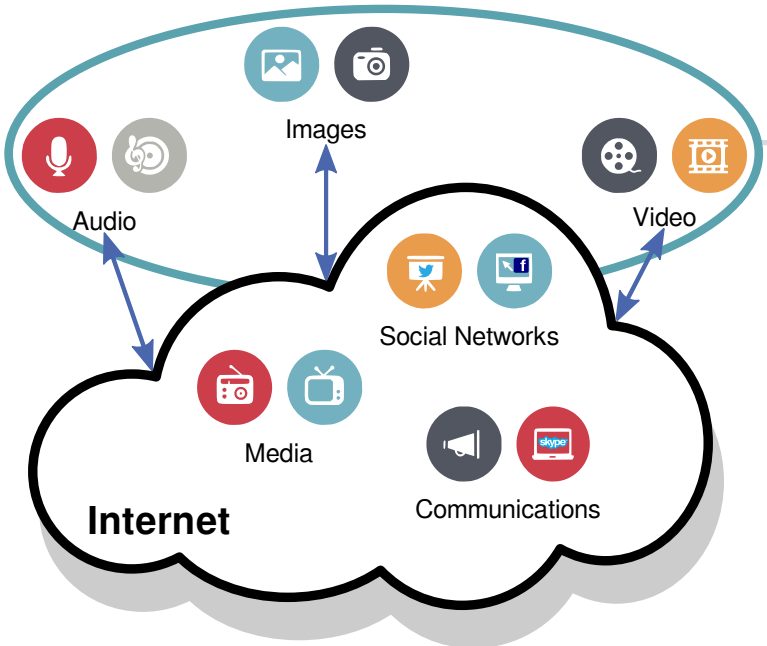
Multimedia contents have become a vehicle for communication:



1. Massive use → valuable asset.
2. Rapid growth of editing tools.

Motivation

Multimedia contents have become a vehicle for communication:



Editing tools: originally devised to enhance the quality of capture moments



Original image

Light and color adjustment

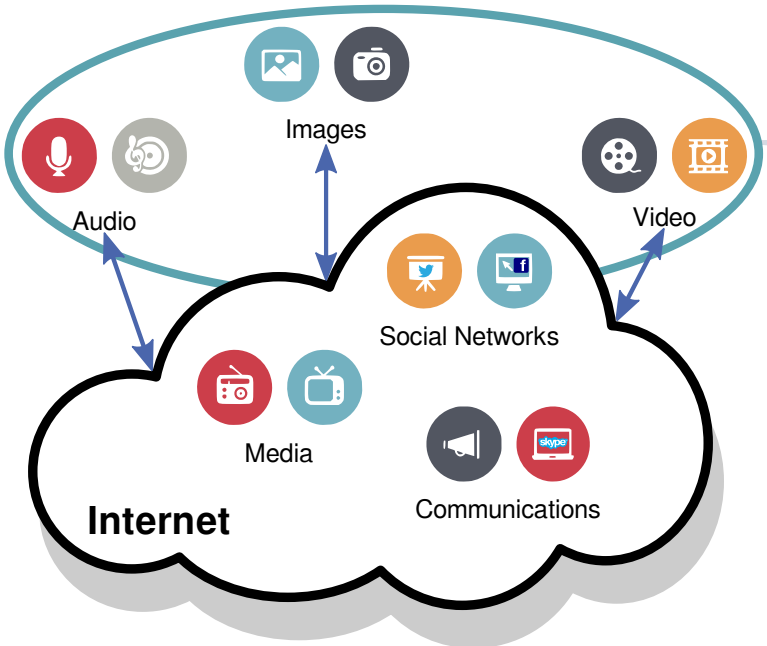


Enhanced image

1. Massive use → valuable asset.
2. Rapid growth of editing tools.
3. Edition by unskilled persons.

Motivation

Multimedia contents have become a vehicle for communication:



Editing tools: originally devised to enhance the quality of capture moments,but...

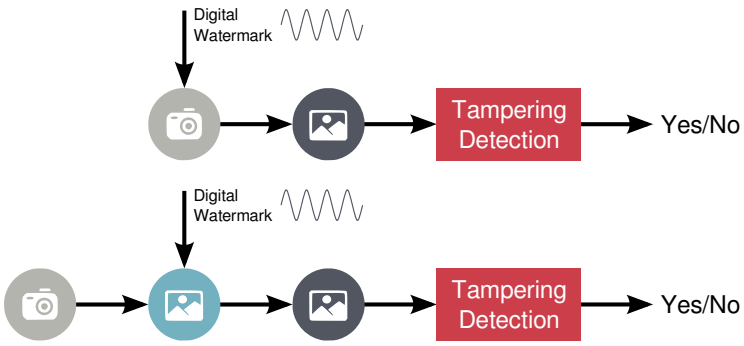


Original image **Forged image**

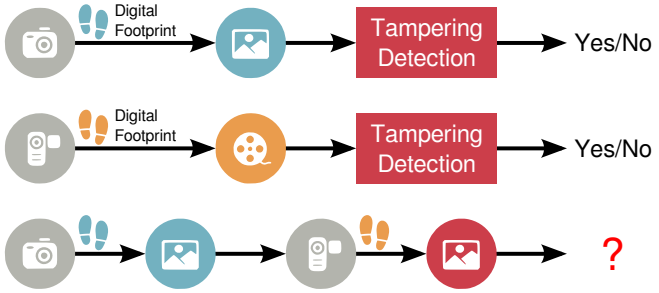
1. Massive use → valuable asset.
2. Rapid growth of editing tools.
3. Edition by unskilled persons.
4. Reliable multimedia contents?

How to rebuild trust in multimedia objects?

Active Forensics:



Passive Forensics:



Advantage

Known signal reduces complexity.

Disadvantage

Complexity grows very fast.

Disadvantage

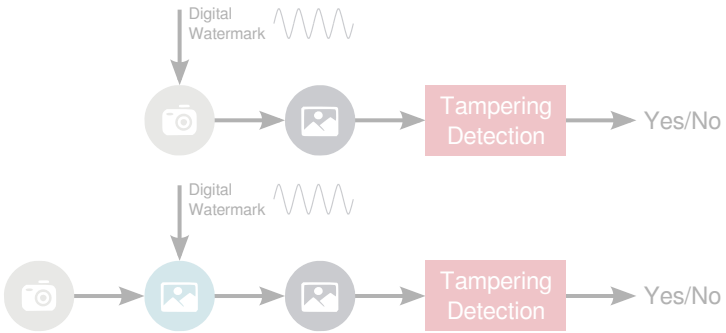
Special-purpose software/hardware.

Advantage

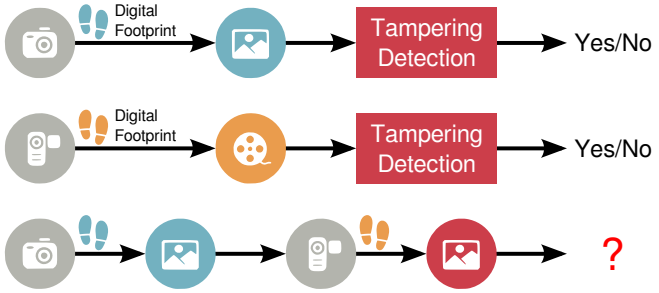
Universal applicability.

How to rebuild trust in multimedia objects?

Active Forensics:



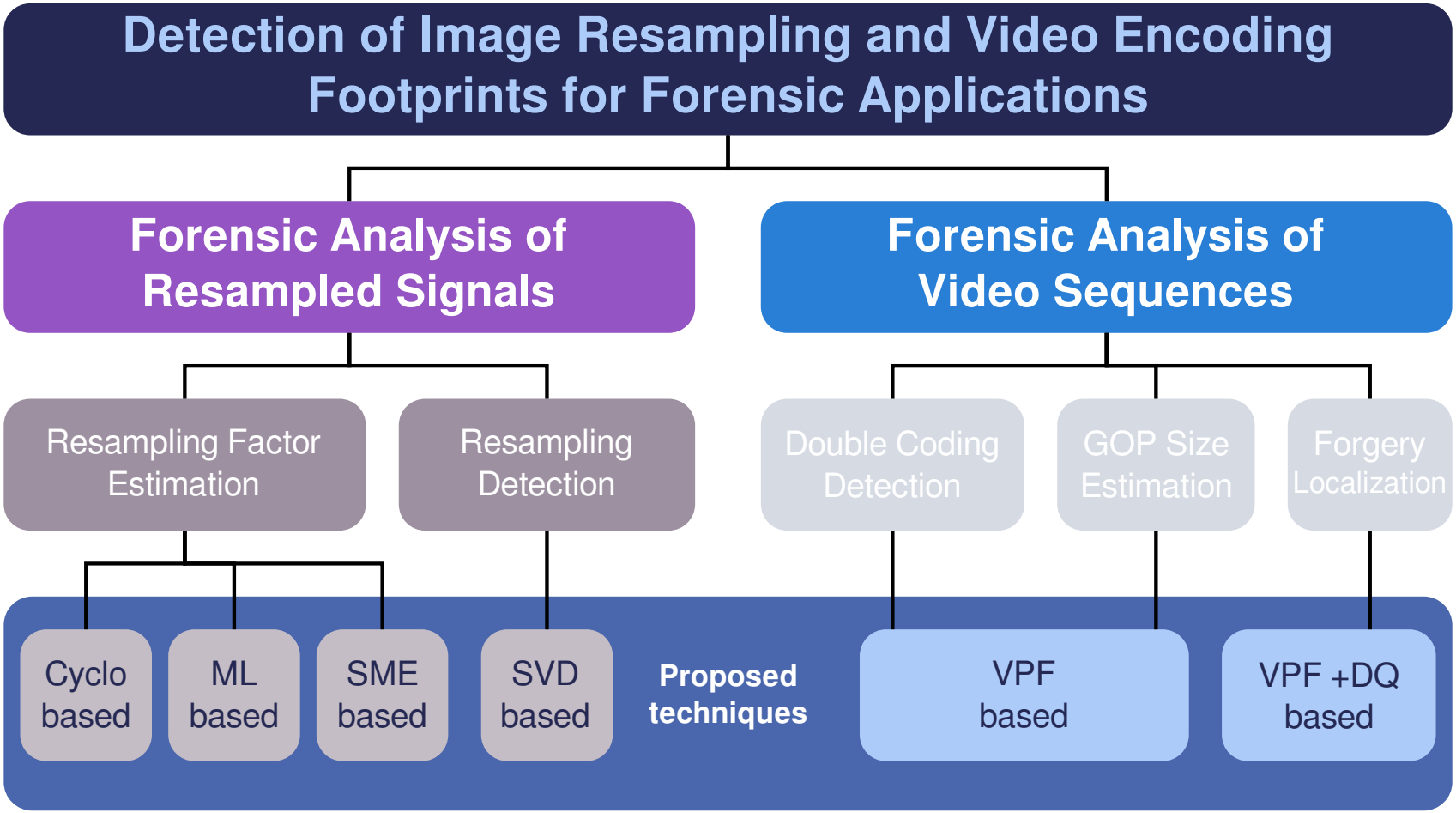
Passive Forensics:



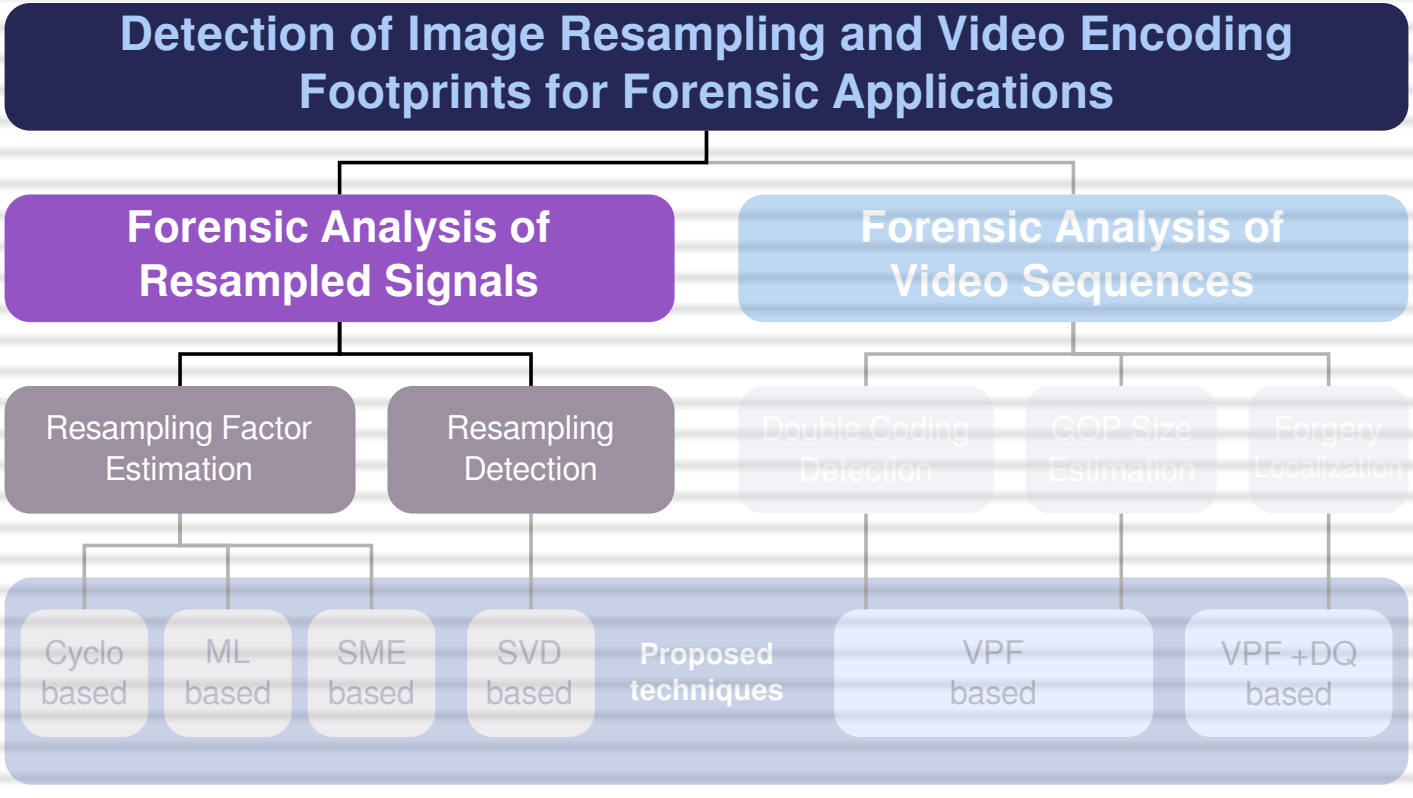
Objectives:

1. Explore **new digital footprints**.
2. **Theoretically model** known digital footprints.
3. Provide information about **authenticity**, **integrity** or **processing history**.

Structure


Detection of Image Resampling and Video Encoding Footprints for Forensic Applications
Forensic Analysis of Resampled Signals
Forensic Analysis of Video Sequences
Resampling Factor Estimation
Resampling Detection
Double Coding Detection
GOP Size Estimation
Forgery Localization
Cyclo based
ML based
SME based
SVD based
Proposed techniques
VPF based
VPF +DQ based

2. Forensic Analysis of Resampled Signals



Problem Description

When a credible forgery is carried out, most of the time it is necessary to adapt added pieces to the original content.

How to perform this image manipulation?



Forged image

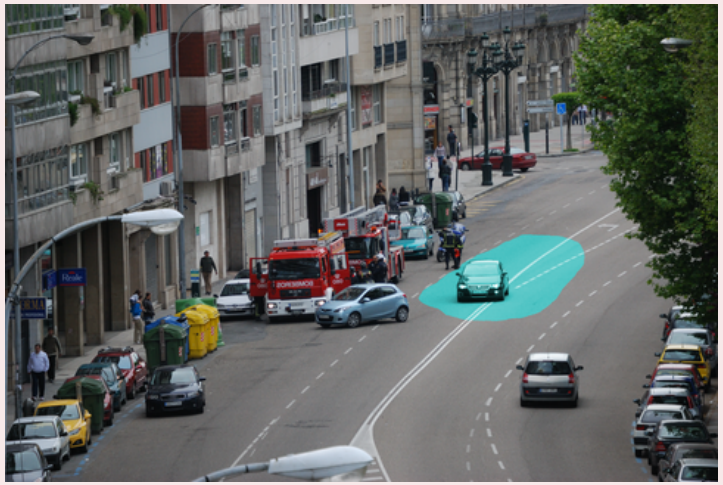


Original image

Problem Description

When a credible forgery is carried out, most of the time it is necessary to adapt added pieces to the original content.

How to perform this image manipulation?

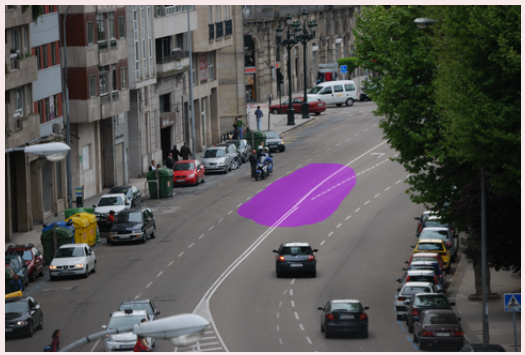


1. Define the region to modify

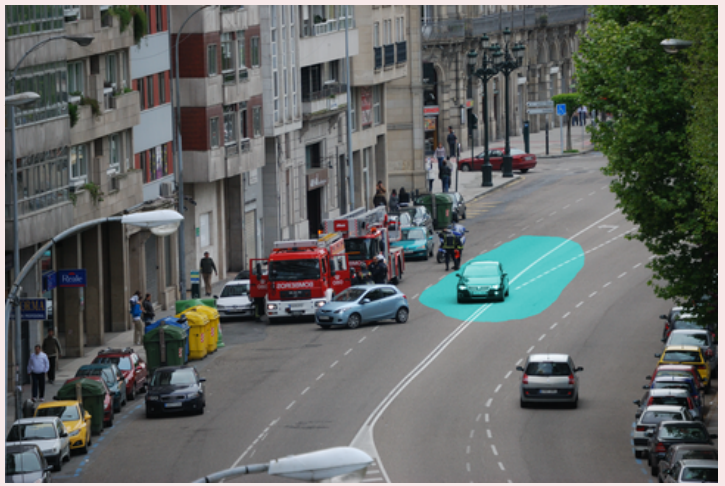
Problem Description

When a credible forgery is carried out, most of the time it is necessary to adapt added pieces to the original content.

How to perform this image manipulation?



2. Find a patch to tamper with

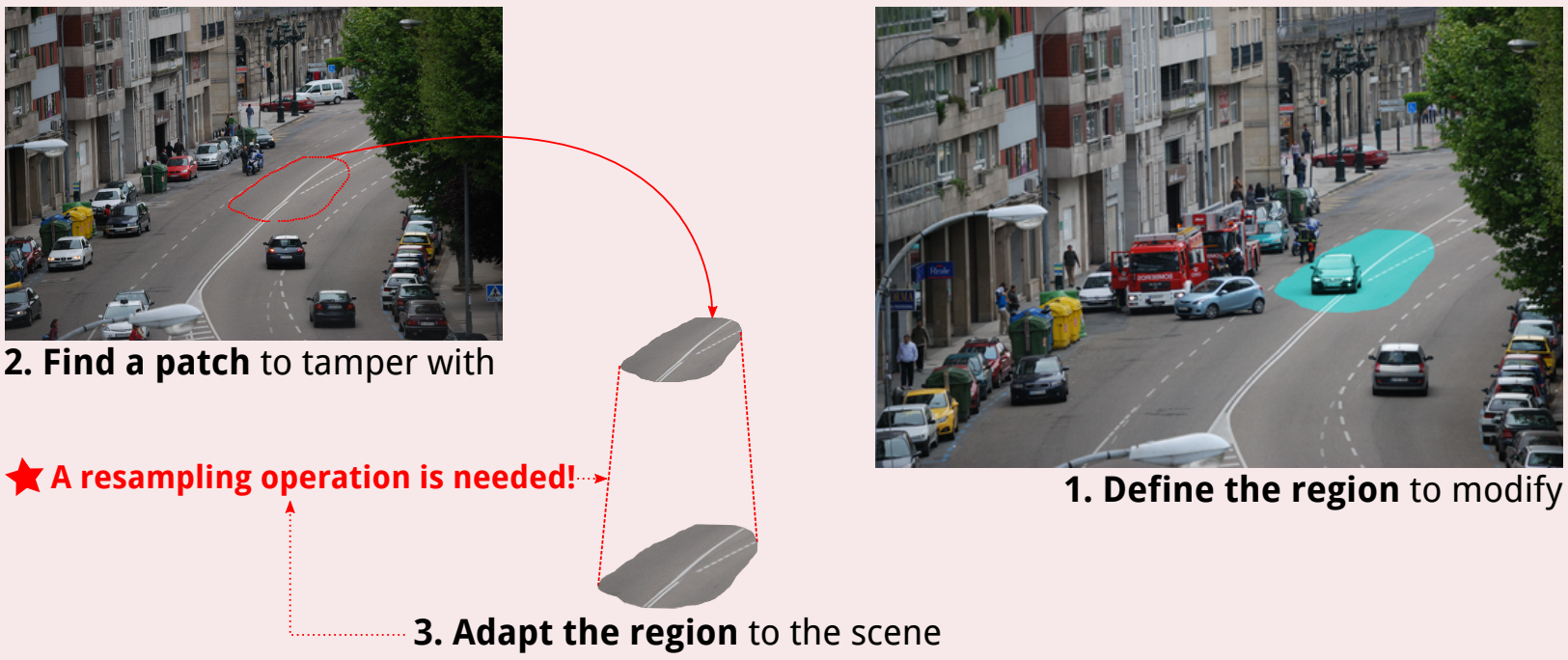


1. Define the region to modify

Problem Description

When a credible forgery is carried out, most of the time it is necessary to adapt added pieces to the original content.

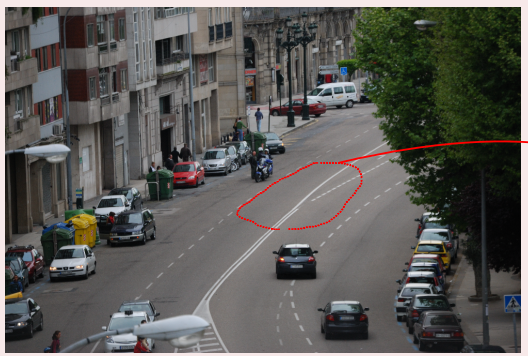
How to perform this image manipulation?



Problem Description

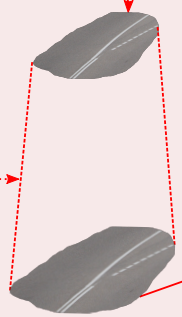
When a credible forgery is carried out, most of the time it is necessary to adapt added pieces to the original content.

How to perform this image manipulation?



2. Find a patch to tamper with

★ **A resampling operation is needed!**





1. Define the region to modify

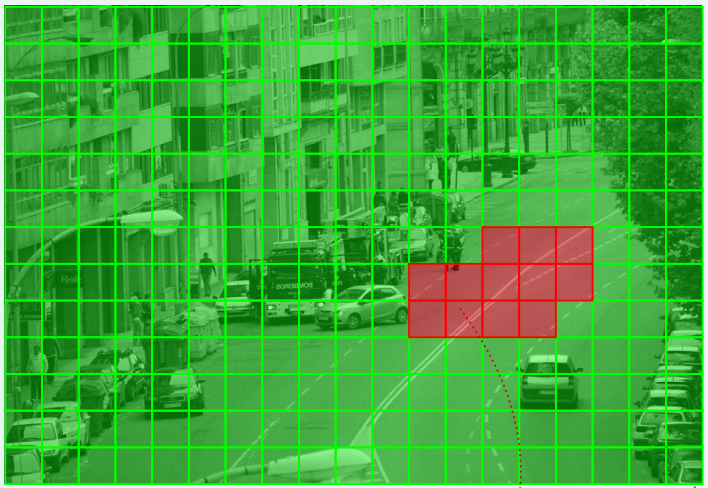
4. Paste the region

3. Adapt the region to the scene

Problem Description

When a credible forgery is carried out, most of the time it is necessary to adapt added pieces to the original content.

Two ways of tackling the analysis of resampled signals:



Example of analysis

$\mathcal{H}_1$: the observed block has been resampled

$\mathcal{H}_0$: the observed block has not been resampled



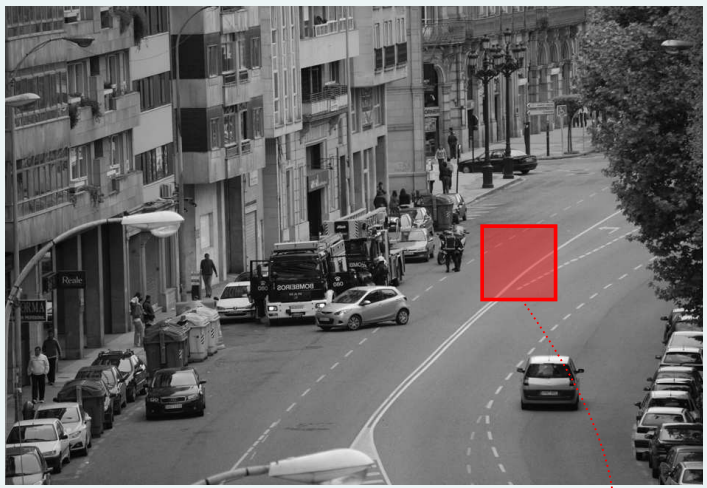
Forged image

❶ **Forensic Image Resampling Detection**

Problem Description

When a credible forgery is carried out, most of the time it is necessary to adapt added pieces to the original content.

Two ways of tackling the analysis of resampled signals:



Example of analysis



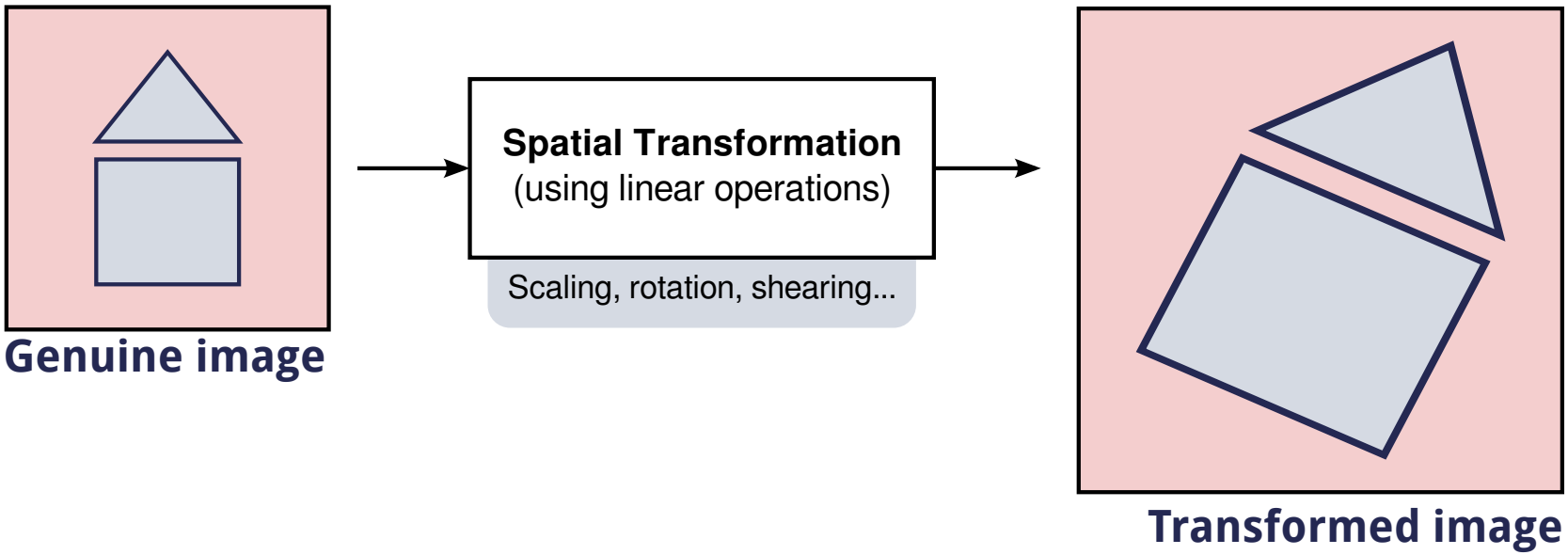
Scaled block by a factor of 1.23



Forged image

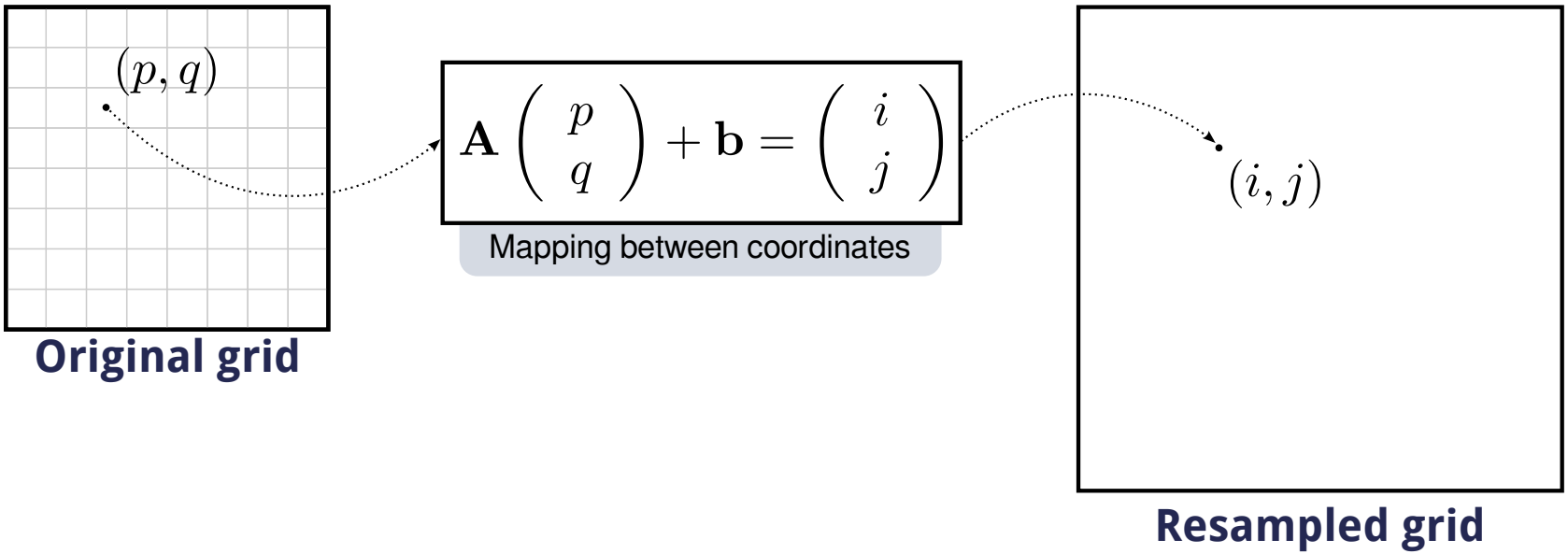
❷ **Forensic Image Resampling Estimation**

Resampling Process Description



Three main steps are involved in the resampling process:

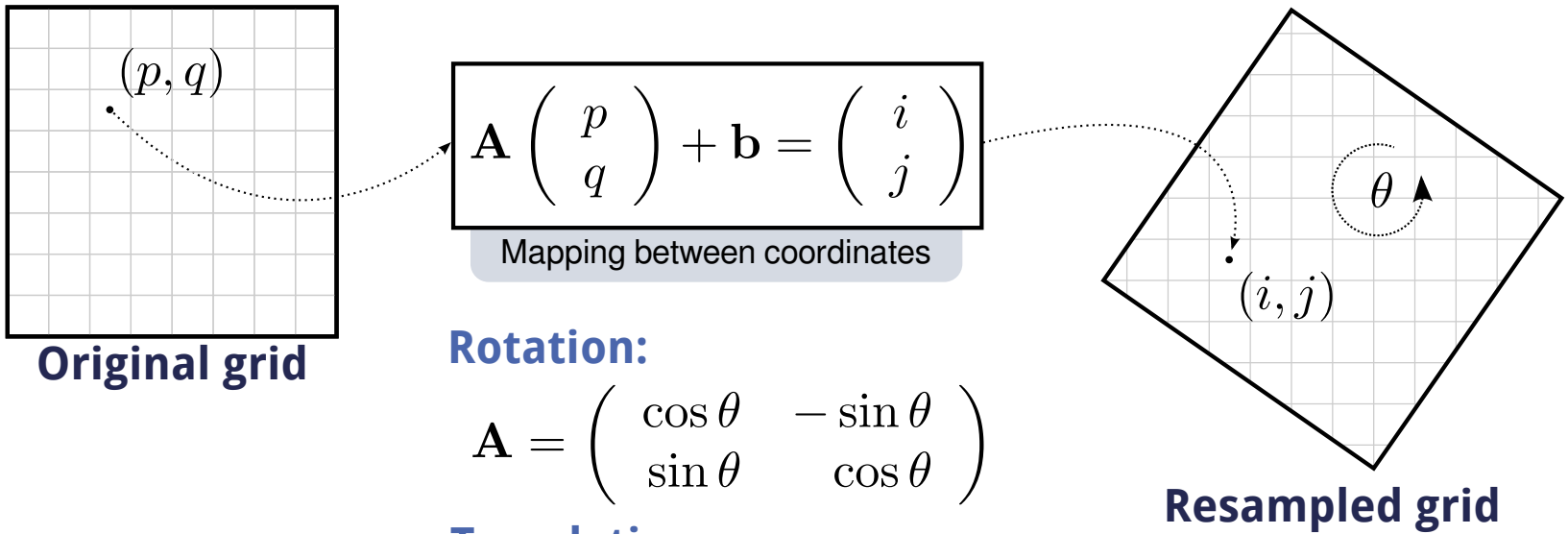
Resampling Process Description



Three main steps are involved in the resampling process:

1. Resampling grid definition.

Resampling Process Description



Rotation:

$$\mathbf{A} = \begin{pmatrix} \cos\theta & -\sin\theta \\ \sin\theta & \cos\theta \end{pmatrix}$$

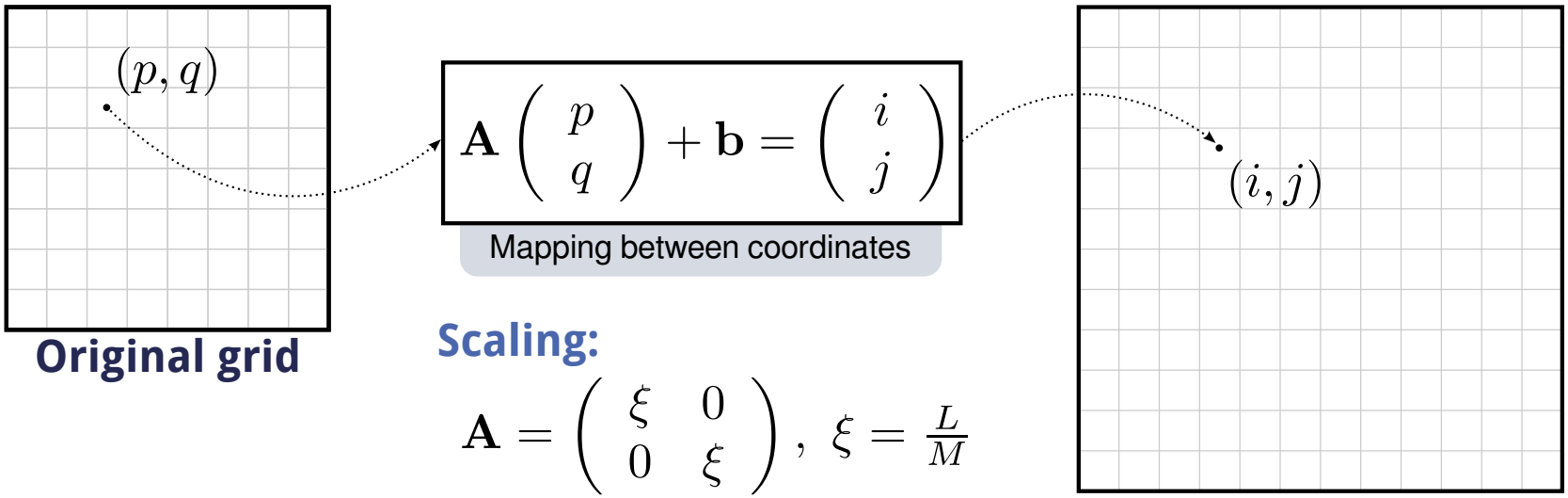
Translation:

$$\mathbf{b} = \mathbf{0}$$

Three main steps are involved in the resampling process:

1. Resampling grid definition.

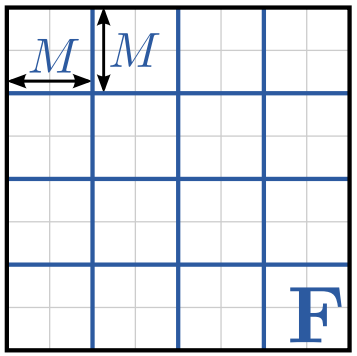
Resampling Process Description



Three main steps are involved in the resampling process:

1. Resampling grid definition.

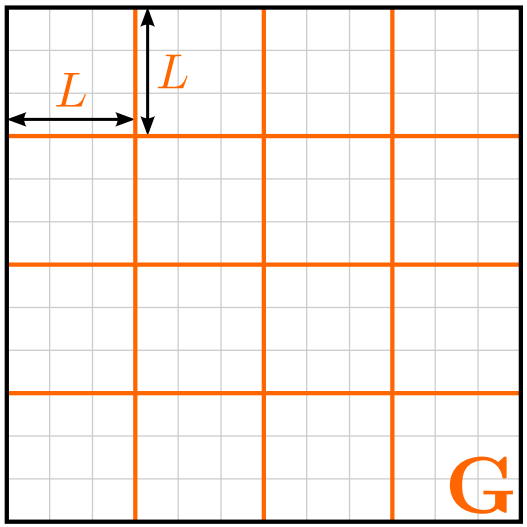
Resampling Process Description



Original image

Interpolation:

$$\sum_{k=0}^{P-1}\sum_{l=0}^{Q-1} F_{k,l}\, h\left(i\frac{M}{L}+\delta-k\right) h\left(j\frac{M}{L}+\delta-l\right) = G_{i,j}$$

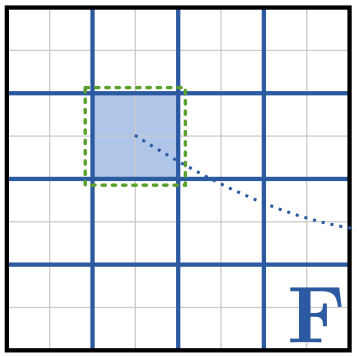


Resampled image

Three main steps are involved in the resampling process:

1. Resampling grid definition.
2. Calculation of pixel values in new locations.

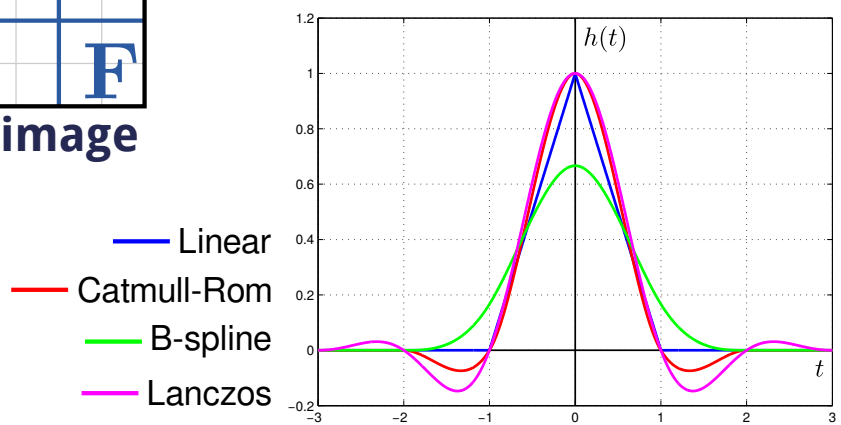
Resampling Process Description

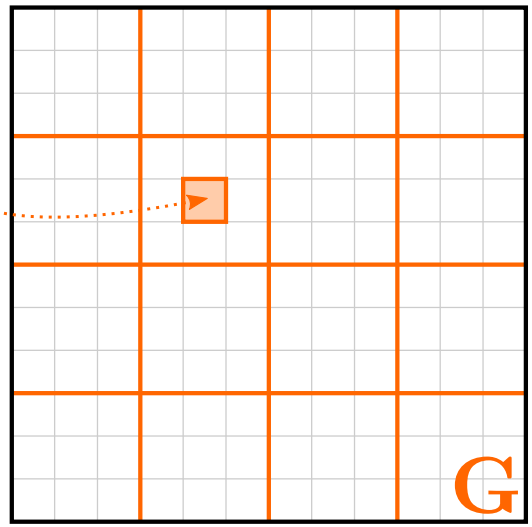


Original image

Interpolation:

$$\sum_{k=0}^{P-1}\sum_{l=0}^{Q-1} F_{k,l}\, h\left(i\frac{M}{L}+\delta-k\right) h\left(j\frac{M}{L}+\delta-l\right) = G_{i,j}$$



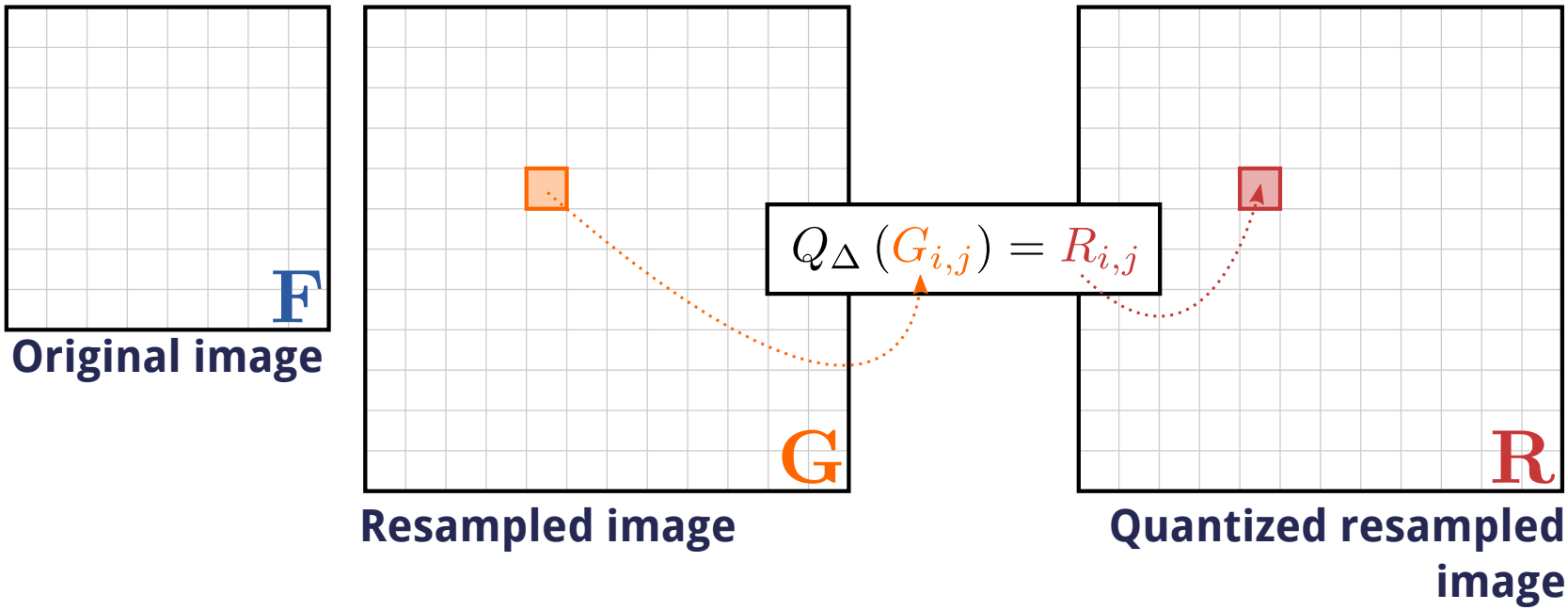


Resampled image

Three main steps are involved in the resampling process:

1. Resampling grid definition.
2. Calculation of pixel values in new locations.

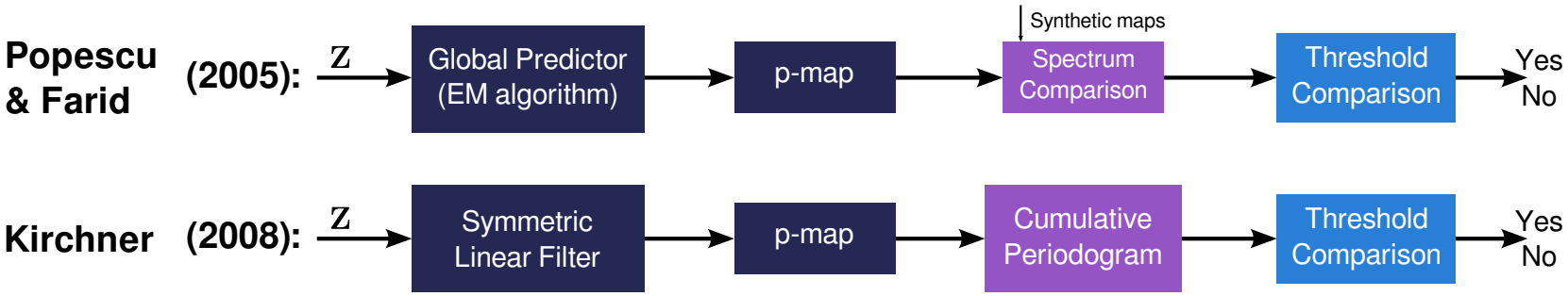
Resampling Process Description



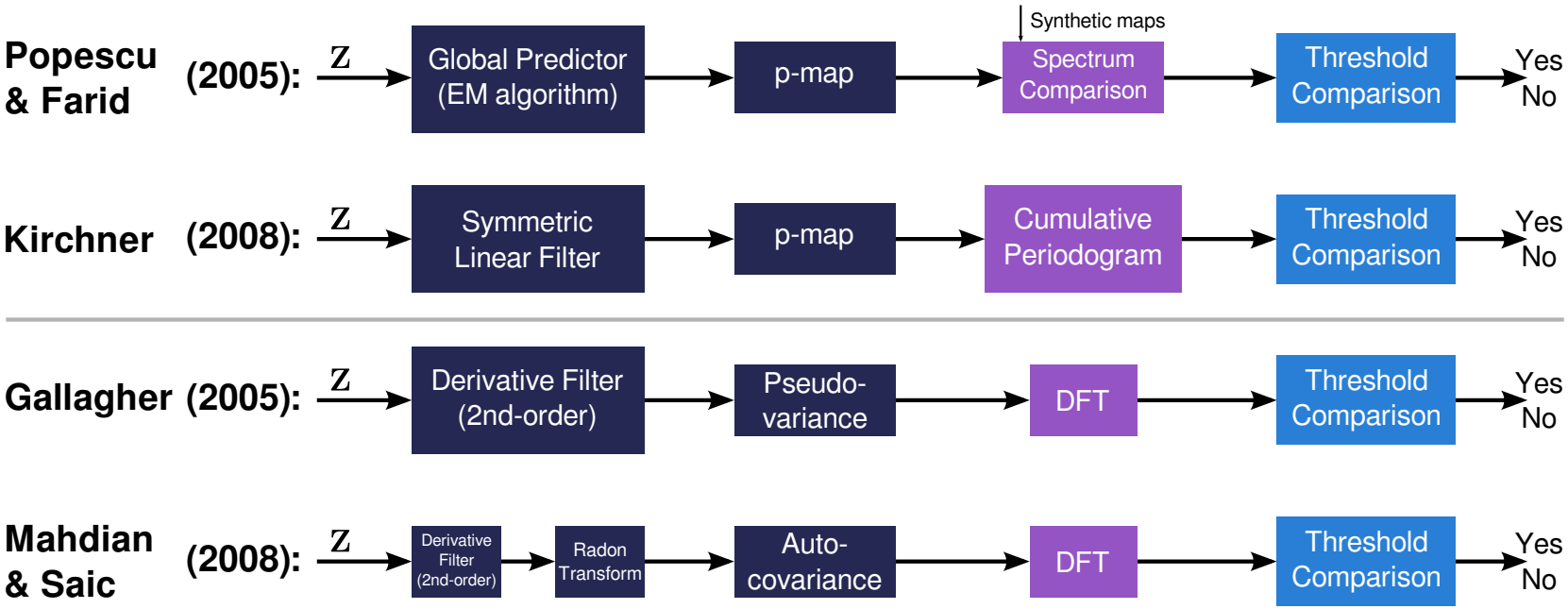
Three main steps are involved in the resampling process:

1. Resampling grid definition.
2. Calculation of pixel values in new locations.
3. Quantization of the interpolated values to fit the original precision.

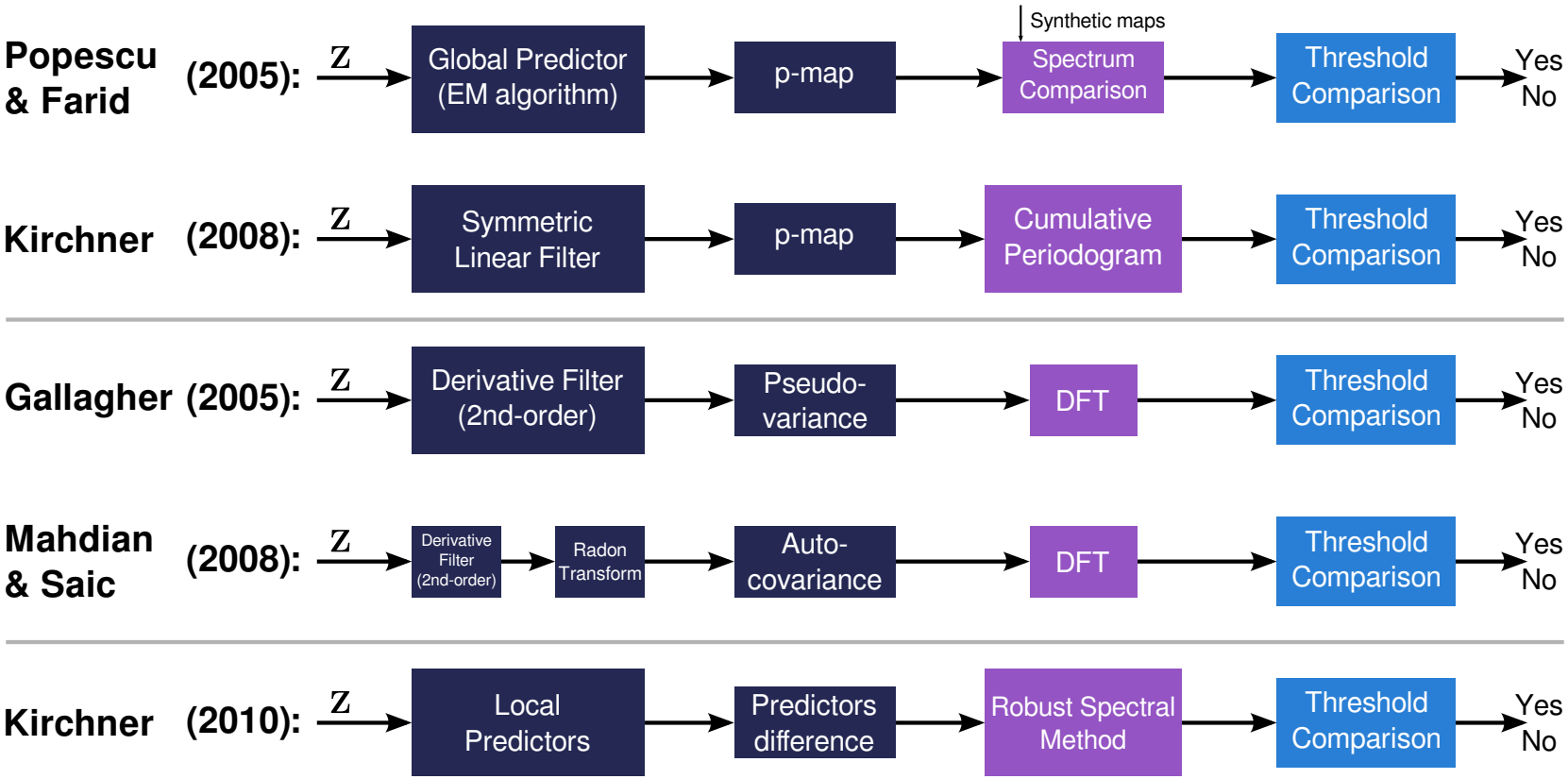
Prior Work


Popescu & Farid (2005):
Z
Global Predictor (EM algorithm)
p-map
Synthetic maps
Spectrum Comparison
Threshold Comparison
Yes
No
Kirchner (2008):
Z
Symmetric Linear Filter
p-map
Cumulative Periodogram
Threshold Comparison
Yes
No

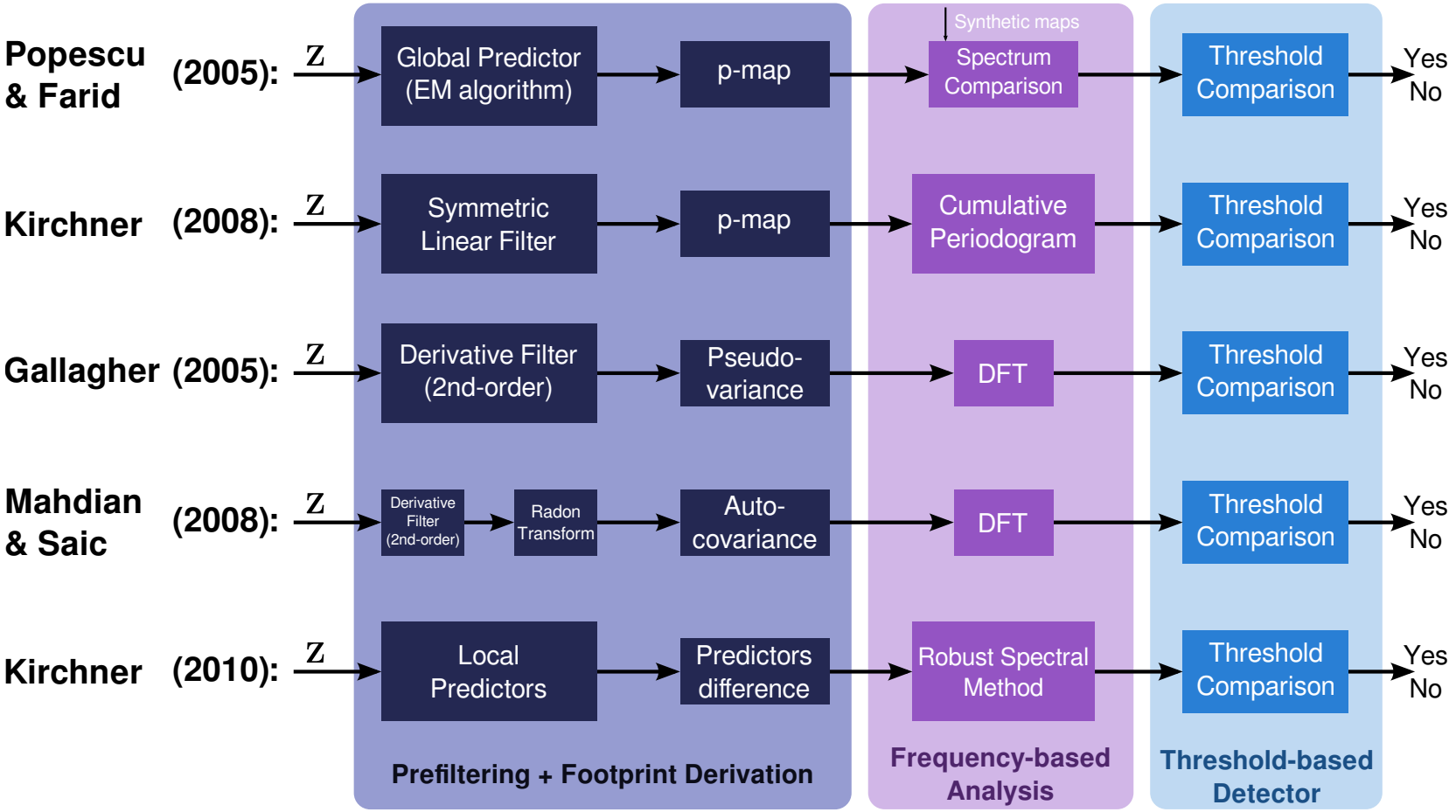
Prior Work


Popescu & Farid (2005):
Z
Global Predictor (EM algorithm)
p-map
Synthetic maps
Spectrum Comparison
Threshold Comparison
Yes
No
Kirchner (2008):
Z
Symmetric Linear Filter
p-map
Cumulative Periodogram
Threshold Comparison
Yes
No
Gallagher (2005):
Z
Derivative Filter (2nd-order)
Pseudo-variance
DFT
Threshold Comparison
Yes
No
Mahdian & Saic (2008):
Z
Derivative Filter (2nd-order)
Radon Transform
Auto-covariance
DFT
Threshold Comparison
Yes
No

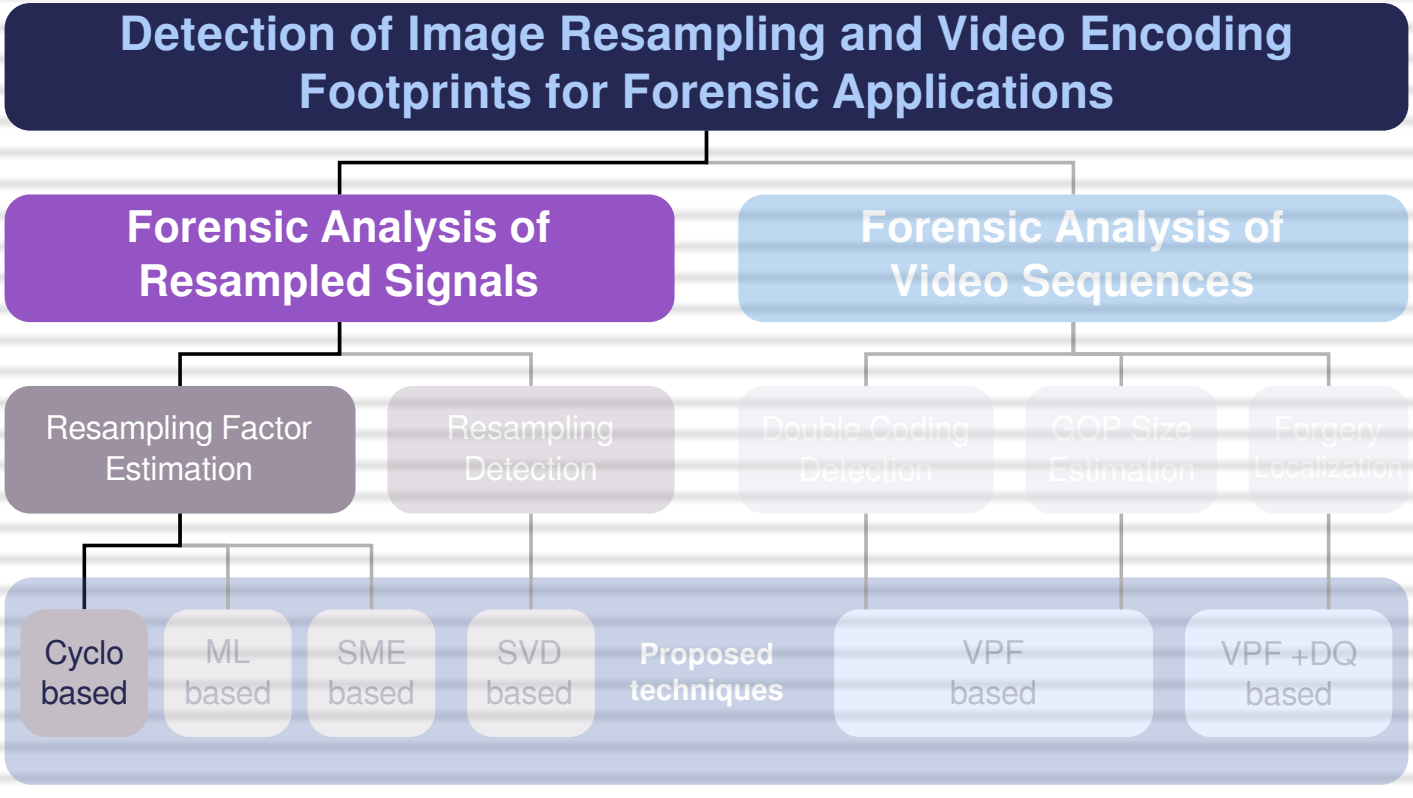
Prior Work


Popescu & Farid (2005):
Z
Global Predictor (EM algorithm)
p-map
Synthetic maps
Spectrum Comparison
Threshold Comparison
Yes
No
Kirchner (2008):
Z
Symmetric Linear Filter
p-map
Cumulative Periodogram
Threshold Comparison
Yes
No
Gallagher (2005):
Z
Derivative Filter (2nd-order)
Pseudo-variance
DFT
Threshold Comparison
Yes
No
Mahdian & Saic (2008):
Z
Derivative Filter (2nd-order)
Radon Transform
Auto-covariance
DFT
Threshold Comparison
Yes
No
Kirchner (2010):
Z
Local Predictors
Predictors difference
Robust Spectral Method
Threshold Comparison
Yes
No

Prior Work

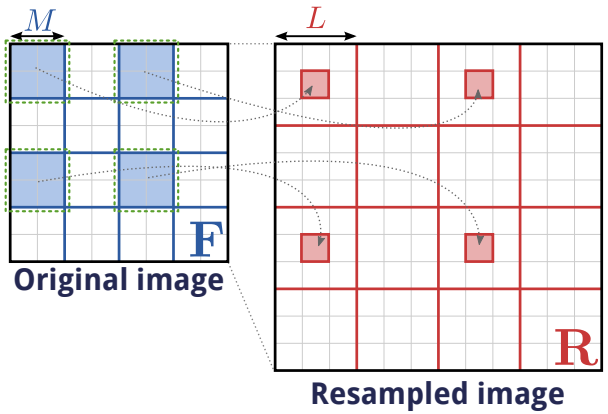

Popescu & Farid (2005):
Kirchner (2008):
Gallagher (2005):
Mahdian & Saic (2008):
Kirchner (2010):
Z
Global Predictor (EM algorithm)
Symmetric Linear Filter
Derivative Filter (2nd-order)
Derivative Filter (2nd-order)
Radon Transform
Local Predictors
p-map
p-map
Pseudo-variance
Auto-covariance
Predictors difference
Synthetic maps
Spectrum Comparison
Cumulative Periodogram
DFT
DFT
Robust Spectral Method
Threshold Comparison
Threshold Comparison
Threshold Comparison
Threshold Comparison
Threshold Comparison
Yes
No
Prefiltering + Footprint Derivation
Frequency-based Analysis
Threshold-based Detector

2.3. **Proposed Techniques**: Method Based on Cyclostationary



Study of Cyclostationarity on Images

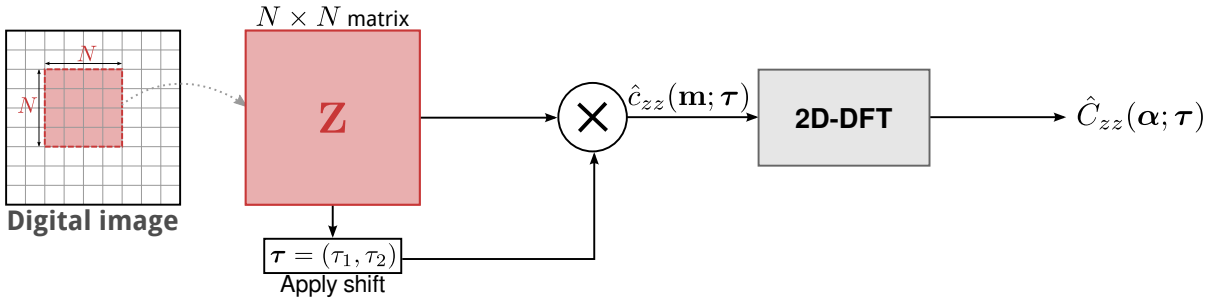
Resampling by $\xi = \frac{L}{M} > 1 \rightarrow$ **periodic filtering** with the **same kernel**.



- Does $\mathbf{R}$ have statistical properties that vary cyclically?
- Under some conditions, its covariance varies cyclically with period ξ.

Study of Cyclostationarity on Images

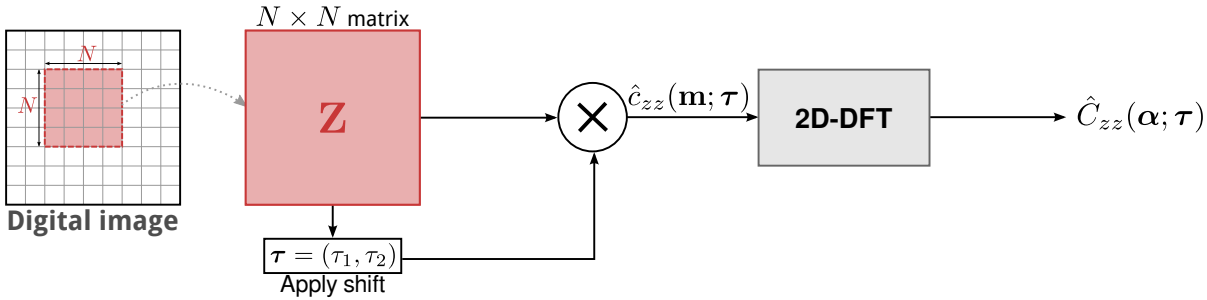
The **Fourier transform** of the **sample covariance** $\hat{c}_{zz}(\mathbf{m};\boldsymbol{\tau})$**:**



shows peaks at cyclic frequencies (α_1, α_2) such that $\alpha_i = \frac{2\pi}{\xi_i},\ i \in \{1, 2\}$.

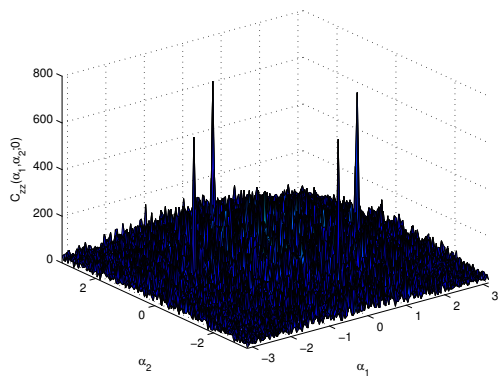
Study of Cyclostationarity on Images

The **Fourier transform** of the **sample covariance** $\hat{c}_{zz}(\mathbf{m};\boldsymbol{\tau})$**:**

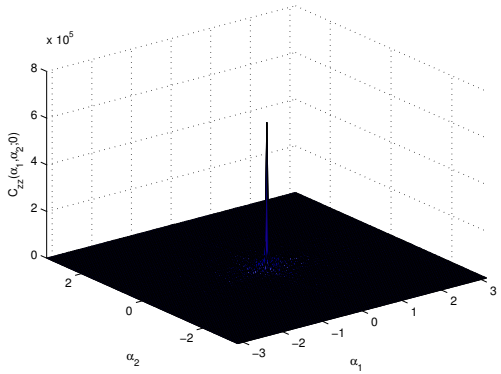


shows peaks at cyclic frequencies (α_1, α_2) such that $\alpha_i = \frac{2\pi}{\xi_i},\ i \in \{1, 2\}$.

Example: $\xi = \frac{3}{2}$ (excluding DC component)



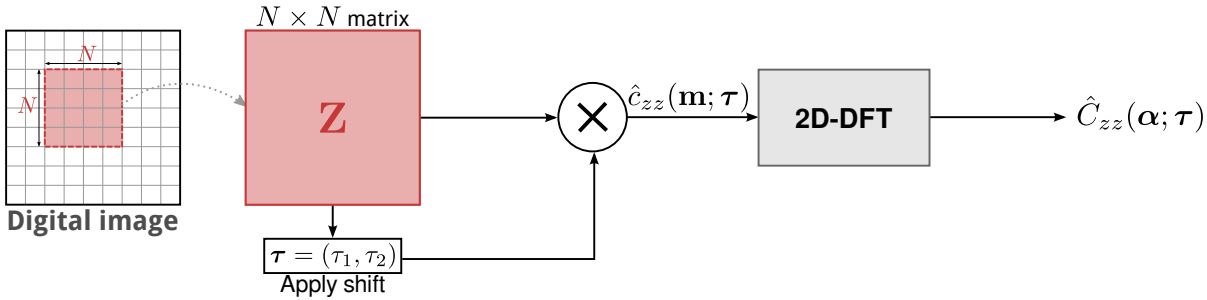
White noise



Real image

Study of Cyclostationarity on Images

The **Fourier transform** of the **sample covariance** $\hat{c}_{zz}(\mathbf{m};\boldsymbol{\tau})$:



shows peaks at cyclic frequencies (α_1, α_2) such that $\alpha_i = \frac{2\pi}{\xi_i},\ i \in \{1, 2\}$.

Problem:

$\hat{C}_{zz}(\boldsymbol{\alpha};\boldsymbol{\tau})$ works well for white noise fields, but not for **real images**.

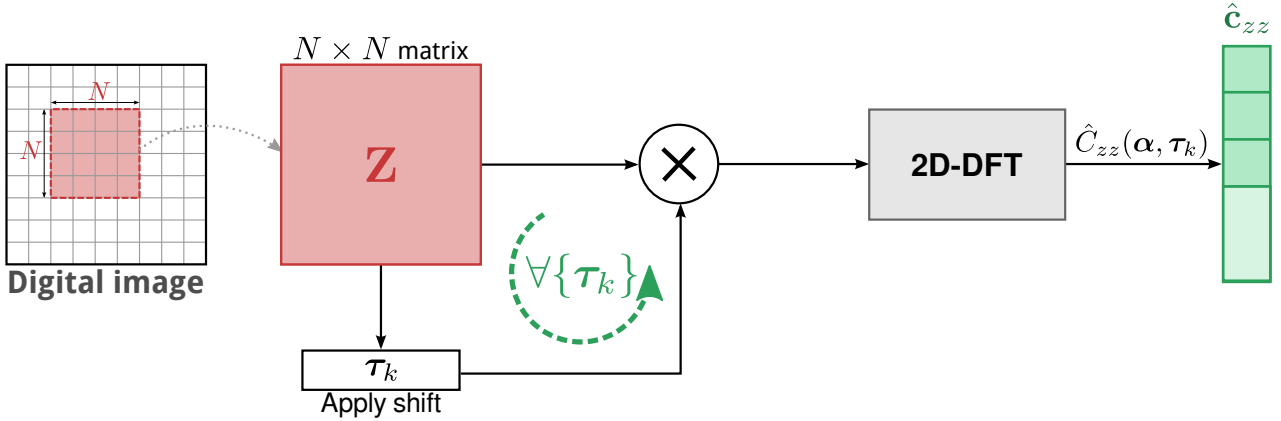
Solution:

Link **resampling problem** with **Digital Communications** field:

$$\text{(1-D)} \quad g_i = \sum_k f_k h\left(i\frac{M}{L} - k\right) \quad \leftrightarrow \quad x(t) = \sum_k a_k p(t - kT_0) \quad \text{(PAM)}$$

Test for the Presence of Cyclostationarity

Two-dimensional extension of **Dandawaté & Giannakis**'s test **(1994)**:



Hypothesis test:

$$\mathcal{H}_0 : \boldsymbol{\alpha} \notin \mathcal{A}_{zz}, \forall\{\boldsymbol{\tau}_k\}_{k=1}^{K} \quad \Rightarrow \quad \hat{\mathbf{c}}_{zz} = \mathbf{e}_{zz},$$

$$\mathcal{H}_1 : \boldsymbol{\alpha} \in \mathcal{A}_{zz}, \text{for some } \{\boldsymbol{\tau}_k\}_{k=1}^{K} \quad \Rightarrow \quad \hat{\mathbf{c}}_{zz} = \mathbf{c}_{zz} + \mathbf{e}_{zz},$$

where $\mathcal{A}_{zz} \triangleq \{\boldsymbol{\alpha} = (\alpha_1, \alpha_2) : C_{zz}(\boldsymbol{\alpha}; \boldsymbol{\tau}) \neq 0, -\pi < \alpha_1, \alpha_2 \leq \pi\}$

Likelihood ratio test:

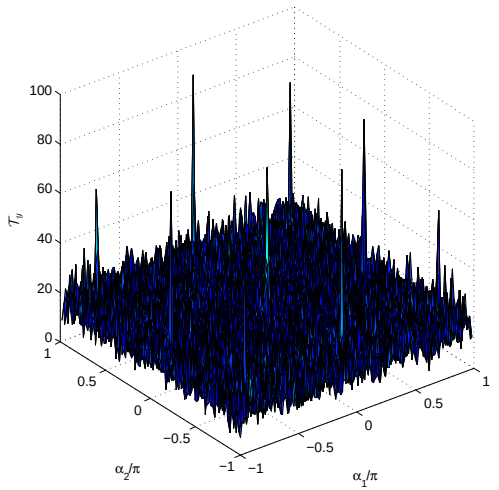
$$\mathcal{T}_{zz} = N^2 \hat{\mathbf{c}}_{zz}^H \hat{\boldsymbol{\Sigma}}_{zz}^{-1} \hat{\mathbf{c}}_{zz} \underset{\mathcal{H}_0}{\overset{\mathcal{H}_1}{\gtrless}} \Gamma$$

Resampling Factor Estimation: examples

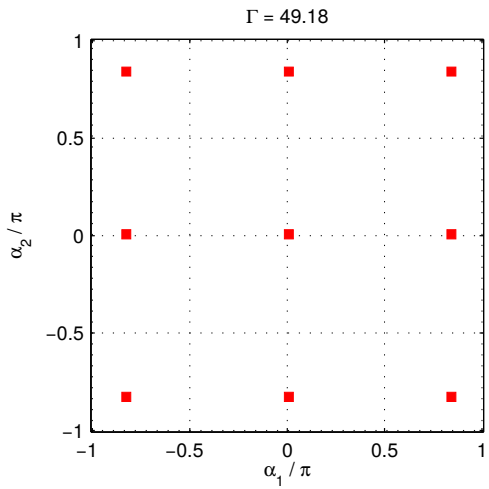
Scaled image by $\xi = (1.7, 1.7)$: image block of size 128×128



Block of analysis



$\mathcal{T}_{zz}$ for $K = 9, P = 11$



$P_F = 10^{-4}$

Detected cyclic frequencies α_i with $i \in \{1, 2\}$:

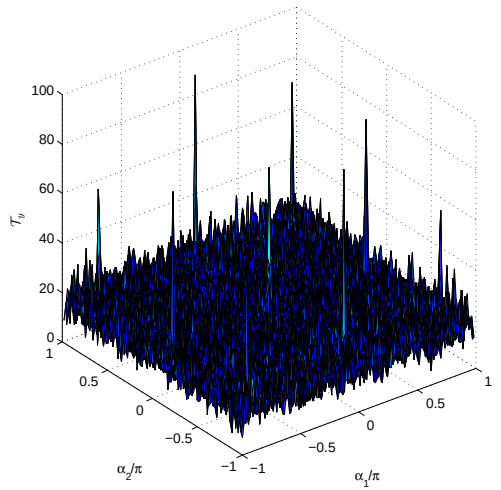
$$\hat{\xi}_i = \begin{cases} \dfrac{2\pi}{2\pi - |\alpha_i|}, & -\pi \leq \alpha_i \leq \pi \quad (1 < \hat{\xi}_i \leq 2) \\ \dfrac{2\pi}{|\alpha_i|}, & -\pi \leq \alpha_i \leq \pi \quad (\hat{\xi}_i \geq 2) \end{cases}$$

Resampling Factor Estimation: examples

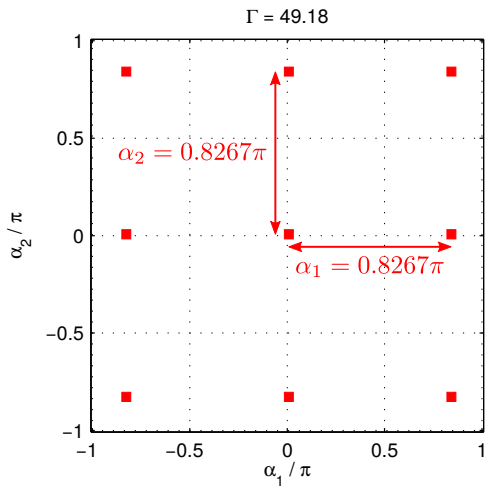
Scaled image by $\xi = (1.7, 1.7)$: image block of size 128×128



Block of analysis



$\mathcal{T}_{zz}$ for $K = 9, P = 11$



$P_F = 10^{-4}$

Detected cyclic frequencies α_i with $i \in \{1, 2\}$:

$$\hat{\xi}_i = \begin{cases} \dfrac{2\pi}{2\pi - |\alpha_i|}, & -\pi \leq \alpha_i \leq \pi \quad (1 < \hat{\xi}_i \leq 2) \\ \dfrac{2\pi}{|\alpha_i|}, & -\pi \leq \alpha_i \leq \pi \quad (\hat{\xi}_i \geq 2) \end{cases}$$

Example:

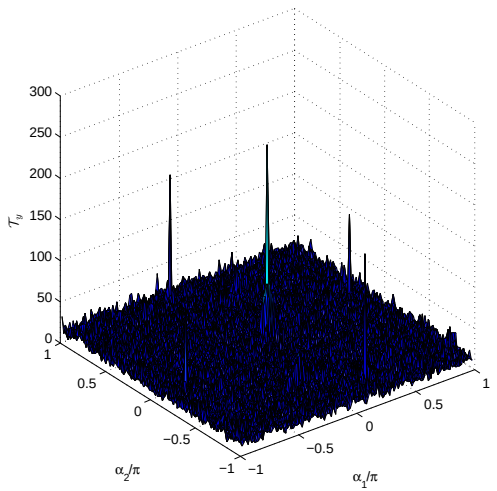
- $\hat{\xi}_1 = 1.7046$
- $\hat{\xi}_2 = 1.7046$

Resampling Factor Estimation: examples

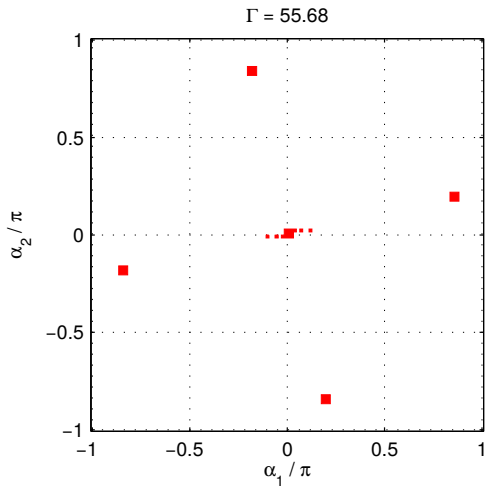
Rotated image by $\theta = -25°$: image block of size 128×128



Block of analysis



$\mathcal{T}_{zz}$ for $K = 9, P = 21$



$P_F = 10^{-5}$

Frequencies: $\phi = \arctan(\alpha_2/\alpha_1) \bmod \pi/2$

$$\hat{\theta} = \begin{cases} -2\phi, & \text{if} \quad 0 \leq \phi \leq \frac{\pi}{12} \\ -\arccos(\kappa), & \text{if} \quad \frac{\pi}{12} < \phi \leq \frac{5\pi}{12} \\ \frac{\pi}{2} - 2\phi, & \text{if} \quad \frac{5\pi}{12} < \phi \leq \frac{\pi}{2} \end{cases}$$

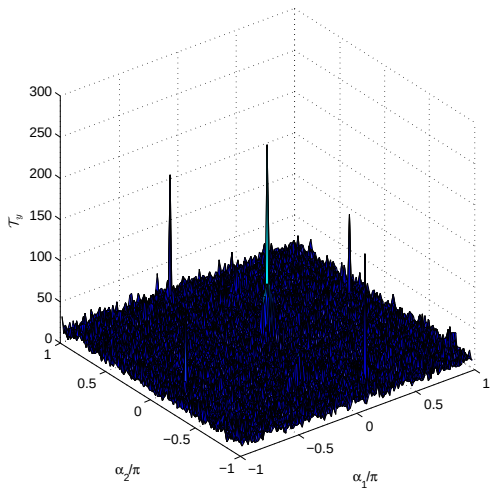
$$\kappa \triangleq \cos^2(\phi)(\sqrt{2\tan(\phi)} - \tan(\phi) + \tan^2(\phi))$$

Resampling Factor Estimation: examples

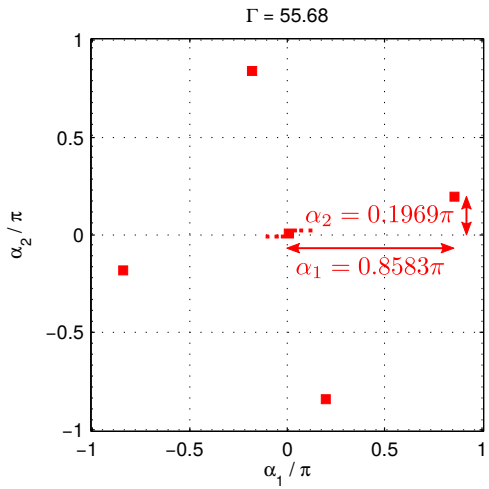
Rotated image by $\theta = -25°$: image block of size 128×128



Block of analysis



$\mathcal{T}_{zz}$ for $K = 9, P = 21$



$P_F = 10^{-5}$

Frequencies: $\phi = \arctan(\alpha_2/\alpha_1) \bmod \pi/2$

$$\hat{\theta} = \begin{cases} -2\phi, & \text{if } \quad 0 \leq \phi \leq \frac{\pi}{12} \\ -\arccos(\kappa), & \text{if } \frac{\pi}{12} < \phi \leq \frac{5\pi}{12} \\ \frac{\pi}{2} - 2\phi, & \text{if } \frac{5\pi}{12} < \phi \leq \frac{\pi}{2} \end{cases}$$

$$\kappa \triangleq \cos^2(\phi)(\sqrt{2\tan(\phi)} - \tan(\phi) + \tan^2(\phi))$$

Example:

- $\phi = 0.2255$
- $\phi < \pi/12$
- $\hat{\theta} = -25.84°$

Experimental Setup

Image Dataset:

40 TIFF images from the **USC-SIPI Image Database** (Miscellaneous).

1. Scaling factor estimation:

- $\xi \in \{1.05, 1.1, \ldots, 2.2, 2.25\}$
- **Lanczos** kernel
- $|\hat{\xi}_i - \xi| < 0.05$ for any $i \in \{1, 2\}$

2. Rotation angle estimation:

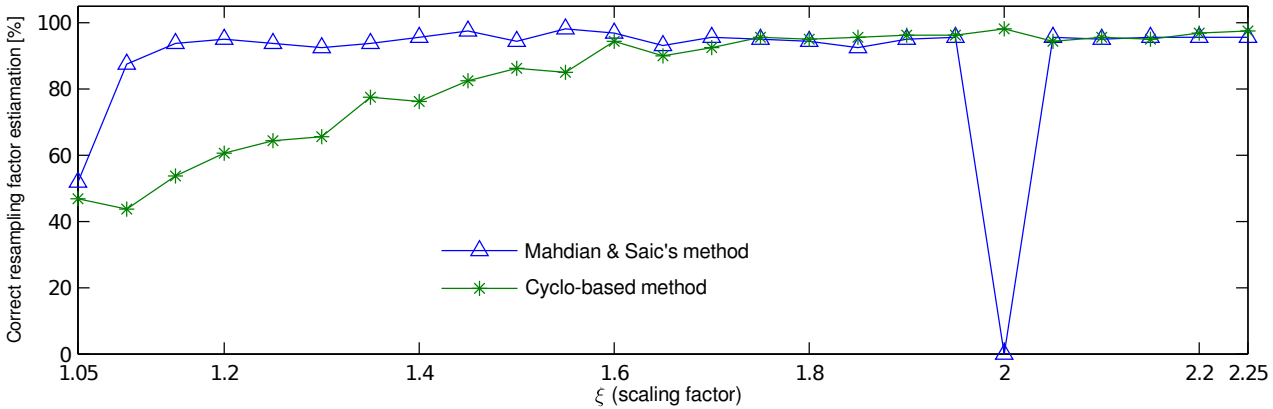
- $-\frac{\pi}{2} < \theta < 0$, sampled by $\frac{\pi}{72}$
- **Catmull-Rom** kernel
- $|\hat{\theta} - \theta| < \frac{\pi}{72}$

Resampling Analysis:

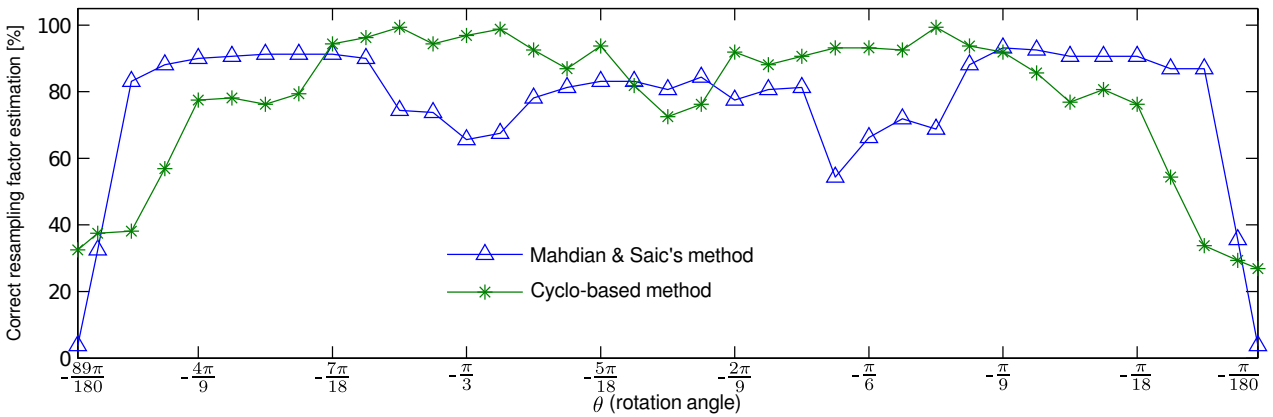
- Average result of **4 blocks** of size 128×128 from the green channel.
- **Comparison:** Mahdian & Saic (2008).

Experimental Results

1. Scaling factor estimation:

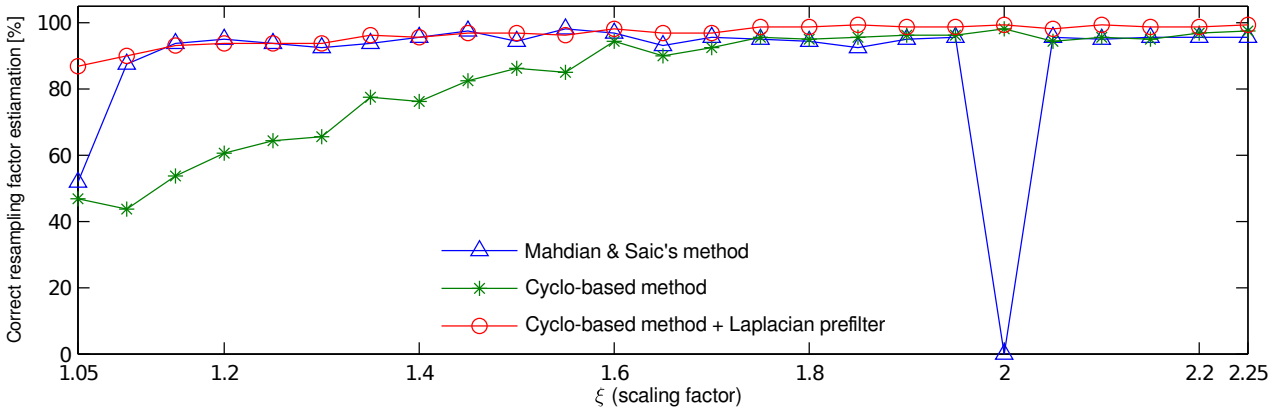


2. Rotation angle estimation:

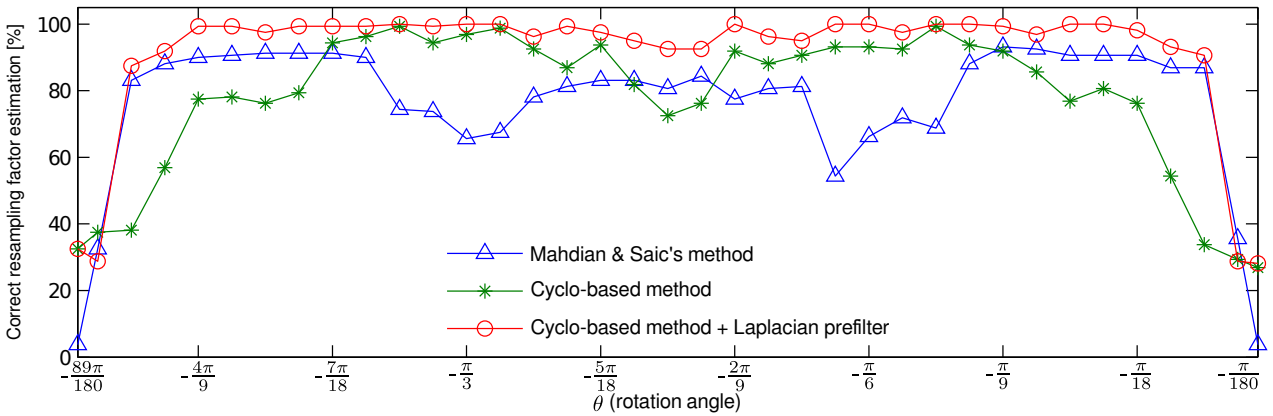


Experimental Results

1. Scaling factor estimation: adding a prefilter

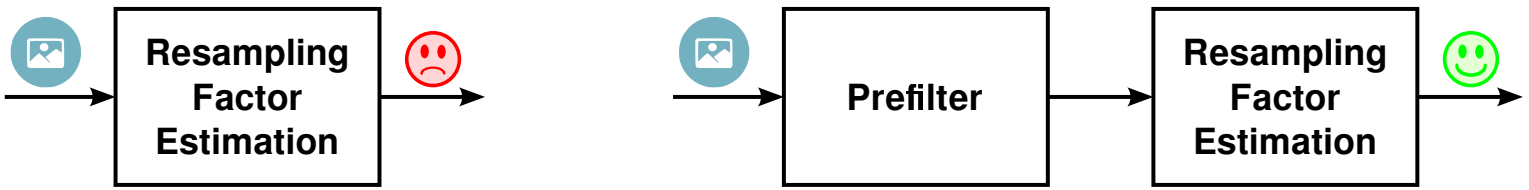


2. Rotation angle estimation: adding a prefilter



Prefilter Design for Resampling Estimation

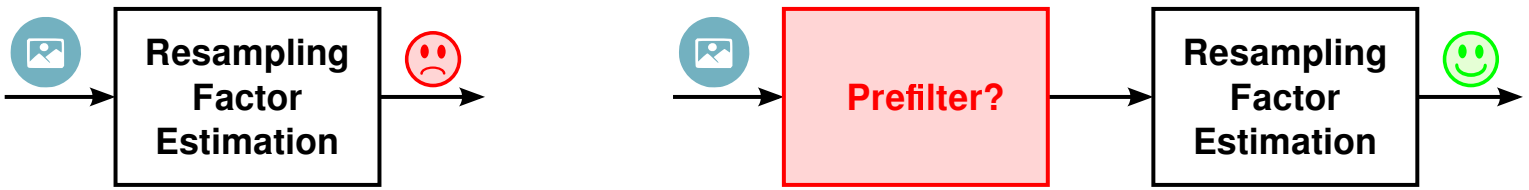
Current situation:



- Derivative prefilters are used as a way of boosting resampling traces.

Prefilter Design for Resampling Estimation

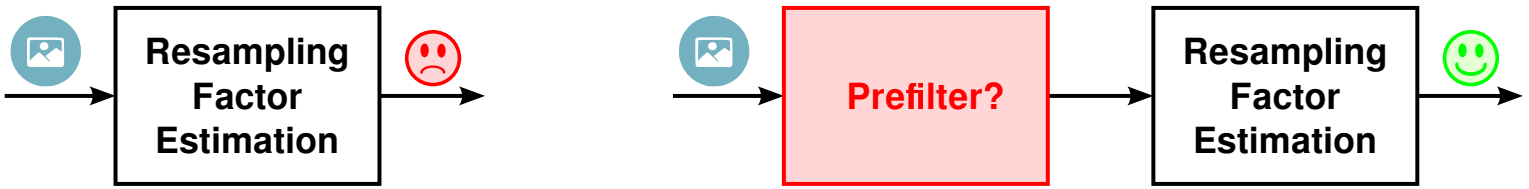
Current situation:



- Derivative prefilters are used as a way of boosting resampling traces.
- Which is the optimum prefilter for resampling estimation?

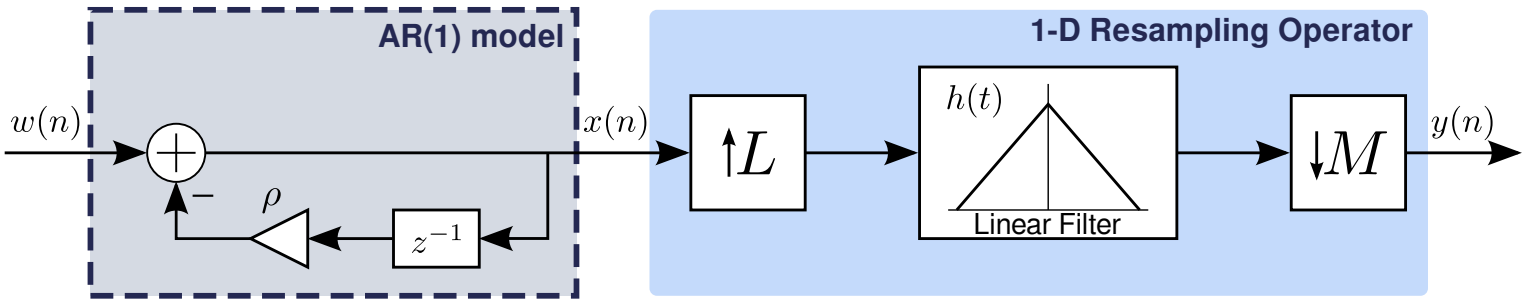
Prefilter Design for Resampling Estimation

Current situation:



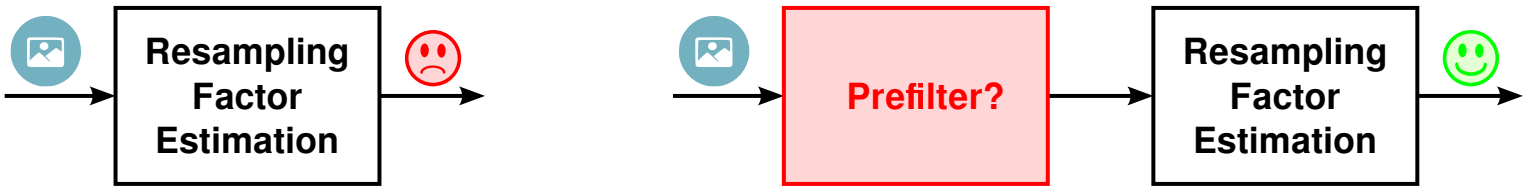
- Derivative prefilters are used as a way of boosting resampling traces.
- Which is the optimum prefilter for resampling estimation?

Complete 1-D model: resampling operation by $\xi = \frac{L}{M} > 1$



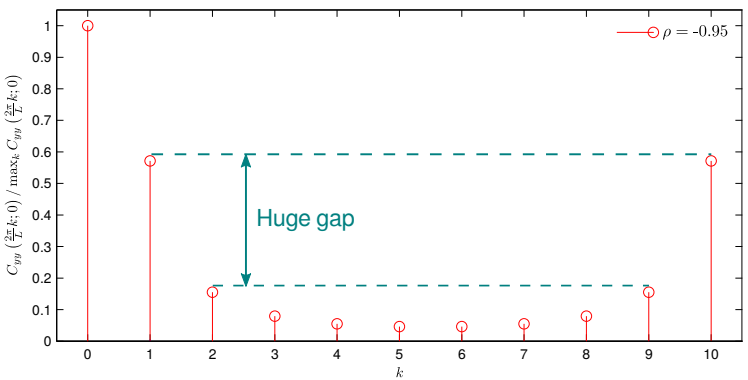
Prefilter Design for Resampling Estimation

Current situation:

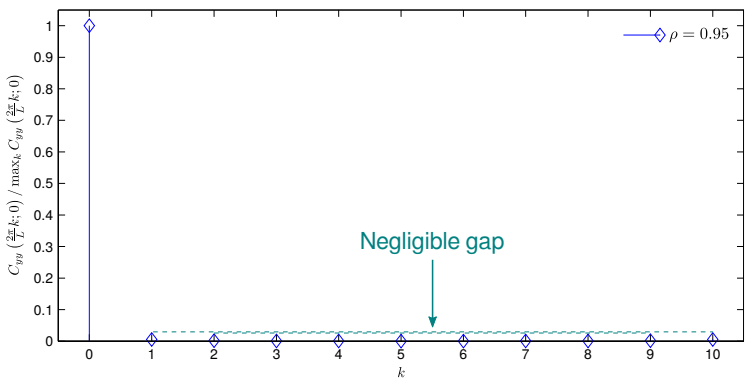


- Derivative prefilters are used as a way of boosting resampling traces.
- Which is the optimum prefilter for resampling estimation?

Example: derivation of the deterministic value of $C_{yy}(k;\tau)$



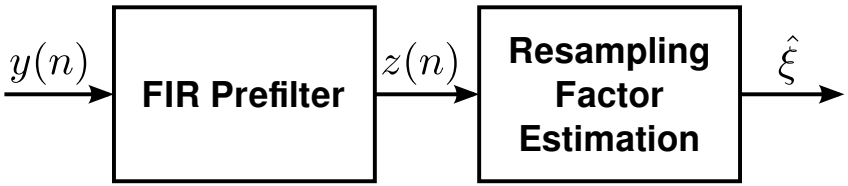
$\xi = \frac{11}{10}$, and $\rho = -0.95$



$\xi = \frac{11}{10}$, and $\rho = 0.95$

Objective Function Definition

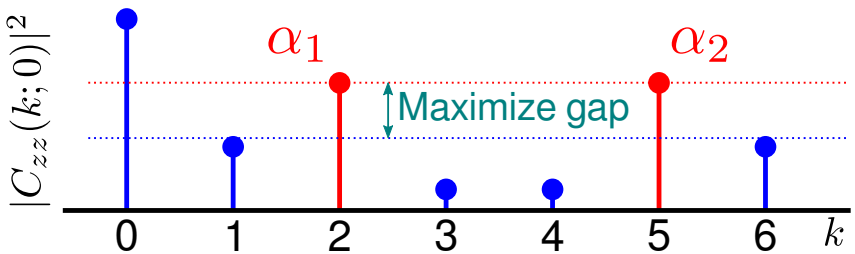
Pth-order **FIR** prefilter $\mathbf{p}$ with coefficients p_i and $i \in \{0, \ldots, P\}$:



Spectral coefficients:

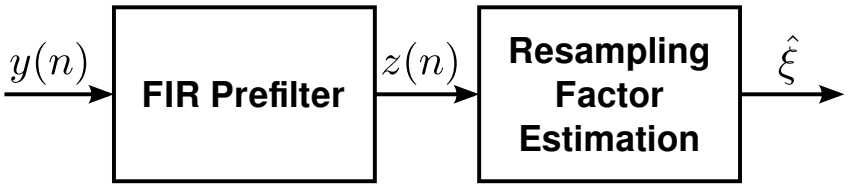
$$C_{zz}(k;\tau) = \sum_{l=0}^{P} \sum_{m=0}^{P} p_l p_m C_{yy}(k;\tau + l - m) e^{-j\frac{2\pi k}{L} l}$$

Cyclic frequencies: $\alpha_1 = \frac{2\pi}{L} M \ (k = M)$, $\alpha_2 = \frac{2\pi}{L}(L - M) \ (k = L - M)$



Objective Function Definition

Pth-order **FIR** prefilter $\mathbf{p}$ with coefficients p_i and $i \in \{0, \ldots, P\}$:



Spectral coefficients:

$$C_{zz}(k;\tau) = \sum_{l=0}^{P} \sum_{m=0}^{P} p_l p_m C_{yy}(k;\tau + l - m) e^{-j\frac{2\pi k}{L} l}$$

Cyclic frequencies: $\alpha_1 = \frac{2\pi}{L} M \ (k = M)$, $\alpha_2 = \frac{2\pi}{L}(L - M) \ (k = L - M)$

Objective function:

$$\Theta(\mathbf{p}) \triangleq \frac{\frac{1}{2}(|C_{zz}(M;0)|^2 + |C_{zz}(L-M;0)|^2)}{\frac{1}{L-2} \sum\limits_{\substack{k=0 \\ k \neq M, L-M}}^{L-1} |C_{zz}(k;0)|^2}$$

Estimate of the optimum prefilter

Estimate of the optimum prefilter for given values of ρ and ξ:

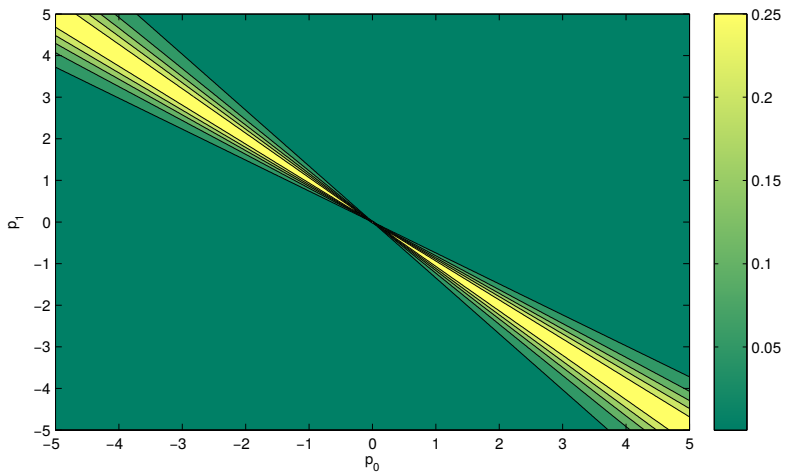
$$\hat{\mathbf{p}} = \arg \max_{\mathbf{p} \in \mathbb{R}^{P+1}} \Theta(\mathbf{p})$$

Estimate of the optimum prefilter

Estimate of the optimum prefilter for given values of ρ and ξ:

$$\hat{\mathbf{p}} = \arg \max_{\mathbf{p} \in \mathbb{R}^{P+1}} \Theta(\mathbf{p})$$

First-order prefilter $(P = 1)$:



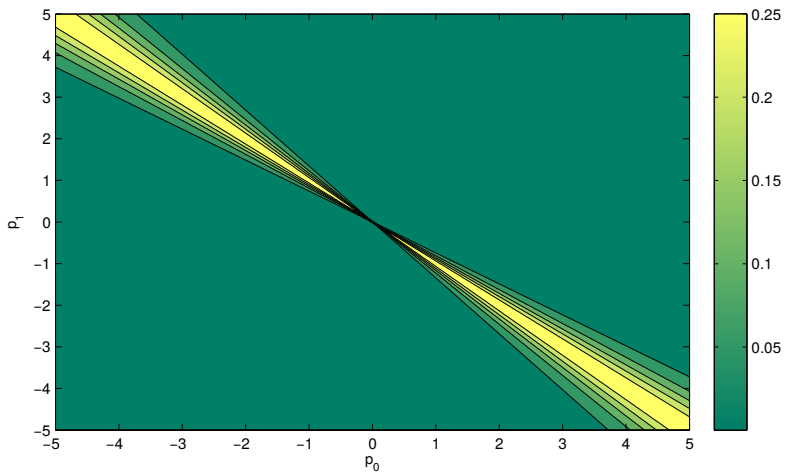
- **Case:** $\rho = 0.95$, $\xi = \frac{11}{10}$
- $\hat{\mathbf{p}} \rightarrow$ 1st-order derivative filter

Estimate of the optimum prefilter

Estimate of the optimum prefilter for given values of ρ and ξ:

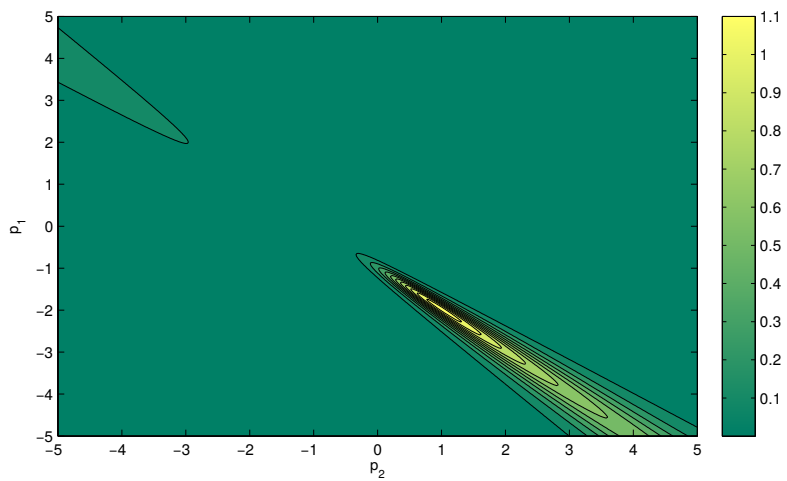
$$\hat{\mathbf{p}} = \arg \max_{\mathbf{p} \in \mathbb{R}^{P+1}} \Theta(\mathbf{p})$$

First-order prefilter $(P = 1)$:



- **Case:** $\rho = 0.95,\ \xi = \frac{11}{10}$
- $\hat{\mathbf{p}} \rightarrow$ 1st-order derivative filter

Second-order prefilter $(P = 2)$:



- **Case:** $p_0 = 1,\ \rho = 0.95,\ \xi = \frac{11}{10}$
- $\hat{\mathbf{p}} \rightarrow$ 2nd-order derivative filter

Experimental Setup

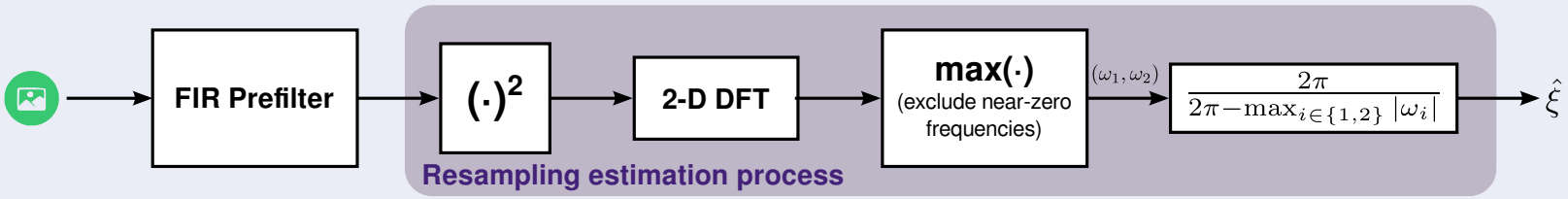
Image Dataset:

- 150 raw format images from a personal image database (Nikon D60).
- Prior **downsampling by 2**, to remove CFA artifacts.

Resampling process:

- **Bilinear** kernel and $1 < \xi < 2$ (sampled with step size 0.05).

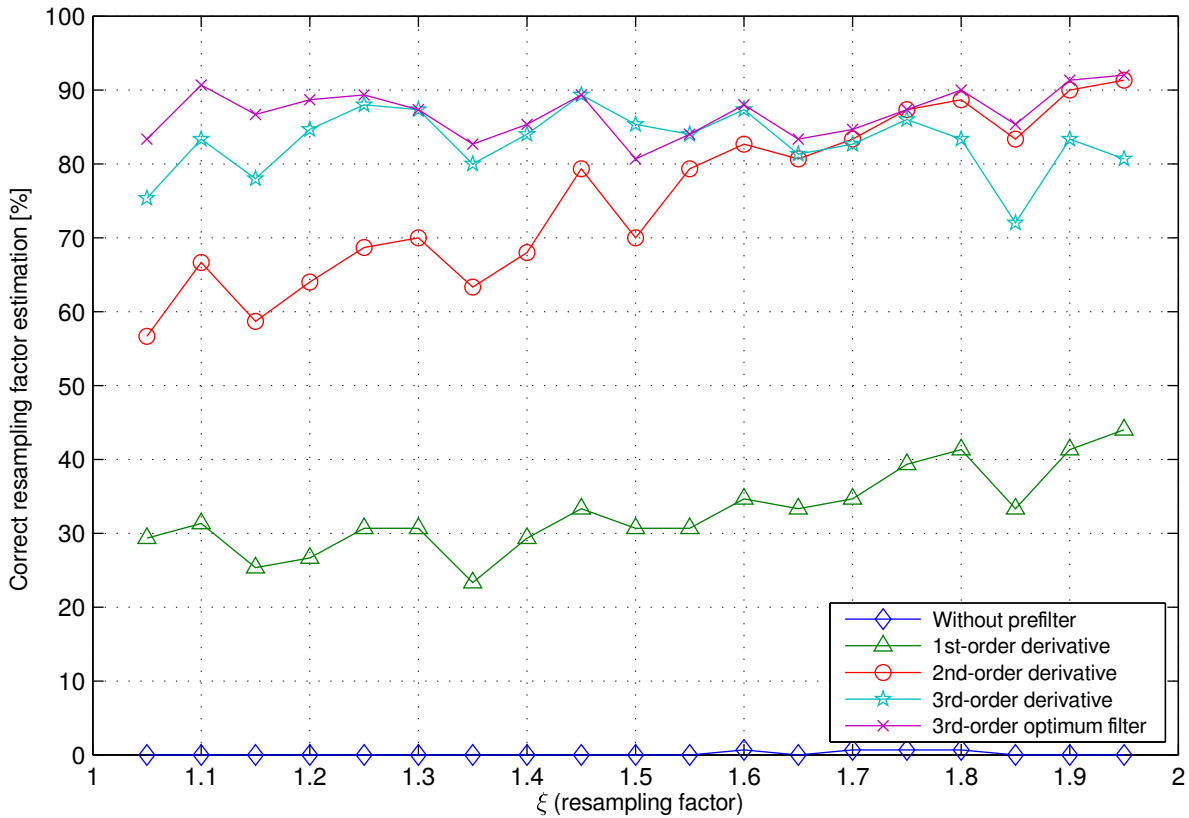
Resampling analysis: block of 1024×1024 pixels from green component.



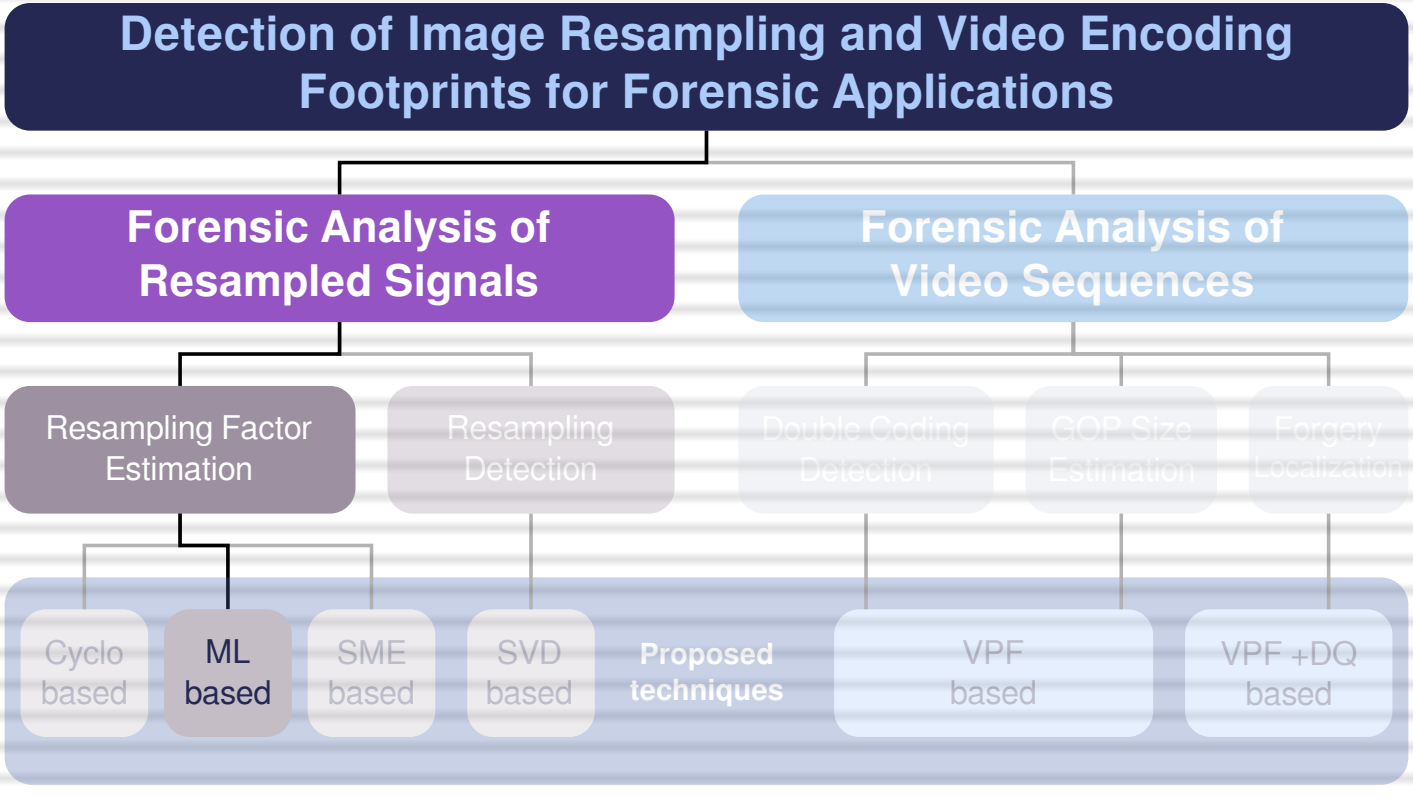
Experimental Results

Correct resampling factor estimation:

- $\left|\max_{i\in\{1,2\}} |\omega_i| - \alpha\right| \leq \frac{2\pi}{1024}$, where $\alpha \triangleq 2\pi\frac{L-M}{L}$ (cyclic frequency)

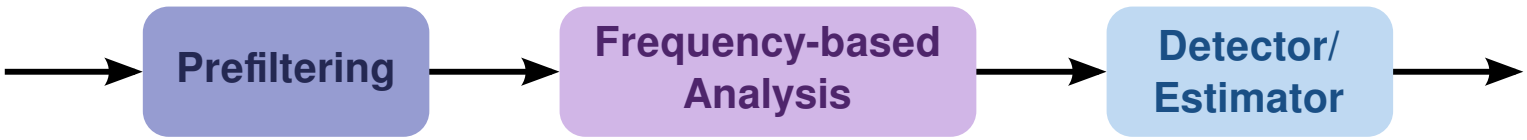


2.3. **Proposed Techniques**: Method based on ML Estimation



Resampling Problem

Previous works share this general structure:

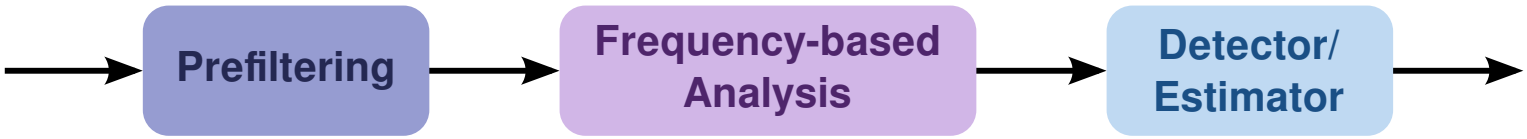


Drawbacks of the **frequency-based analysis:**

1. A **large amount of samples** is needed.
2. Presence of **periodic patterns** misleads the detectors.

Resampling Problem

Previous works share this general structure:

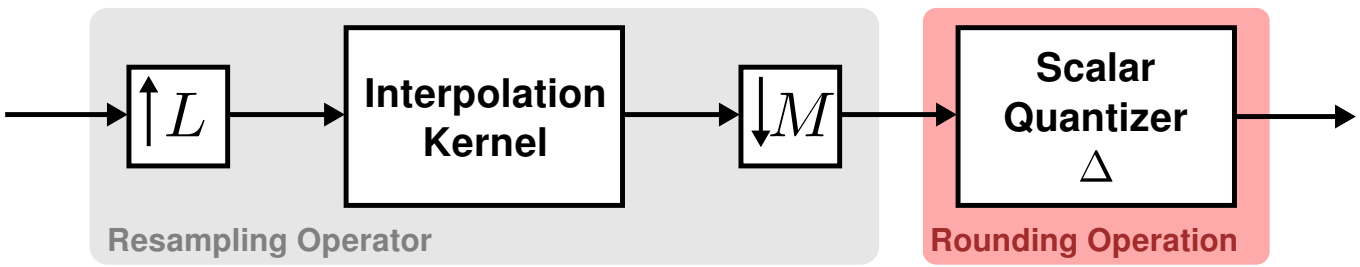


Drawbacks of the **frequency-based analysis:**

1. A **large amount of samples** is needed.
2. Presence of **periodic patterns** misleads the detectors.

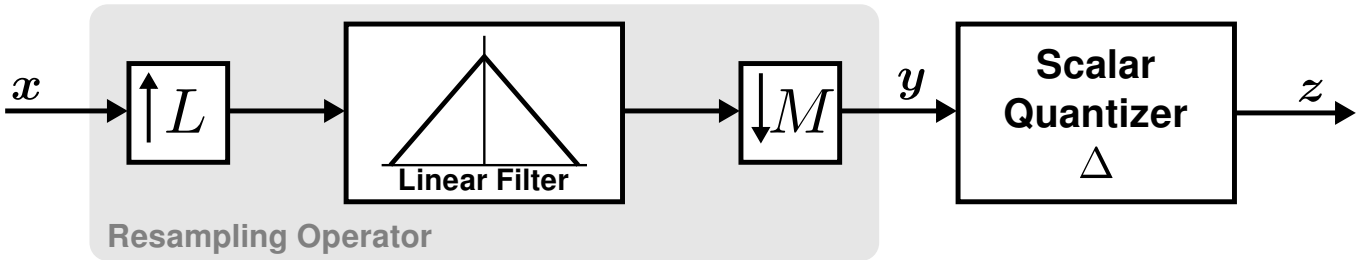
New approach:

- Analysis of the **rounding operation** applied after resampling.



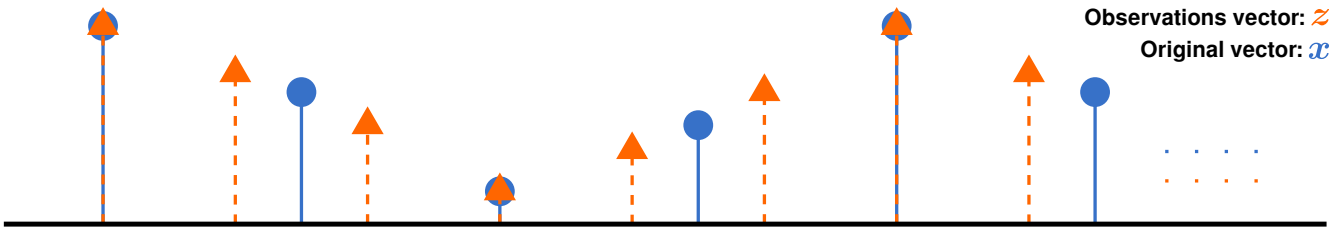
ML Approach to Resampling Estimation

One-dimensional resampling by $\xi = \frac{L}{M} > 1$:



ML Approach to Resampling Estimation

Example: linear kernel and $\xi = \frac{3}{2}$



Goal:

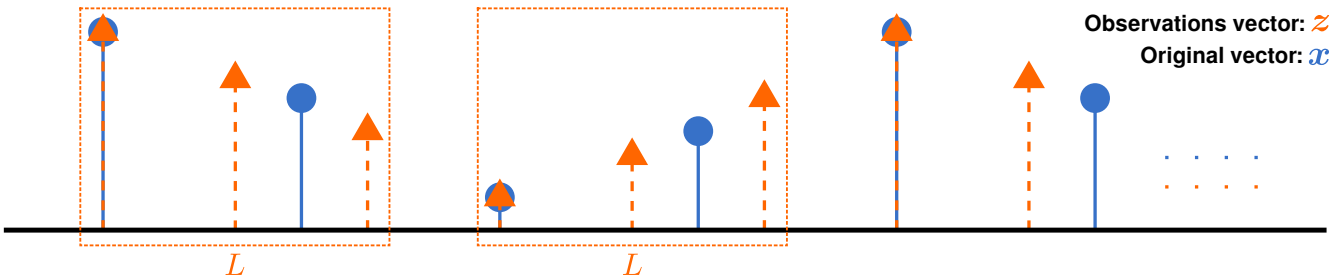
- Given a vector of observations z, we want to know the resampling factor ξ applied to the original vector x.

Maximum Likelihood Estimate:

- $\hat{\xi} = \arg\max_{\xi>1} f_{\boldsymbol{Z}|\Xi}(\boldsymbol{z}|\xi)$, where $f_{\boldsymbol{Z}|\Xi}(\boldsymbol{z}|\xi) = \int_{\mathbb{R}^{N+1}} f_{\boldsymbol{Z}|\boldsymbol{X}}(\boldsymbol{z}|\boldsymbol{x}) f_{\boldsymbol{X}}(\boldsymbol{x})\, d\boldsymbol{x}$

ML Approach to Resampling Estimation

Example: linear kernel and $\xi = \frac{3}{2}$



Goal:

- Given a vector of observations z, we want to know the resampling factor ξ applied to the original vector x.

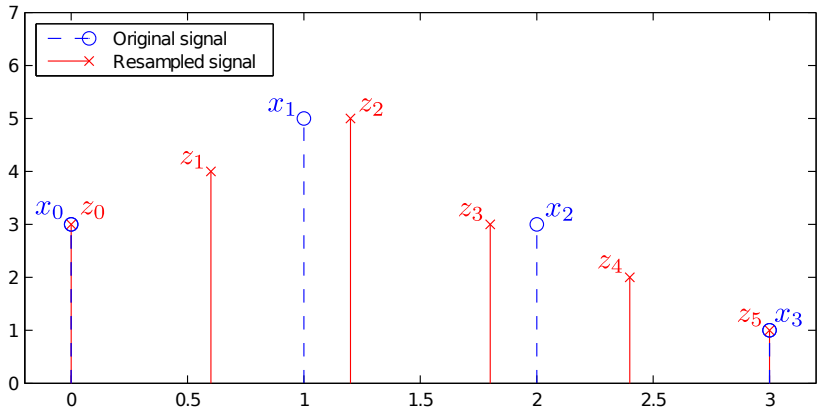
Maximum Likelihood Estimate:

- $\hat{\xi} = \arg\max_{\xi>1} f_{\boldsymbol{Z}|\Xi}(\boldsymbol{z}|\xi)$, where $f_{\boldsymbol{Z}|\Xi}(\boldsymbol{z}|\xi) = \int_{\mathbb{R}^{N+1}} f_{\boldsymbol{Z}|\boldsymbol{X}}(\boldsymbol{z}|\boldsymbol{x}) f_{\boldsymbol{X}}(\boldsymbol{x}) d\boldsymbol{x}$

Derivation of $f_{\boldsymbol{Z}|\Xi}(\boldsymbol{z}|\xi)$: through disjoint blocks of L samples from z, i.e.,

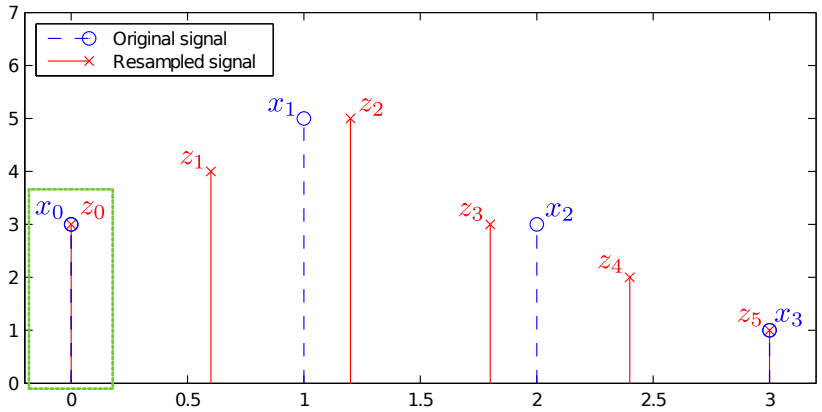
$$f_{\boldsymbol{Z}|\Xi}(\boldsymbol{z}|\xi) \approx \prod_{j=0}^{N/M-1} \int_{\mathbb{R}^M} f_{\boldsymbol{Z}_{Lj}|\boldsymbol{X}_{Mj}}(\boldsymbol{z}_{Lj}|\boldsymbol{x}_{Mj}) d\boldsymbol{x}_{Mj}$$

Method Description with an Example ($\xi = 5/3$)

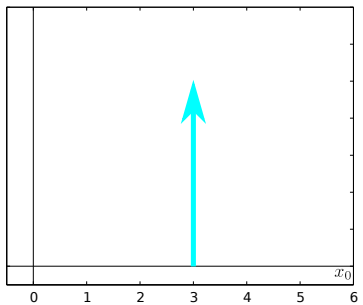


Original and resampled signals

Method Description with an Example ($\xi = 5/3$)

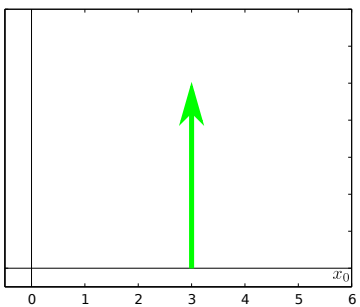


Original and resampled signals



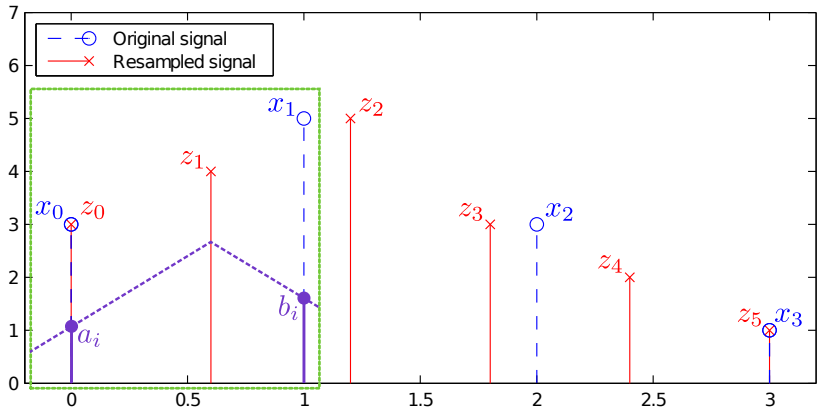
Feasible range for x_0

$$f_{Z_i|X_k}(z_i|x_k) = \delta(z_i - x_k)$$

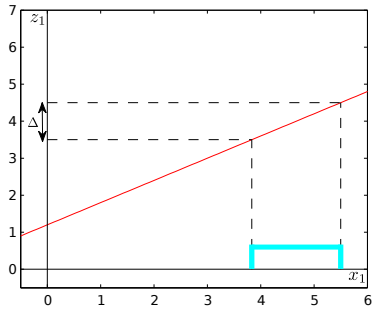


Resulting pdf for x_0

Method Description with an Example ($\xi = 5/3$)

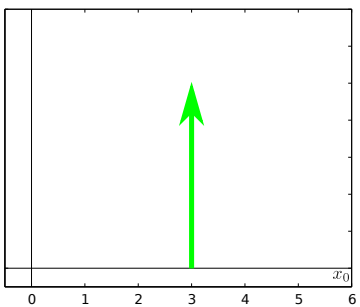


Original and resampled signals

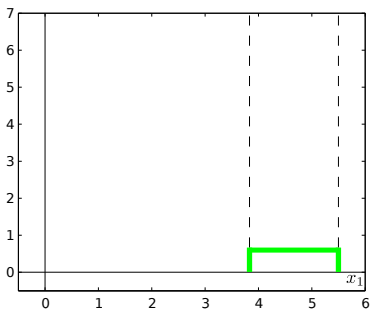


Feasible range for x_1

$$f_{Z_i|X_k,X_{k+1}}(z_i|x_k,x_{k+1}) = \Pi\left(\frac{a_i x_k + b_i x_{k+1} - z_i}{\Delta}\right)$$

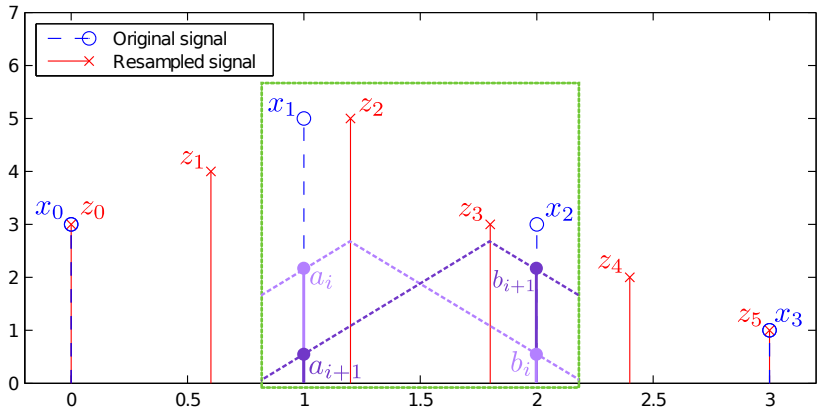


Resulting pdf for x_0

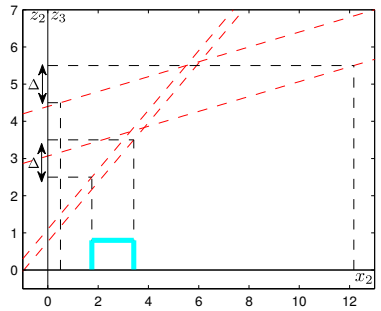


Resulting pdf for x_1

Method Description with an Example ($\xi = 5/3$)

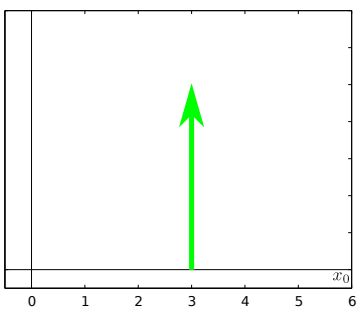


Original and resampled signals

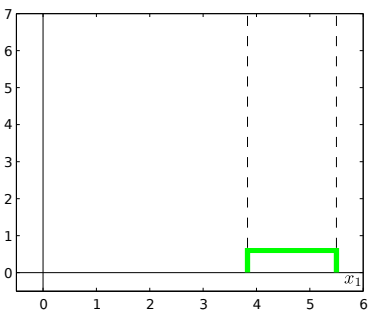


Feasible range for x_2

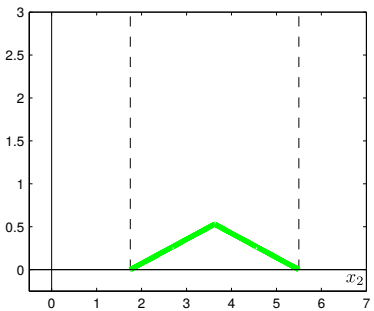
$$f_{\boldsymbol{z}_i|X_k,X_{k+1}}(\boldsymbol{z}_i|x_k,x_{k+1}) = \prod_m \Pi\left(\frac{a_m x_k + b_m x_{k+1} - z_m}{\Delta}\right)$$



Resulting pdf for x_0

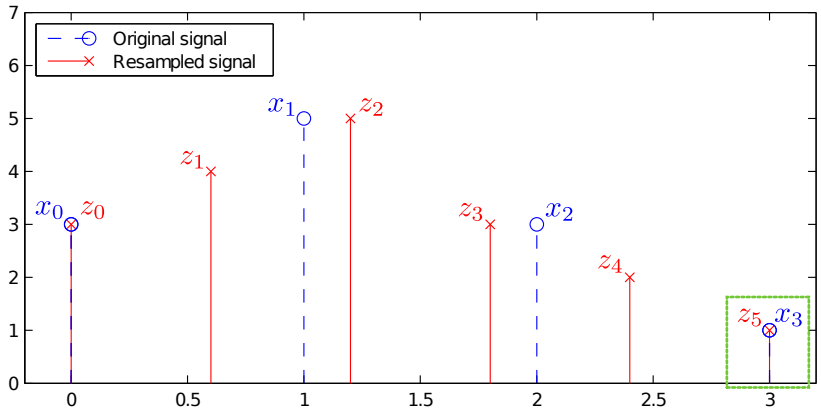


Resulting pdf for x_1

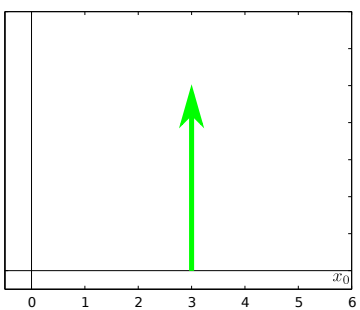


Resulting pdf for x_2

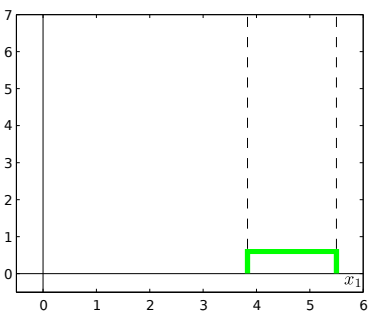
Method Description with an Example ($\xi = 5/3$)



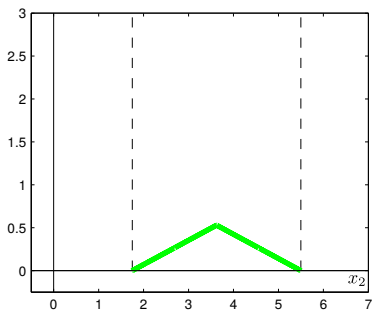
Original and resampled signals



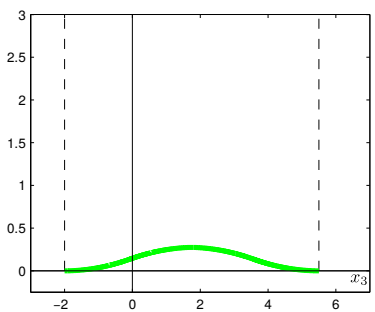
Resulting pdf for x_0



Resulting pdf for x_1



Resulting pdf for x_2

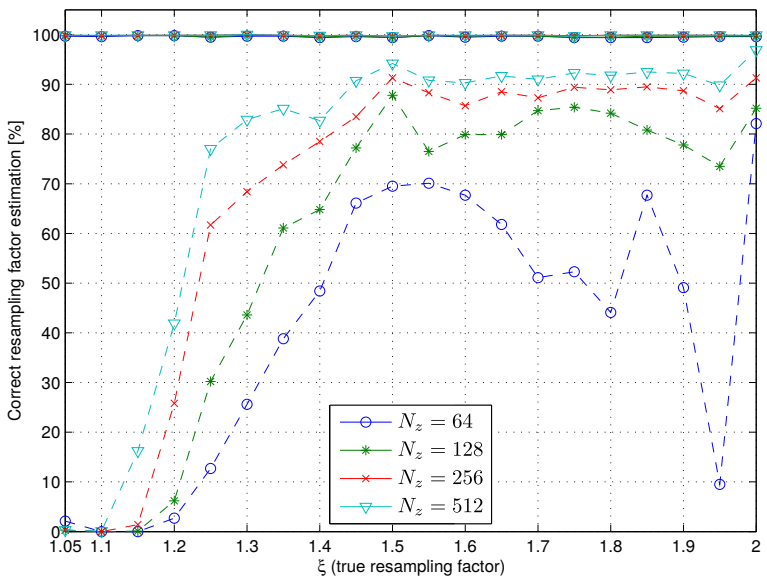


Resulting pdf for x_3

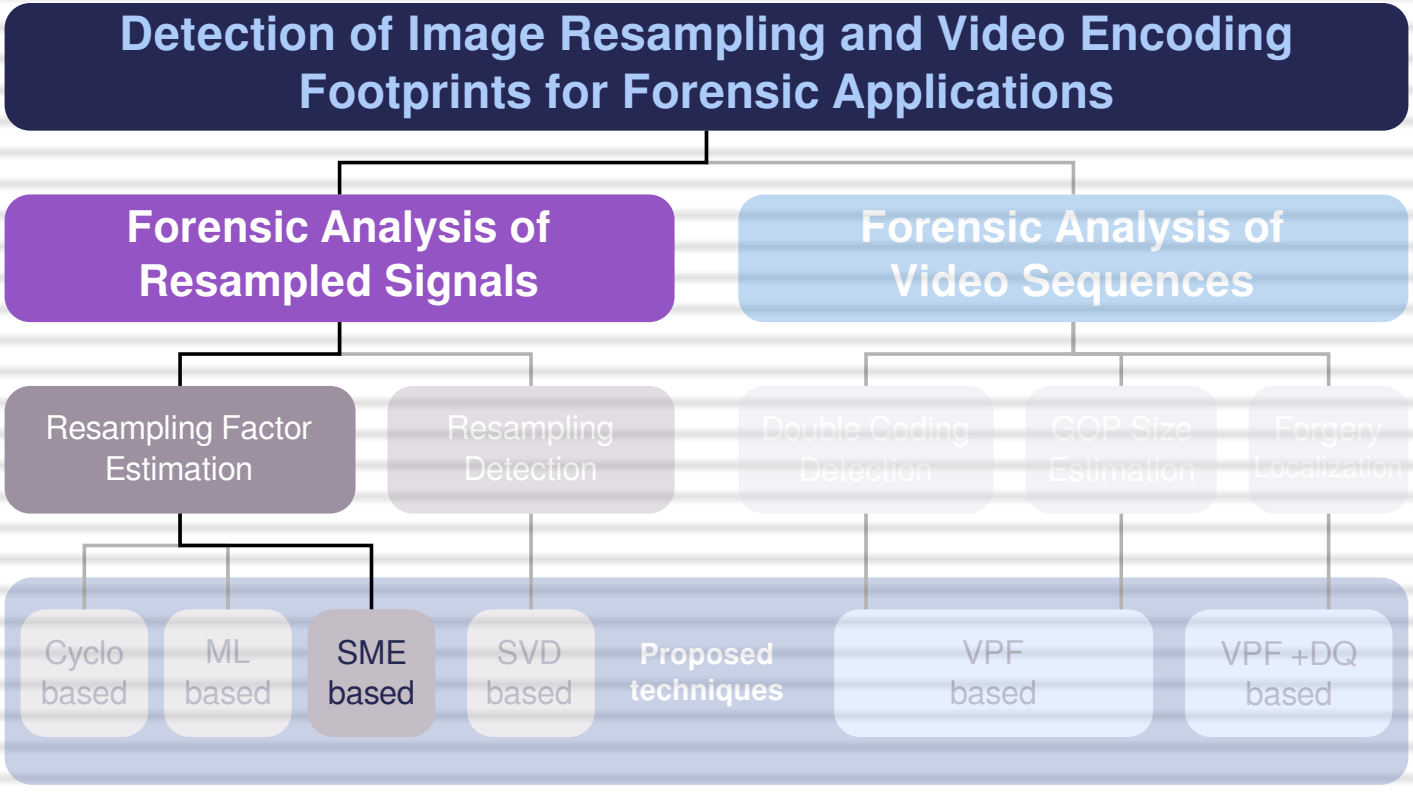
Experimental Validation

Experimental setup:

- "Music Genres" audio database: 1000 uncompressed audio files.
- **Linear filter** for interpolation and $\xi \in \{1.05, 1.1, \ldots, 1.95, 2\}$.
- **Comparison:** Popescu and Farid's method in 1-D (dashed lines).

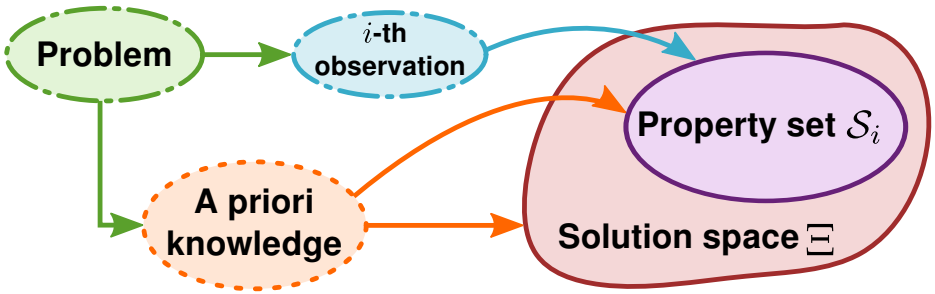


2.3. **Proposed Techniques**: Method based on Set Membership Estimation



Set-Membership Theory

Set-membership theory is governed by the concept of feasibility:



- $\mathcal{S}_i = \{a \in \Xi : a \text{ satisfies } \Psi_i\}$

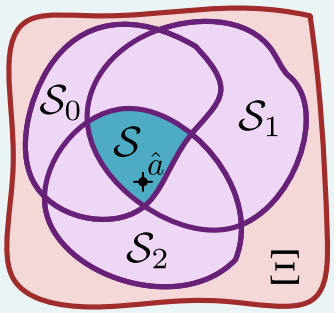
  Ψ_i: i-th problem constraint
- **Feasible set of solutions**:

$$\mathcal{S} = \cap_{i=0}^{N-1} \mathcal{S}_i$$

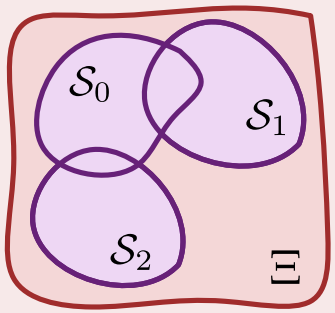
Final goal: find a solution that satisfies all the constraints.

- Given N observations: find $a \in \mathcal{S}$, where $\mathcal{S} = \cap_{i=0}^{N-1} \mathcal{S}_i$.

$a \in \mathcal{S}$ (a feasible solution exists)

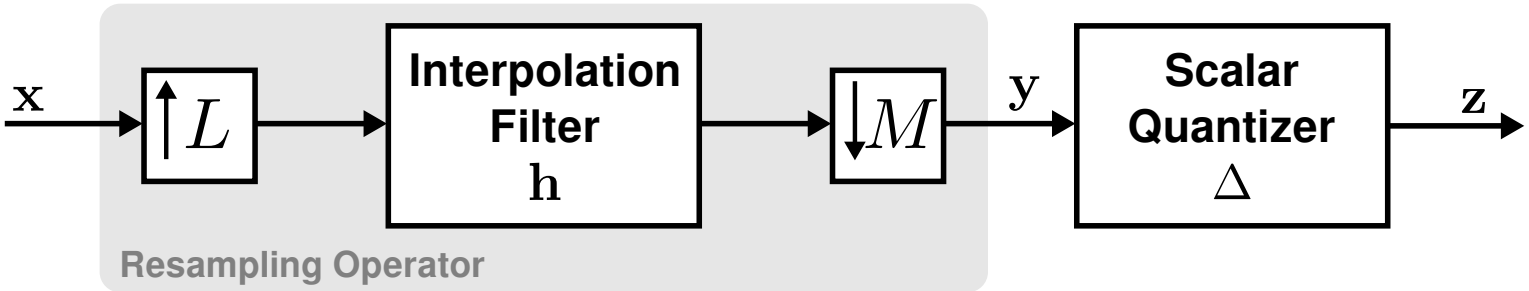


$\mathcal{S} = \emptyset$ (no feasible solution exists)



Set-Membership Formulation

Block diagram representation of the resampling process by $\xi \triangleq \frac{L}{M}$:



A priori knowledge:

- $\mathcal{X} = \{\mathbf{x} \in \mathbb{R}^{N_x} : x_{\min} \leq x_i \leq x_{\max}, i = 0, \ldots, N_x - 1\}$
- $\mathcal{H} = \{\mathbf{h} \in \mathbb{R}^{N_h} : h_{\min} \leq h_i \leq h_{\max}, i = 0, \ldots, N_h - 1\}$
- Solution space: $\Xi = \mathcal{X} \times \mathcal{H}$
- From the quantization: $z_i - \frac{\Delta}{2} < y_i \leq z_i + \frac{\Delta}{2}, \quad \text{for} \quad i = 0, \ldots, N_z - 1$

From each i-th observation:

$$\mathcal{S}_i = \left\{ (\mathbf{x}, \mathbf{h}) \in \Xi : -\frac{\Delta}{2} < \mathbf{x}_i^T \mathbf{h} - z_i \leq \frac{\Delta}{2} \right\}$$

Feasibility Problem

Given:

- a vector of observations $\tilde{\mathbf{z}}$ of length $\tilde{N}_z$
- a candidate resampling factor $\xi \triangleq \frac{L}{M}$
- the length of the interpolation filter N_h

$$
\begin{aligned}
\text{find} \quad & \mathbf{x}, \mathbf{h}, \\
\text{subject to} \quad & \mathbf{x} \in \mathbb{R}^{N_x}, \mathbf{h} \in \mathbb{R}^{N_h}, \\
& x_{\text{min}} \leq x_i \leq x_{\text{max}}, && i = 0, \ldots, N_x - 1, \\
& h_{\text{min}} \leq h_j \leq h_{\text{max}}, && j = 0, \ldots, N_h - 1, \\
& -\tfrac{\Delta}{2} < \mathbf{x}_k^T \mathbf{h} - \tilde{z}_k \leq \tfrac{\Delta}{2}, && k = 0, \ldots, \tilde{N}_z - 1.
\end{aligned}
$$

- **No feasible solution is found**: $\mathbf{z}$ has not been resampled by ξ.
- **A feasible solution is found**: $\mathbf{z}$ might have been resampled by ξ.

Practical Algorithms

Optimal Value Ellipsoid (OVE) algorithm

Cannot be applied! The feasibility problem has bilinear constraints.

Nonlinear programming algorithms

- **Global optimization techniques**: branch-and-bound strategy.
  - Difficulties handling large-scale problems.
- **Local optimization techniques**: interior-point method.
  - A starting point is needed for $\mathbf{x}$ and $\mathbf{h}$.

Derivation of the starting point: $\mathbf{x}^{(0)}$ and $\mathbf{h}^{(0)}$



- $\mathbf{z} = Q_{\Delta}(\mathbf{Xh}) \approx \mathbf{Xh}$

From $\mathbf{x}^{(0)}$, we derive $\mathbf{X}^{(0)}$:

- $\mathbf{h}^{(0)} = \left(\mathbf{X}^{(0)}\right)^{+} \tilde{\mathbf{z}}$

Experimental Setup

1. Synthetic signals: $\mathbf{x}$

- Discrete uniform distribution
- 8-bit precision samples
- $x_{\text{min}} = 0, x_{\text{max}} = 2^8 - 1$
- $\tilde{\xi} \in \{0.6, 0.7, \ldots, 1.9, 2, 2.5, 3\}$

2. Audio signals: $\mathbf{x}$

- 100 files from "Music Genres"
- 16-bit precision samples
- $x_{\text{min}} = 0, x_{\text{max}} = 2^{16} - 1$
- $\tilde{\xi} \in \{1.1, 1.2, \ldots, 1.9, 2\}$

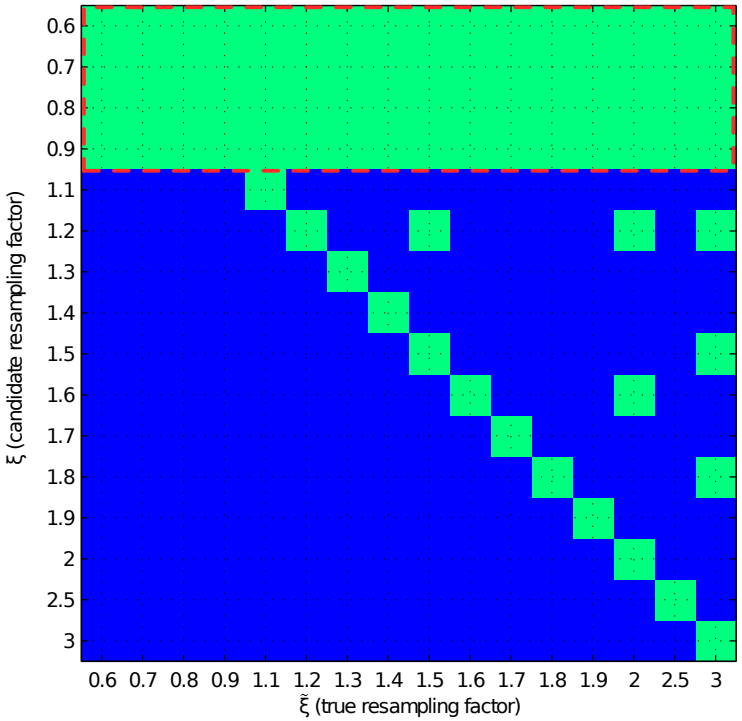
Interpolation filters: $\mathbf{h}$

- $\tilde{\xi} < 1$: **Kaiser** filter, $\tilde{N}_h = 2\tilde{M} + 1$
- $\tilde{\xi} > 1$: **Linear** filter, $\tilde{N}_h = 2\tilde{L} + 1$

Quantization:

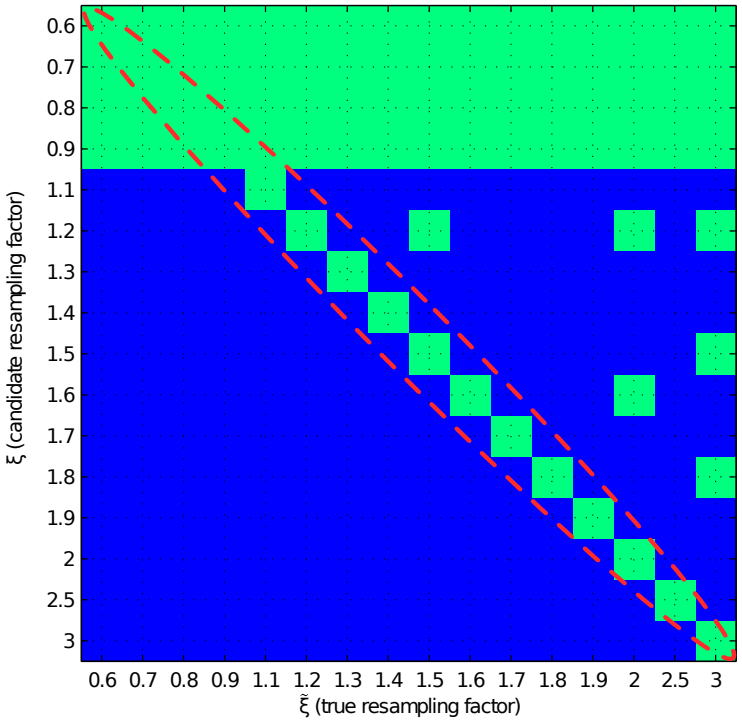
Scalar quantizer with step size $\Delta = 1$

Performance Analysis with Synthetic Signals



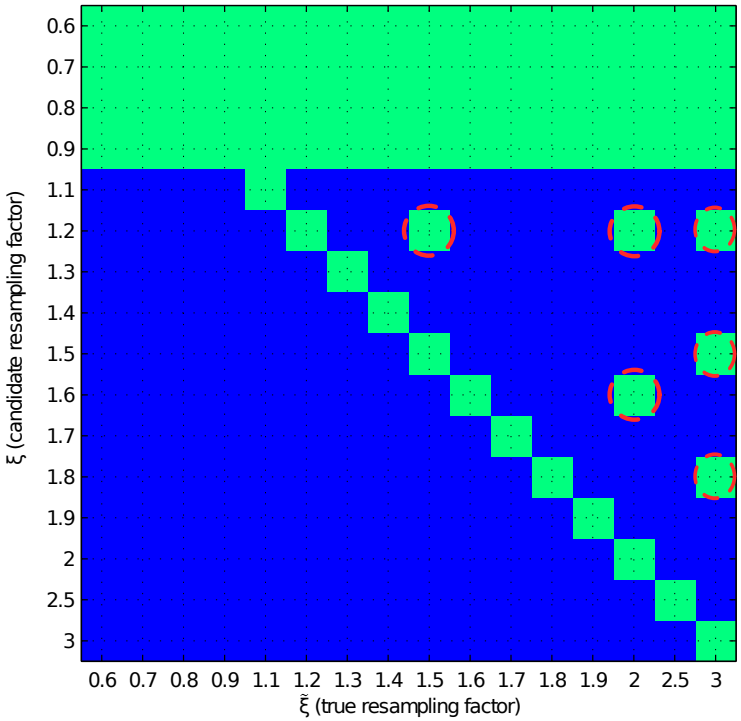
1. For $\xi < 1$, there is always a feasible solution.
   There is not sufficient information (prior or observed).

Performance Analysis with Synthetic Signals



1. For $\xi < 1$, there is always a feasible solution.
   There is not sufficient information (prior or observed).
2. For $\xi = \tilde{\xi}$, a feasible solution is always found.
   Reliable solutions are obtained.

Performance Analysis with Synthetic Signals



1. For $\xi < 1$, there is always a feasible solution.
   There is not sufficient information (prior or observed).
2. For $\xi = \tilde{\xi}$, a feasible solution is always found.
   Reliable solutions are obtained.
3. For $\xi \leq \tilde{\xi}$ $(\tilde{\xi} > 1)$, multiple candidates are feasible.

Set of possible candidates:

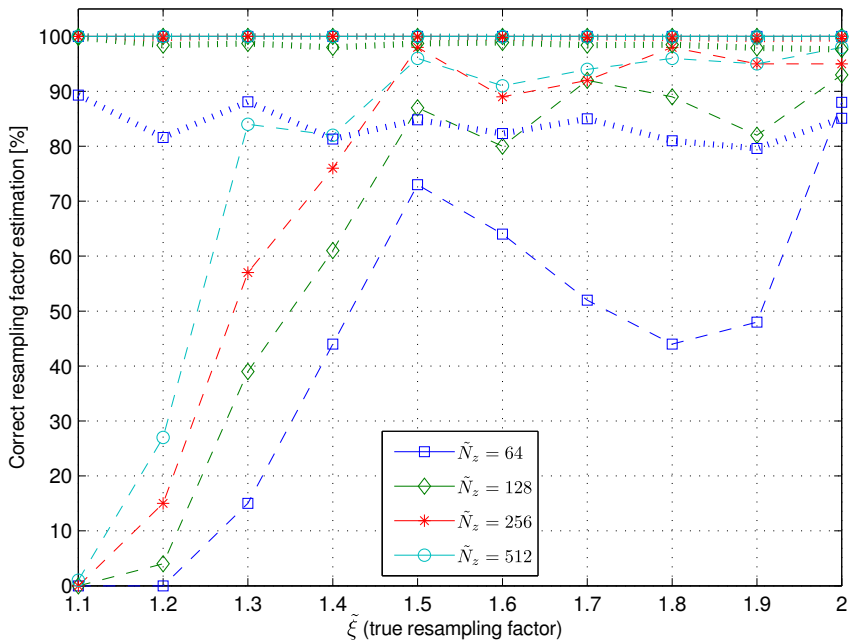
$$\mathcal{C} = \left\{ \frac{L}{M} \ : \ \frac{L}{M} < \tilde{\xi}, (L = k\tilde{L}) \wedge (M > k\tilde{M}), k \in \mathbb{N}^+ \right\}$$

where $L \in \mathbb{N}^+$ and $M \in \mathbb{N}^+$ are coprime.

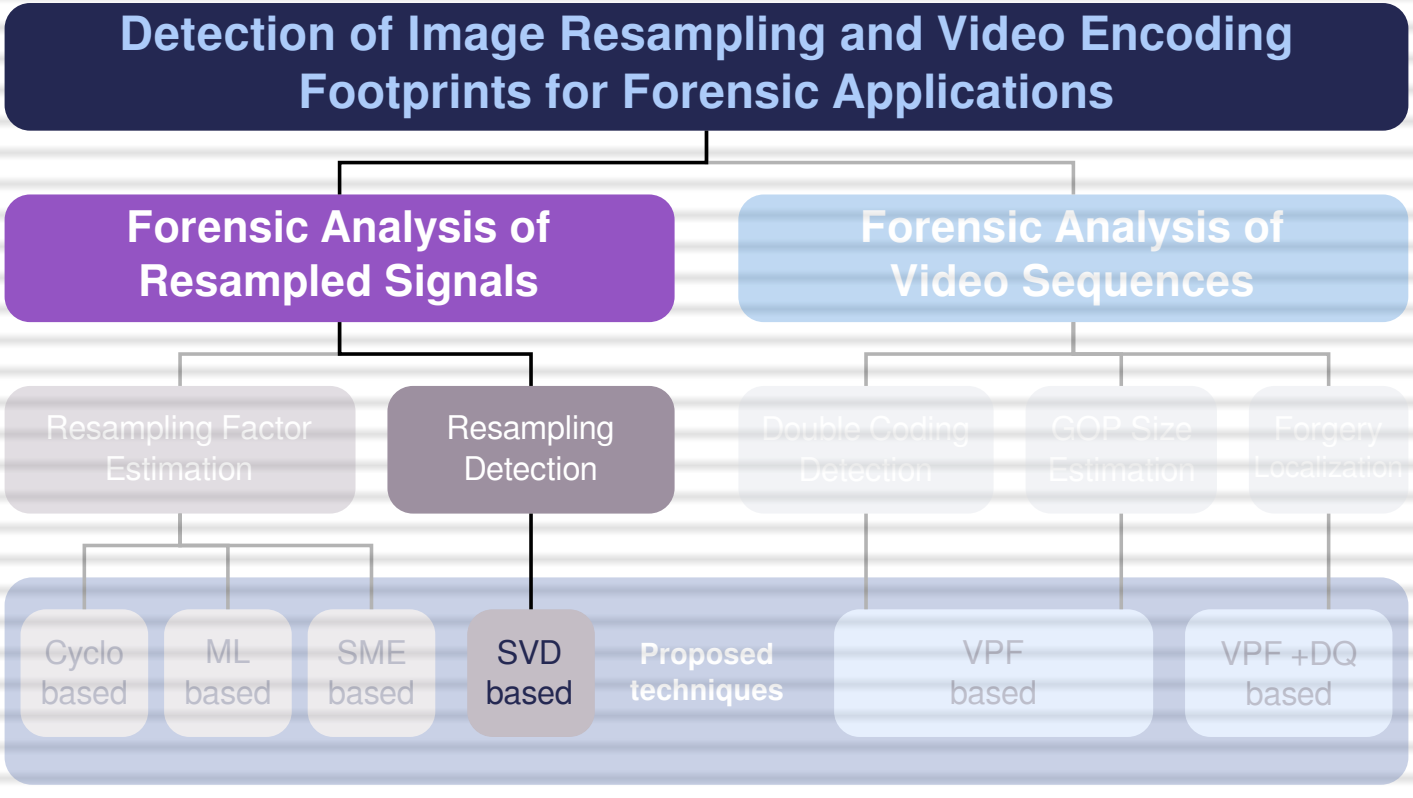
Performance Analysis with Real Audio Signals

Comparative results

- **Popescu & Farid (2005)**: frequency-based analysis (dashed lines).
- **ML-based**: quantization analysis (solid lines).
- **This work**: set-membership approach (dotted lines).

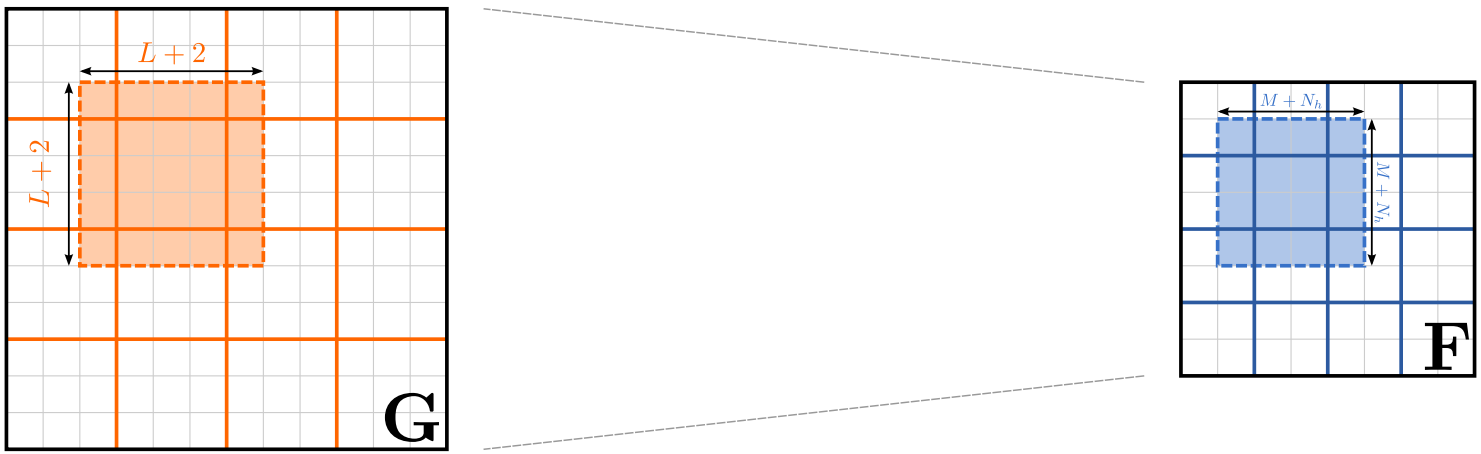


2.3. **Proposed Techniques**: Method based on SVD



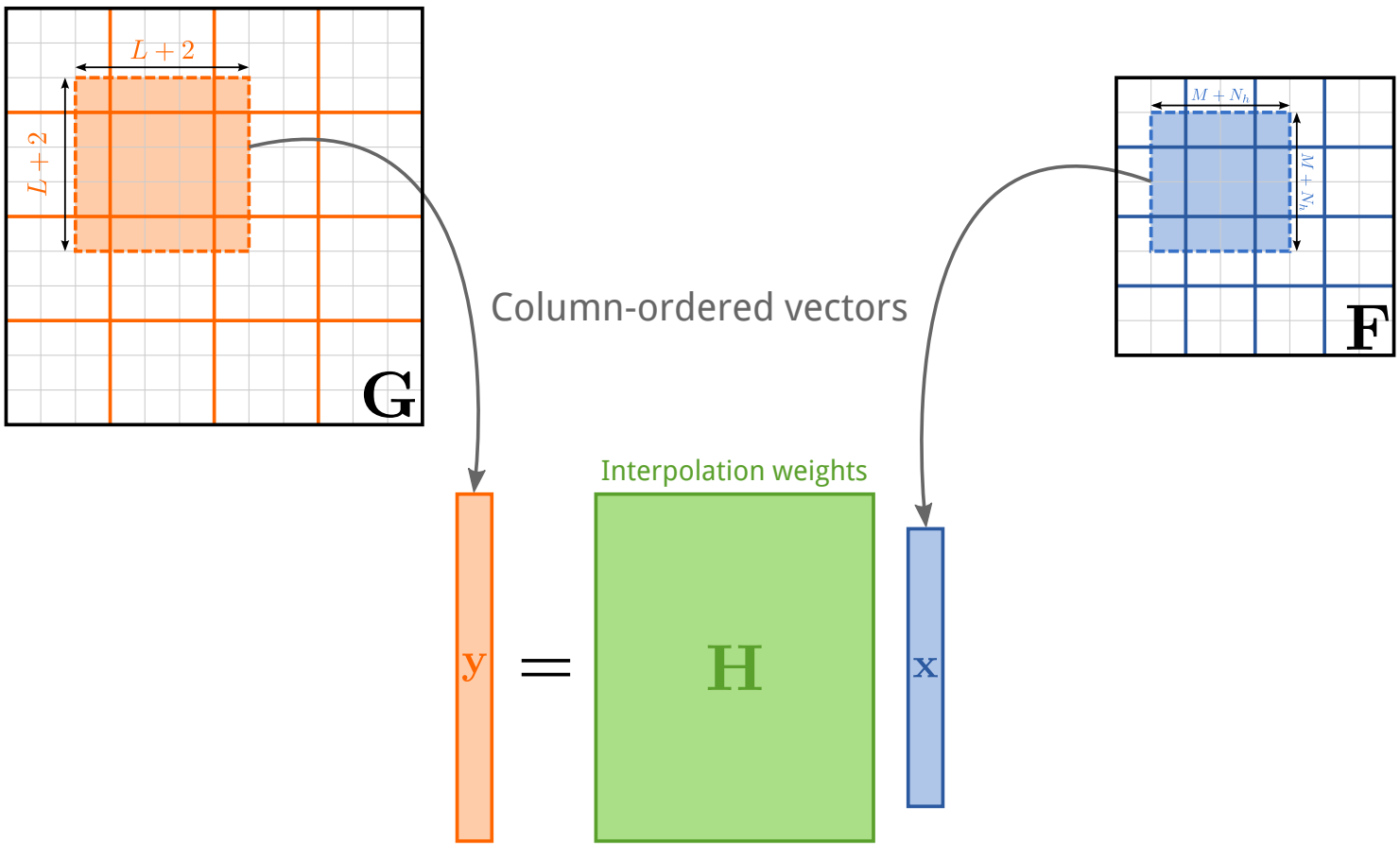
Analysis of Image Resampling

1. **Periodic linear relation:** each block is always computed in the same way.



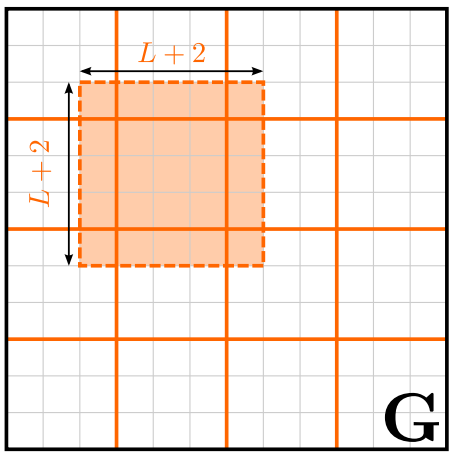
Analysis of Image Resampling

1. **Periodic linear relation:** the following linear transformation arises.



Analysis of Image Resampling

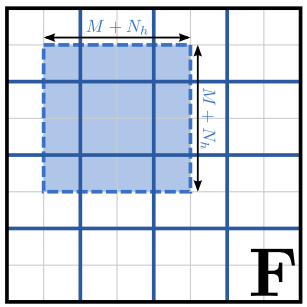
1. Periodic linear relation:



$$\mathbf{y} \in \mathbb{R}^{(L+2)^2}$$

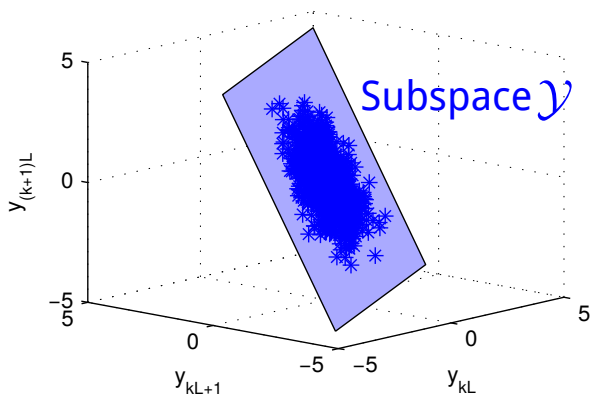
$$\mathbf{H} \in \mathbb{R}^{(L+2)^2 \times (M+N_h)^2}$$

$$\mathbf{x} \in \mathbb{R}^{(M+N_h)^2}$$



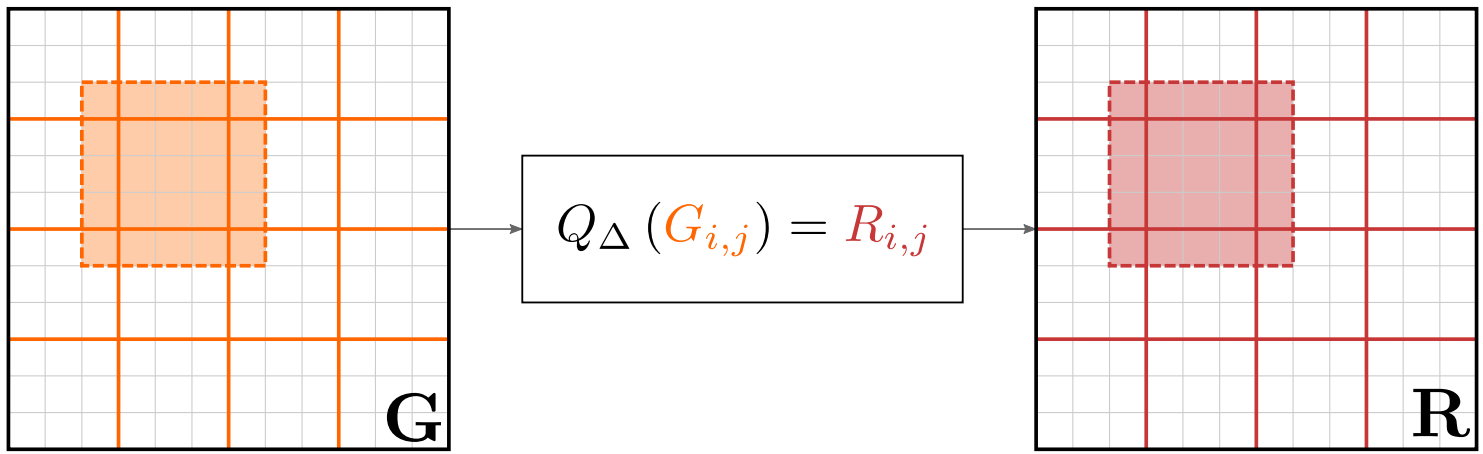
Example (1-D): $L/M = 2, x_i \sim \mathcal{N}(0,1)$

$$\begin{bmatrix} y_{2k} \\ y_{2k+1} \\ y_{2k+2} \end{bmatrix} = \begin{bmatrix} 1 & 0 \\ 0.5 & 0.5 \\ 0 & 1 \end{bmatrix} \begin{bmatrix} x_k \\ x_{k+1} \end{bmatrix}$$



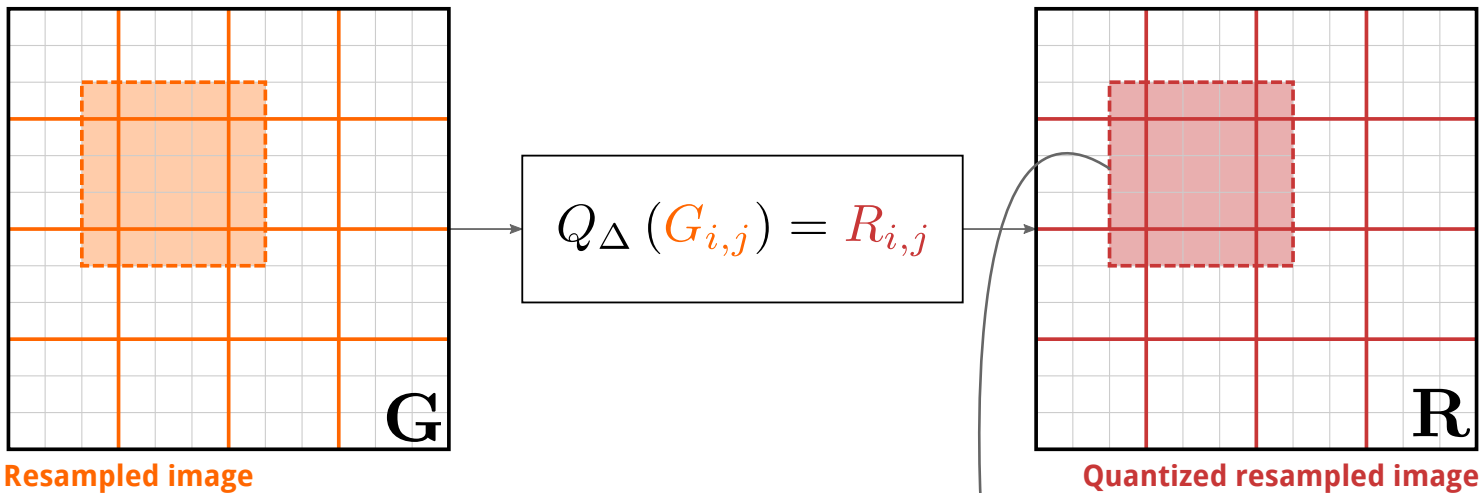
Analysis of Image Resampling (II)

2. Quantization:

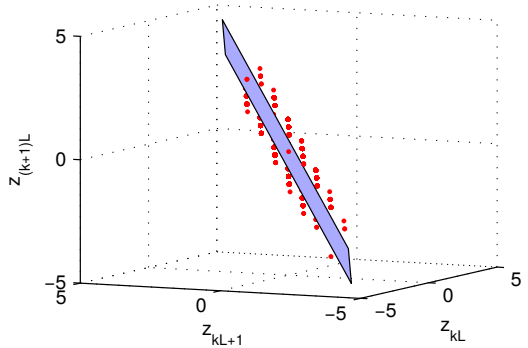


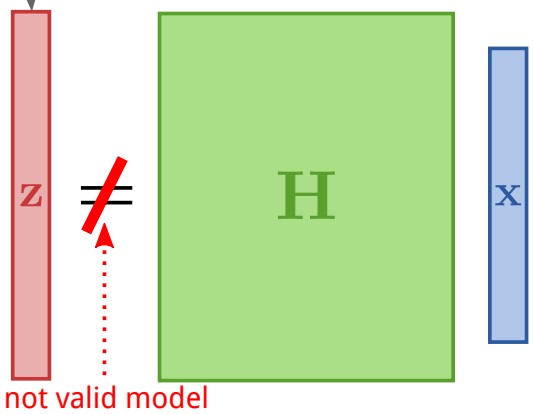
Analysis of Image Resampling (II)

2. Quantization: previous linear model is no longer valid.



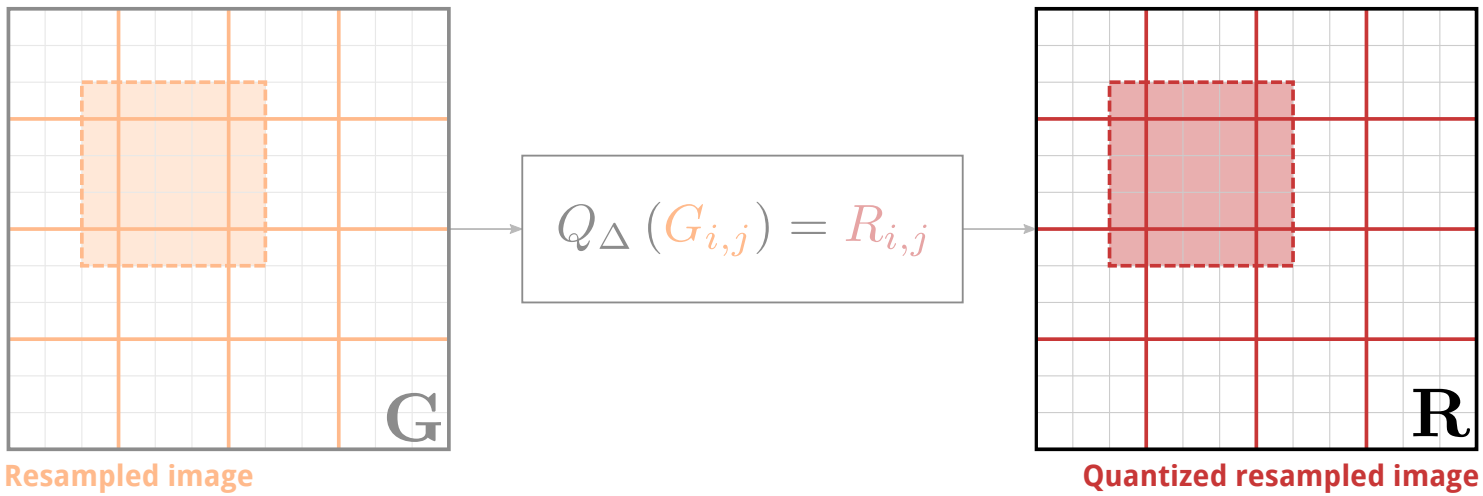
Example (1-D): $L/M = 2, x_i \sim \mathcal{N}(0,1)$





Analysis of Image Resampling (II)

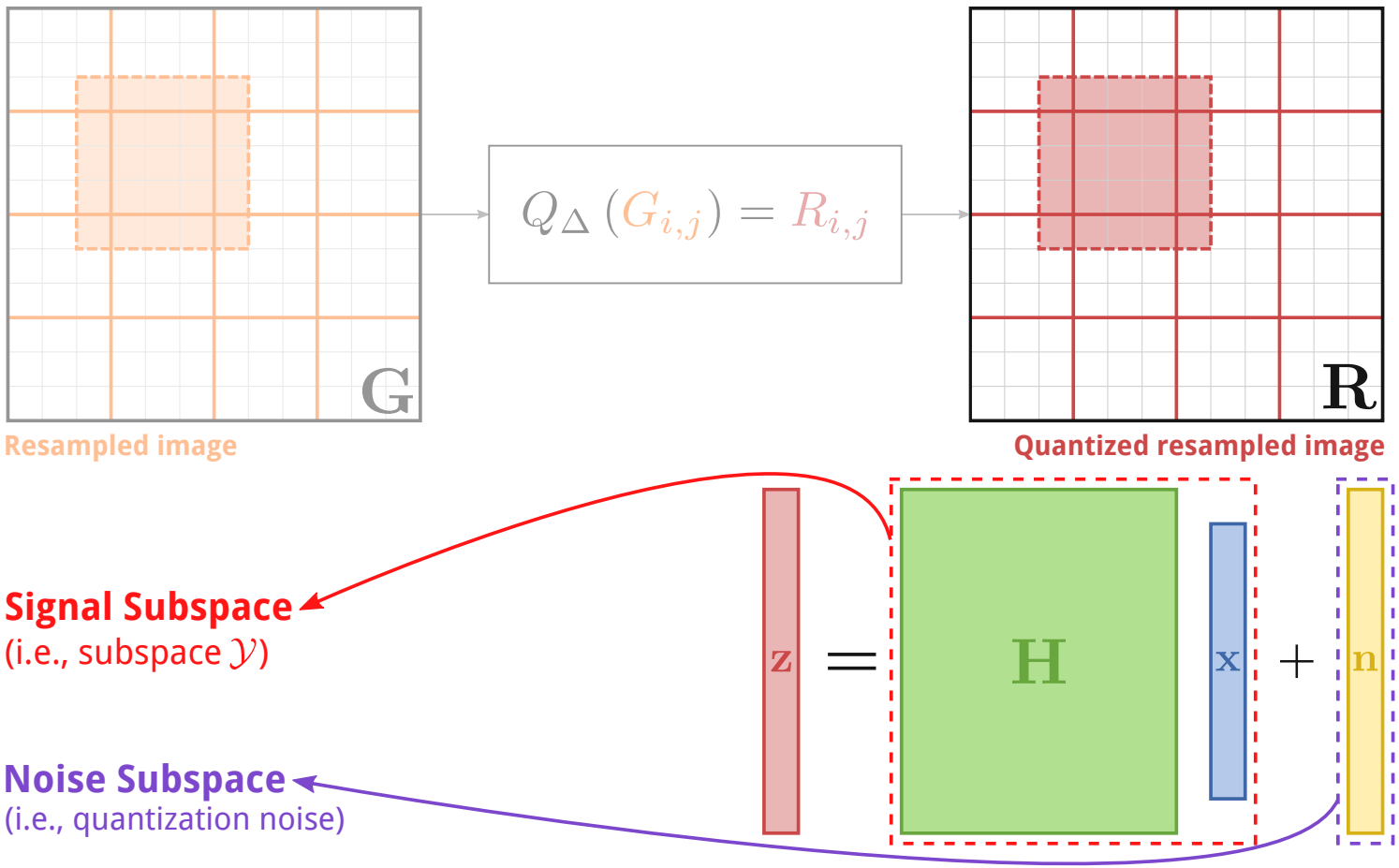
2. **Quantization:** a noise component is added to the model.



$$\mathbf{z} = \mathbf{H}\,\mathbf{x} + \mathbf{n}$$

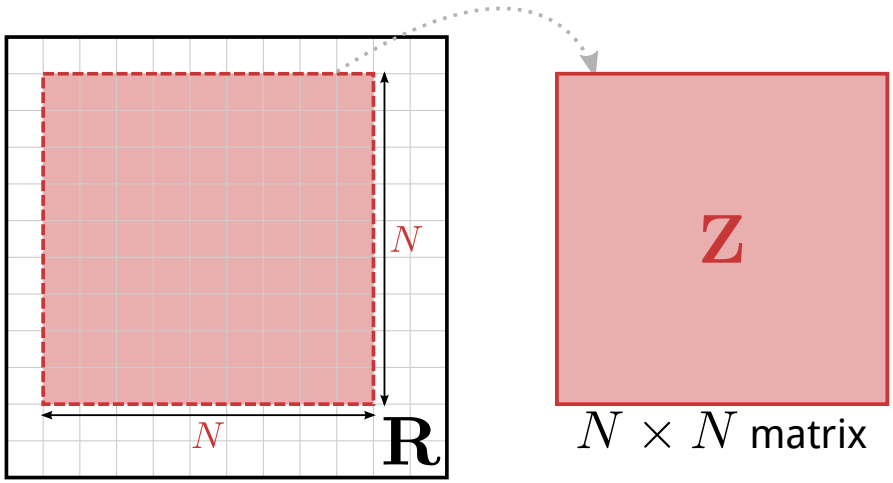
Analysis of Image Resampling (II)

2. **Quantization:** upsampled images belong to this sum of subspaces.



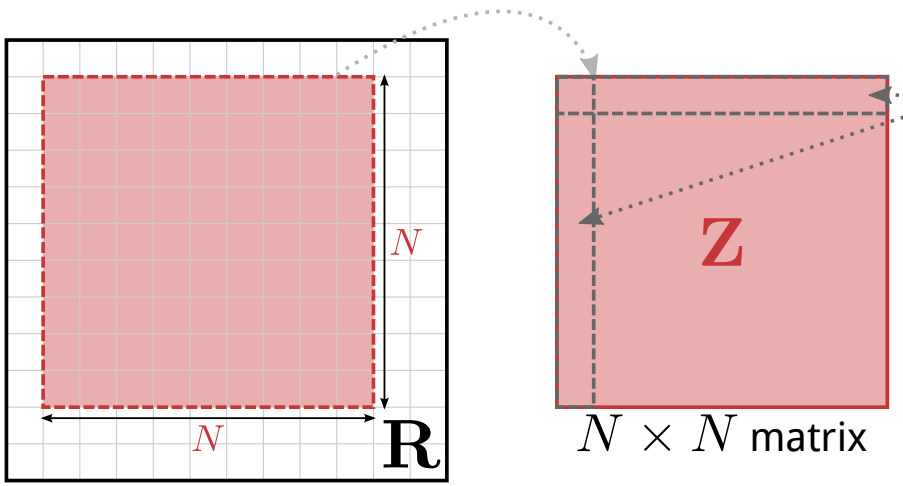
Practical Solution: subspace decomposition

Analysis of a block of $N \times N$ samples:



Practical Solution: subspace decomposition

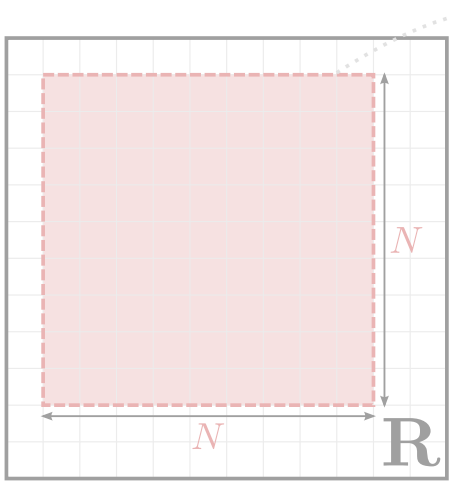
Analysis of a block of $N \times N$ samples:

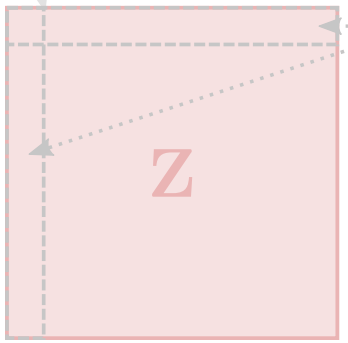


- Each **row/column** belongs to an N-dimensional space.
- **But, upsampling** by ξ induces **linear** dependencies.
- **Thus,** the set of N **points** can be represented by a **smaller** number of **dimensions** $k \approx \frac{N}{\xi}$.

Practical Solution: subspace decomposition

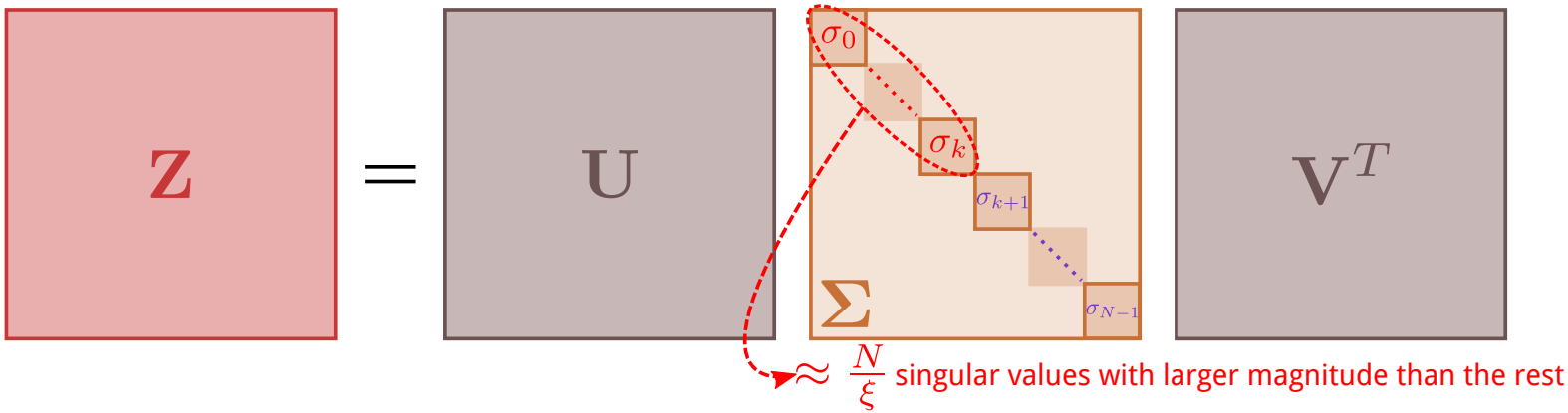
Singular Value Decomposition of matrix Z:





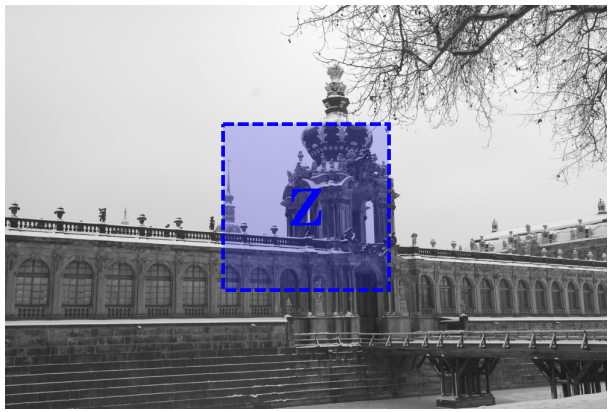
$N \times N$ matrix

- Each **row/column** belongs to an N-dimensional space.
- **But, upsampling** by ξ induces **linear** dependencies.
- **Thus,** the set of N **points** can be represented by a **smaller** number of **dimensions** $k \approx \frac{N}{\xi}$.

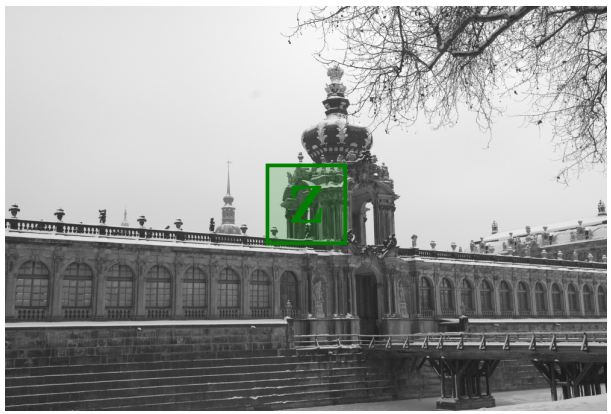


Practical Solution: subspace decomposition

Example: non-resampled vs. resampled images (center 512×512 block).

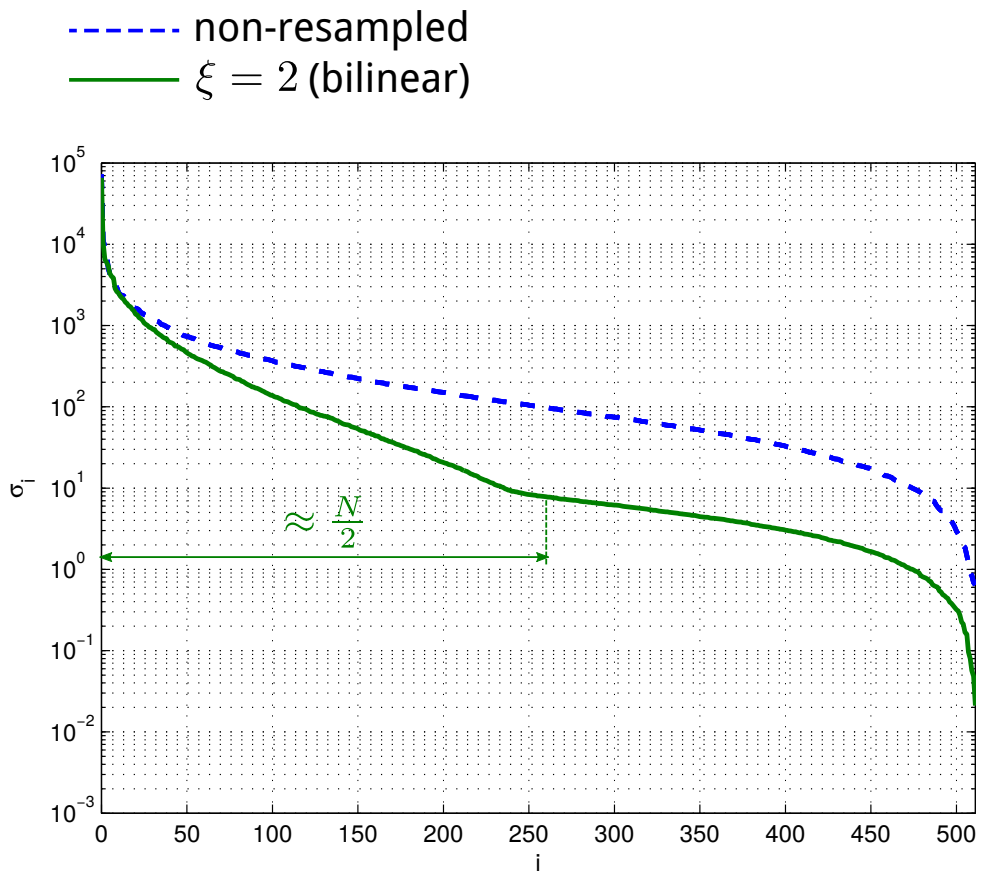


Non-resampled image



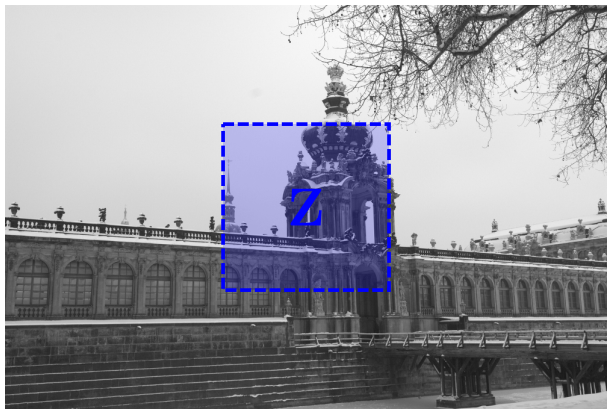
Quantized resampled image

Evolution of the singular values of Z:

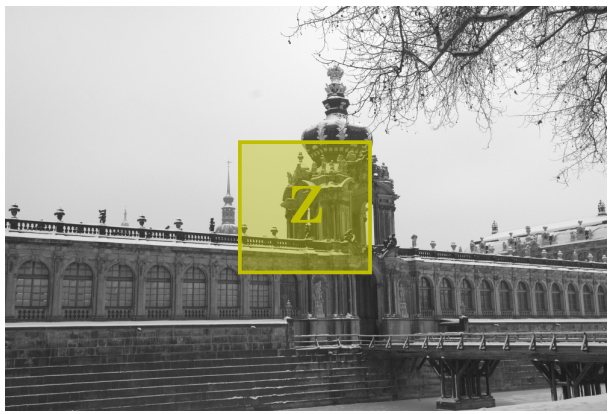


Practical Solution: subspace decomposition

Example: non-resampled vs. resampled images (center 512×512 block).

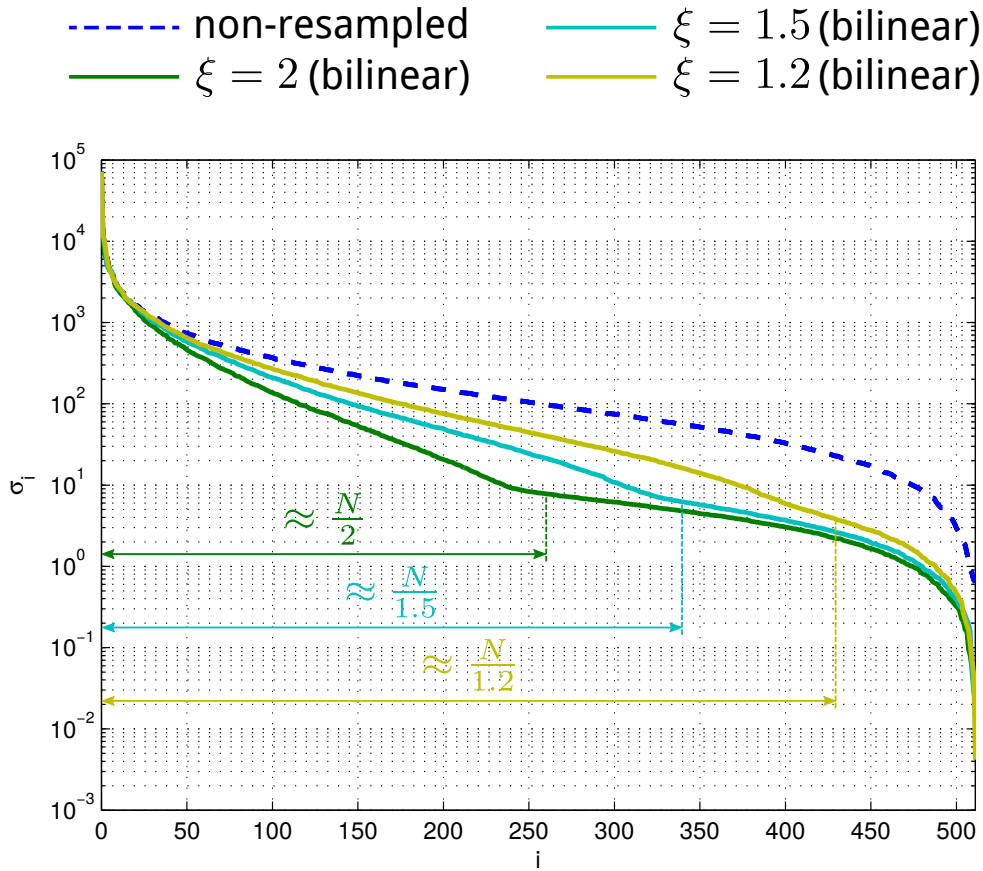


Non-resampled image



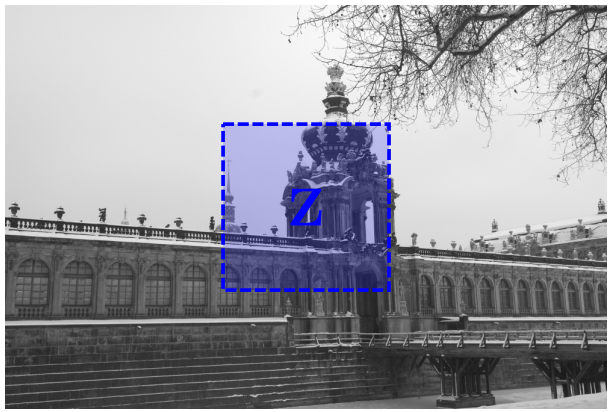
Quantized resampled image

Evolution of the singular values of Z:

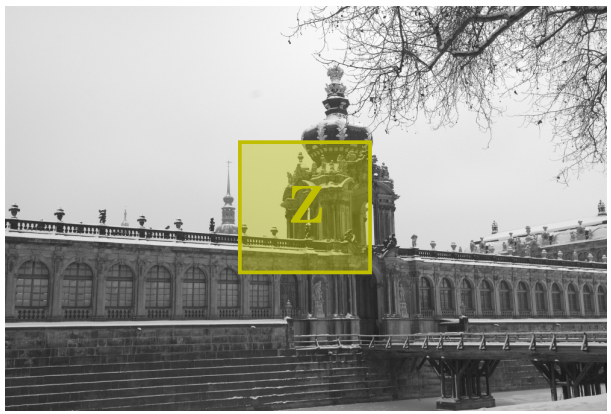


Practical Solution: subspace decomposition

Example: non-resampled vs. resampled images (center 512×512 block).

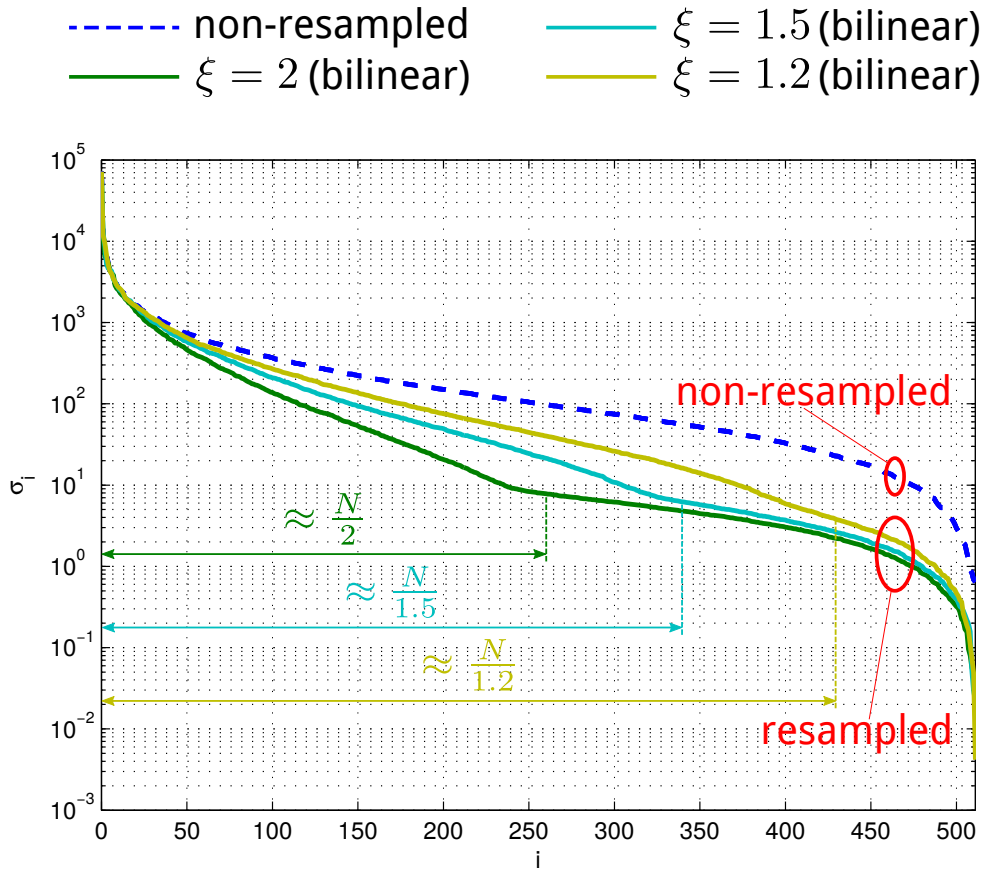


Non-resampled image



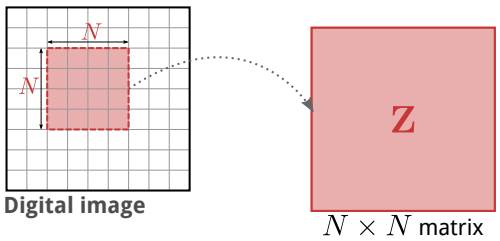
Quantized resampled image

Evolution of the singular values of Z:



Proposed Detector for $\xi > 1$

Observed Data:



Hypothesis Test

- $\mathcal{H}_0$: $\mathbf{Z}$ has never been resampled.
- $\mathcal{H}_1$: $\mathbf{Z}$ has been resampled by any $\xi > 1$.

Test statistic: ρ

Will measure the magnitude of singular values at a certain index.

Degree of Saturation: s

- $\gamma_{\text{row}} \triangleq \frac{\#\text{ saturated pixels in } \mathbf{Z}}{\#\text{ rows}}$
- $s \triangleq \frac{1}{N} \max\{\gamma_{\text{row}}, \gamma_{\text{column}}\}$



$s = 0.8389$



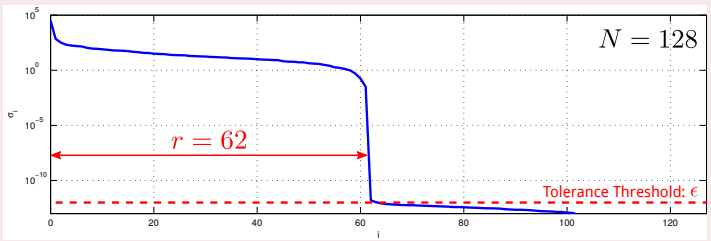
$s = 0.5272$



$s = 0.0344$

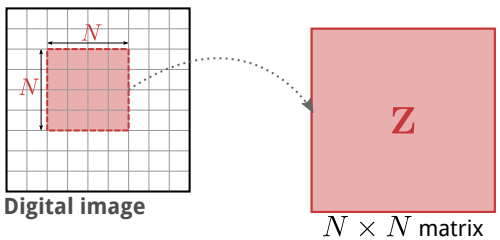
Non-zero Singular Values: r

- $r \triangleq \#\left(\sigma_{\forall i} > N\epsilon(\sigma_0)\right)$



Proposed Detector for $\xi > 1$

Observed Data:



Hypothesis Test

- $\mathcal{H}_0$: $\mathbf{Z}$ has never been resampled.
- $\mathcal{H}_1$: $\mathbf{Z}$ has been resampled by any $\xi > 1$.

Test statistic: ρ

$$\rho \triangleq \begin{cases} 0, & \text{if } r < 0.1N, \\ \log\left(\sigma_{\nu - \lfloor 0.05N \rfloor - 1}\right), & \text{if } s \geq 0.45 \text{ and } r > 0.95N, \\ \log\left(\sigma_{\nu-2}\right), & \text{otherwise.} \end{cases}$$

Selected index: ν

- Maximum number of significant dimensions achieved by any $\xi \geq \xi_{\min} \rightarrow \nu = \text{round}\left(\frac{r}{\xi_{\min}}\right)$.

Decision

$$\begin{aligned} \mathcal{H}_0 &: \quad \rho > T, \\ \mathcal{H}_1 &: \quad \rho \leq T. \end{aligned}$$

Experimental Setup

Image Dataset

- 1317 images from the **Dresden Image Database** (Nikon cameras).

Full-frame resampling through `convert` from ImageMagick

- **Interpolation kernels:** *Bilinear*, *Catmull-Rom*, *B-spline*, *Lanczos*.
- **Set of resampling factors:** $\xi \in \{1.05, 1.1, \ldots, 1.95, 2\}$, $(\xi_{\min} = 1.05)$.

Experimental Setup

Image Dataset

- 1317 images from the **Dresden Image Database** (Nikon cameras).

Full-frame resampling through `convert` from ImageMagick

- **Interpolation kernels:** *Bilinear*, *Catmull-Rom*, *B-spline*, *Lanczos*.
- **Set of resampling factors:** $\xi \in \{1.05, 1.1, \ldots, 1.95, 2\}$, $(\xi_{\min} = 1.05)$.

Benchmark detector

- **Kirchner's detector:** based on row/column predictors $(K = 3)$.

Resampling Analysis

- **Blocks of small size:** center 32×32 block of the green channel.

Experimental Setup

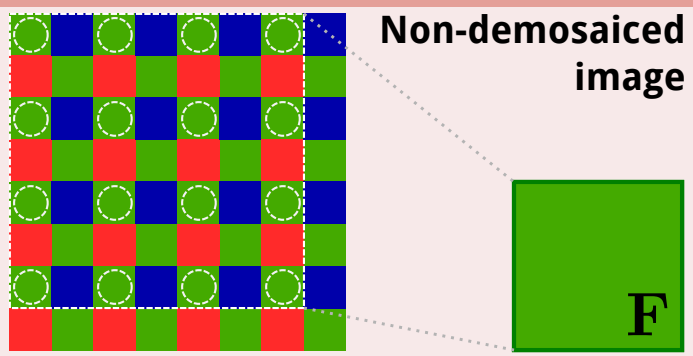
Image Dataset

- 1317 images from the **Dresden Image Database** (Nikon cameras).

Full-frame resampling through `convert` from ImageMagick

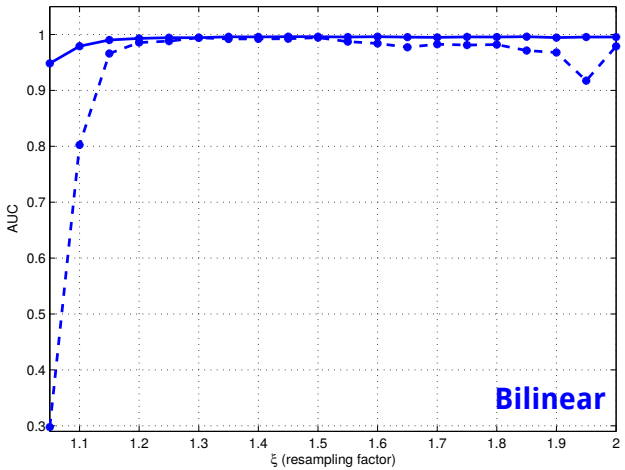
- **Interpolation kernels:** *Bilinear*, *Catmull-Rom*, *B-spline*, *Lanczos*.
- **Set of resampling factors:** $\xi \in \{1.05, 1.1, \ldots, 1.95, 2\}$, $(\xi_{\min} = 1.05)$.

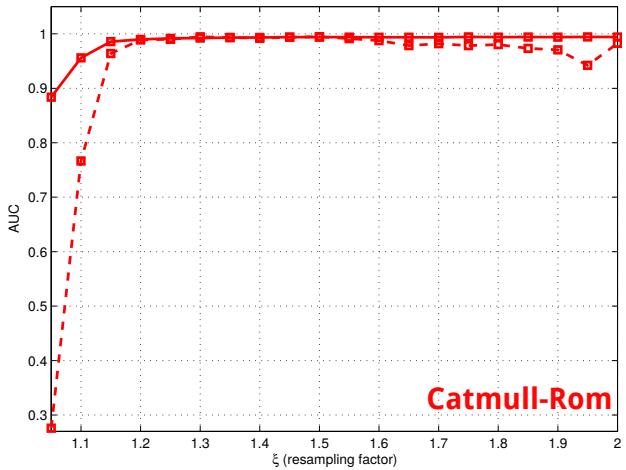
Without demosaicing traces:

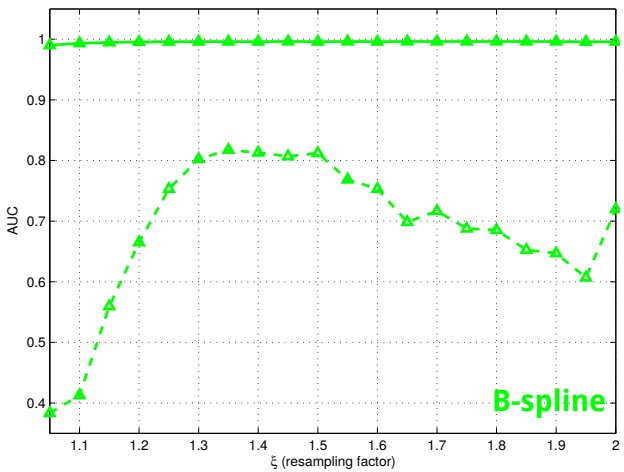


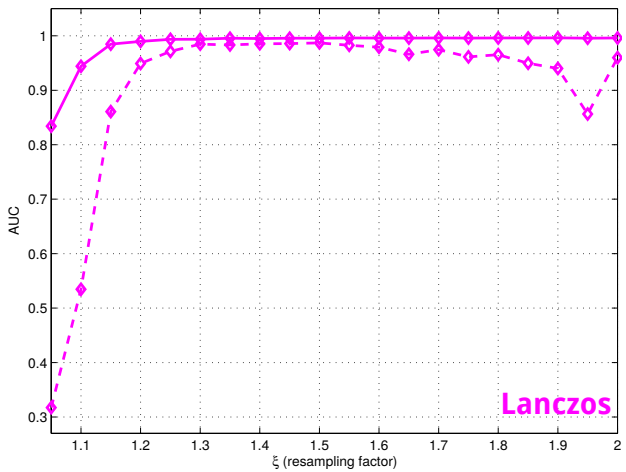
Experimental Results: without demosaicing

Area under the ROC curve (AUC):









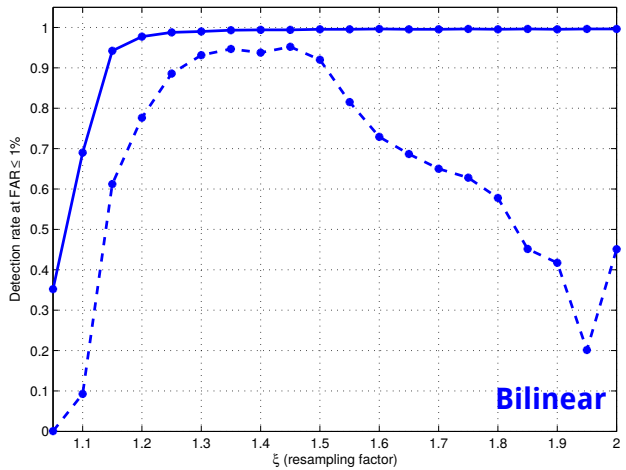
Detectors:

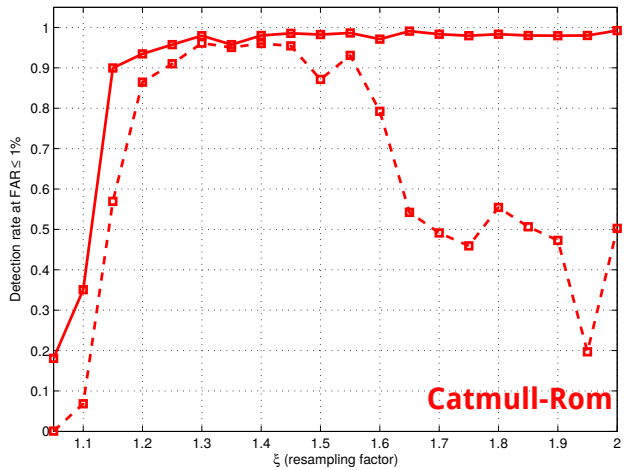
—— SVD-based

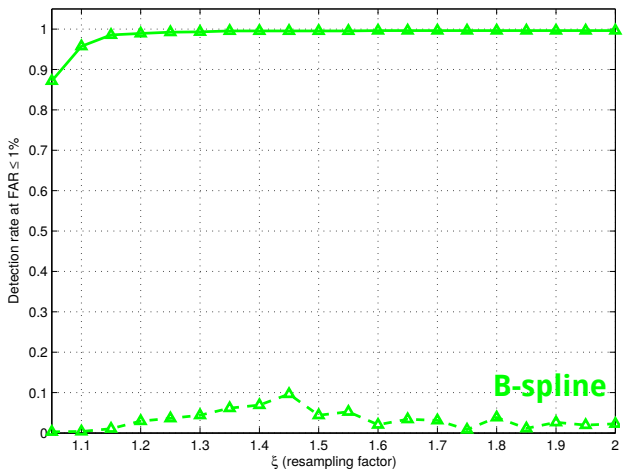
- - - - Kirchner

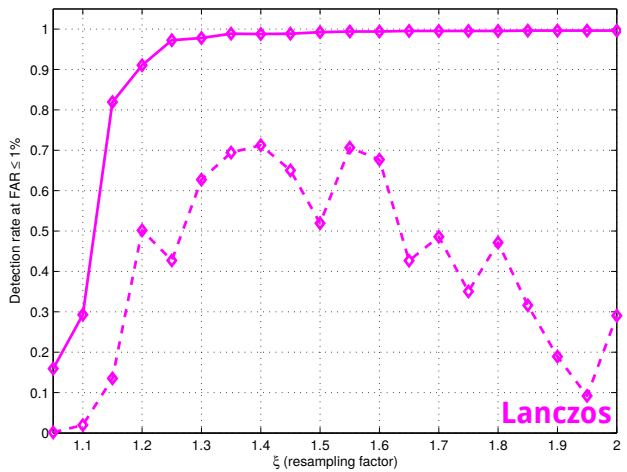
Experimental Results: without demosaicing

Detection rate at 1% False Alarm Rate:







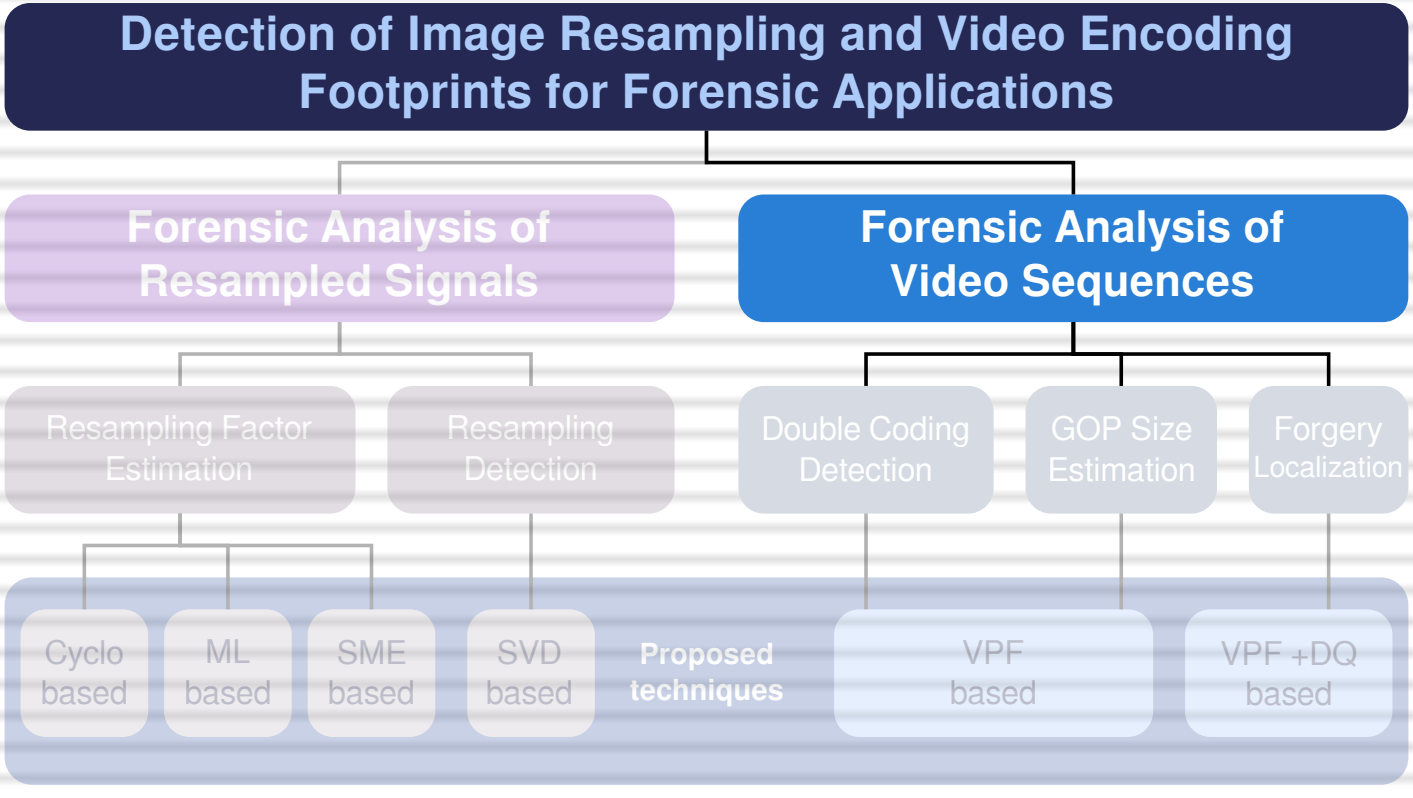


Detectors:

—— SVD-based

- - - - Kirchner

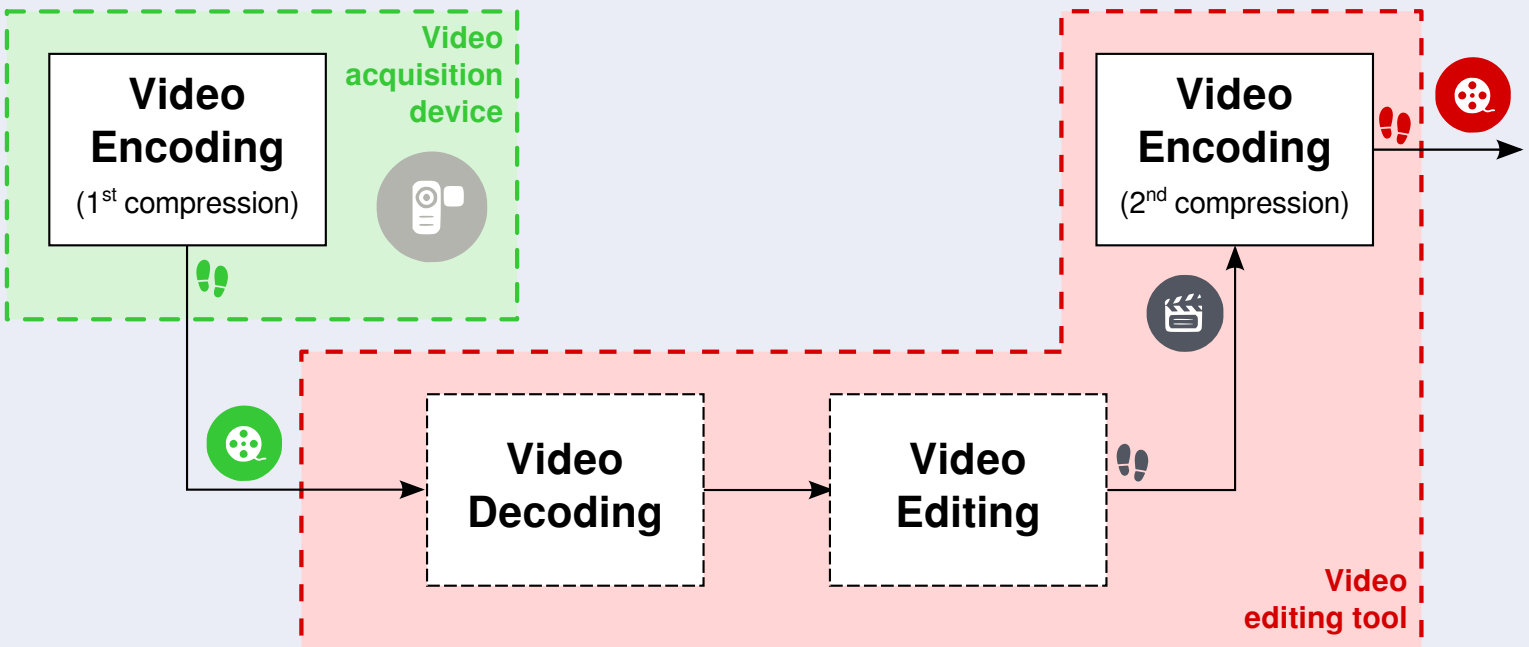
3. Forensic Analysis of Video Sequences



Problem Description

Generally, existing video editing tools do not work directly on the compressed domain, but in the reconstructed spatio-temporal domain.

Typical processing chain for video manipulation:



Passive Video Forensics

First approaches:

- **Double encoding detection:** analysis of double quantization.
- **Adaptation** of **working methods** on **images** to **video**.
  - Useful for MJPEG or specific scenarios (GOP=1).

Current approaches:

- Take advantage of **temporal information**: prediction error
  - Applicable to different video encoders and more complex scenarios.
- **Forgery localization:** inter-frame and intra-frame

Final Goal:

Identify all the operations applied to a video sequence.

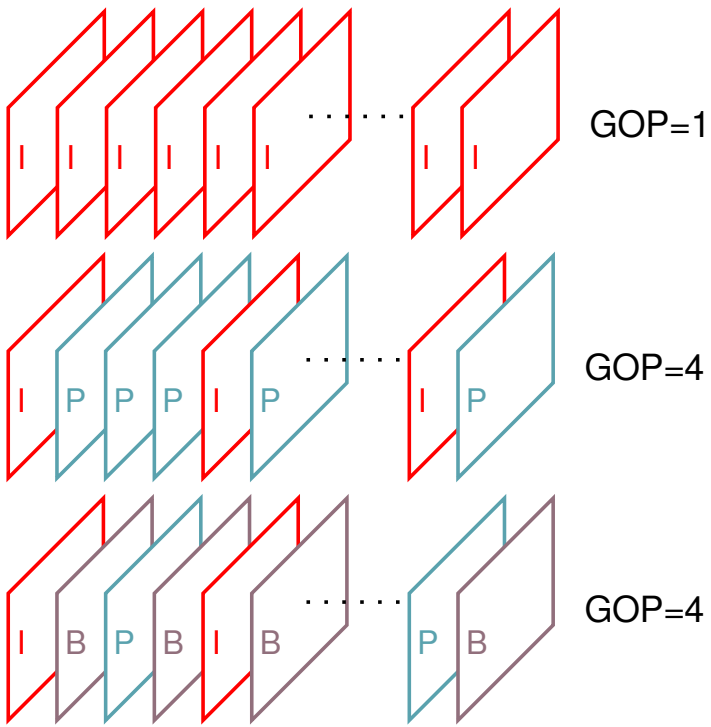
Basics on Video Coding: GOP and MBs

Group of Pictures (GOP):

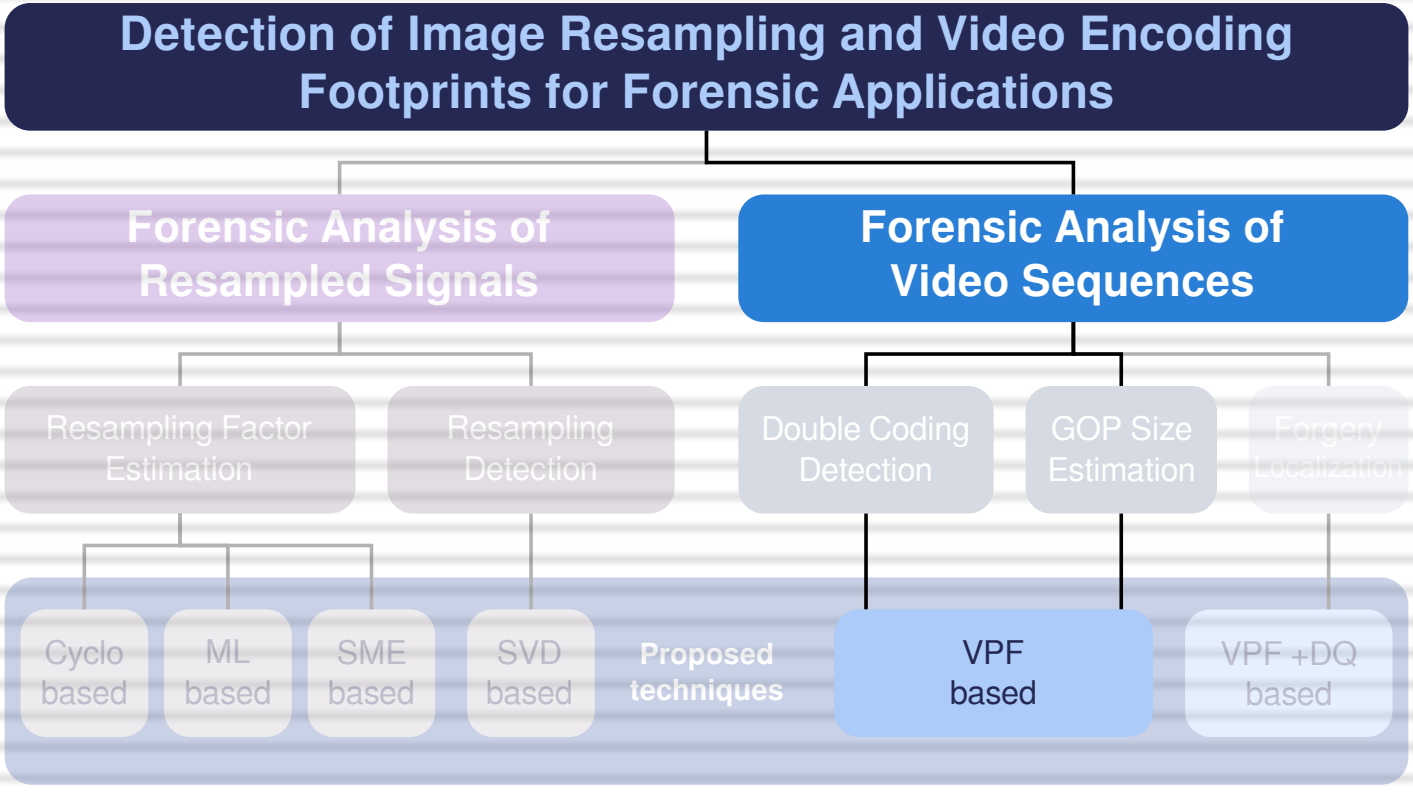
A GOP is an encoding of a sequence of frames that contains all the information that can be completely decoded within that group of pictures.

Available macroblock types:

- **I-frame:**
  - I-MB
- **P-frame:**
  - I-MB
  - P-MB
  - S-MB (SKIP)
- **B-frame:**
  - Same as P-frames
  - B-MB



3.3. **Proposed Techniques**: Method based on the VPF



Scenario Under Analysis

Basic video processing chain:

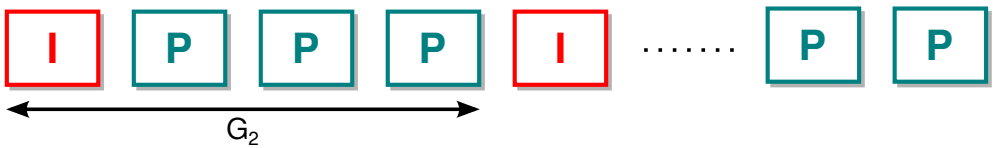


Output of the 1st encoder:



- **GOP size value:** G_1
- **CBR value:** B_1
- **Encoder:** MPEG-2, MPEG-4, H.264

Output of the 2nd encoder:



- **GOP size value:** G_2
- **CBR value:** B_2
- **Encoder:** MPEG-2, MPEG-4, H.264

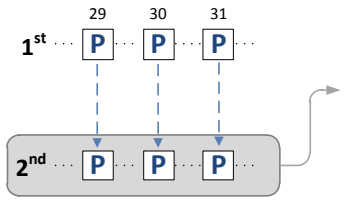
Assumptions:

- **GOP:** constant size with only I- and P-frames.
- $G_1 \neq mG_2$ for any $m \in \mathbb{N}$, and $G_1, G_2 \neq 1$.

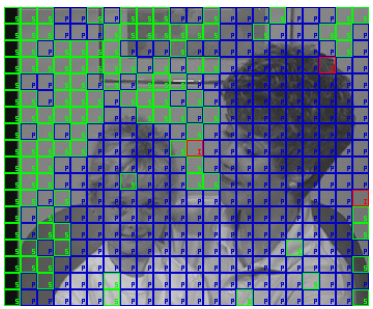
Variation of Prediction Footprint (VPF)

A specific variation of the number of macroblocks coded as I-MB and S-MB shows up in the P-frames previously encoded as I-frames.

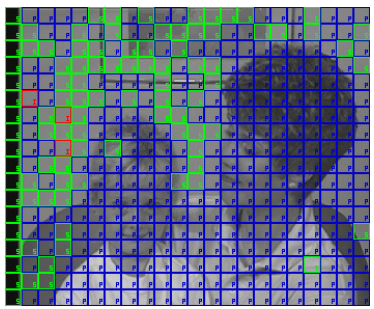
Illustrative example with macroblock types: I-MB P-MB S-MB



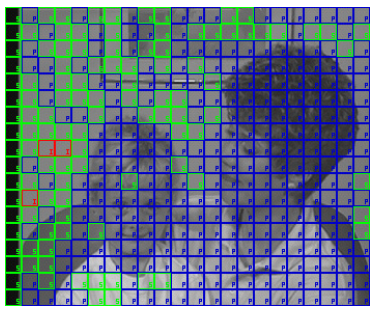
$G_1 = 45,\ G_2 = 50$



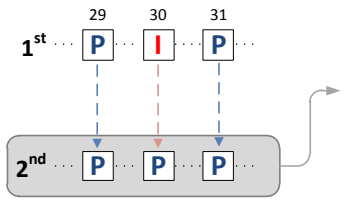
Frame 29



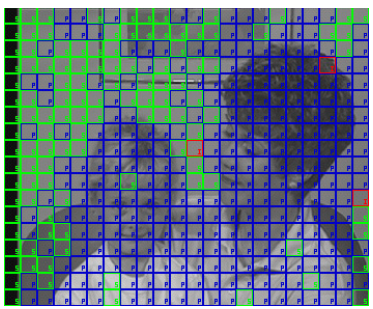
Frame 30



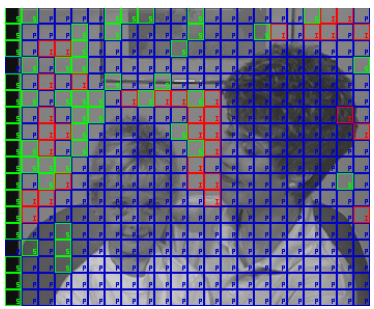
Frame 31



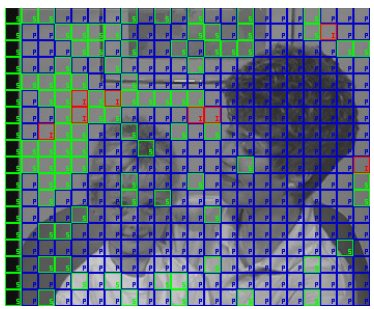
$G_1 = 30,\ G_2 = 50$



Frame 29



Frame 30

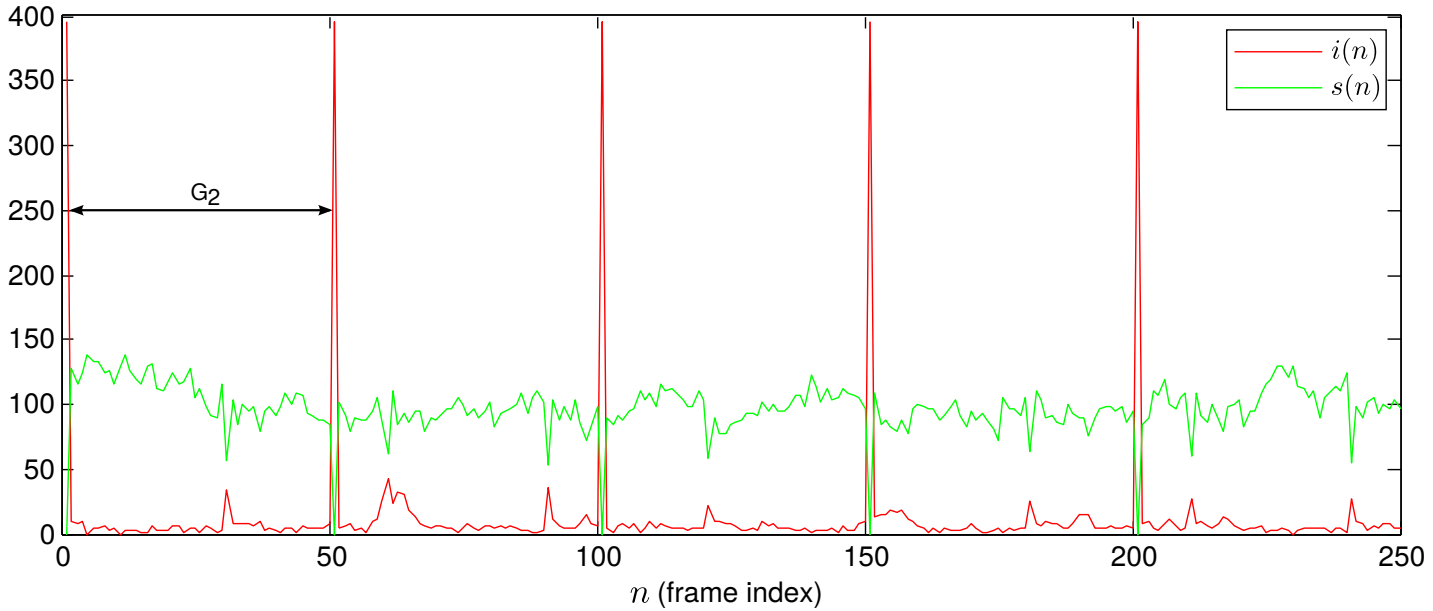


Frame 31

VPF Localization & Measurement

From the previous example:

- $i(n) \rightarrow$ number of I-MB at nth frame
- $s(n) \rightarrow$ number of S-MB at nth frame

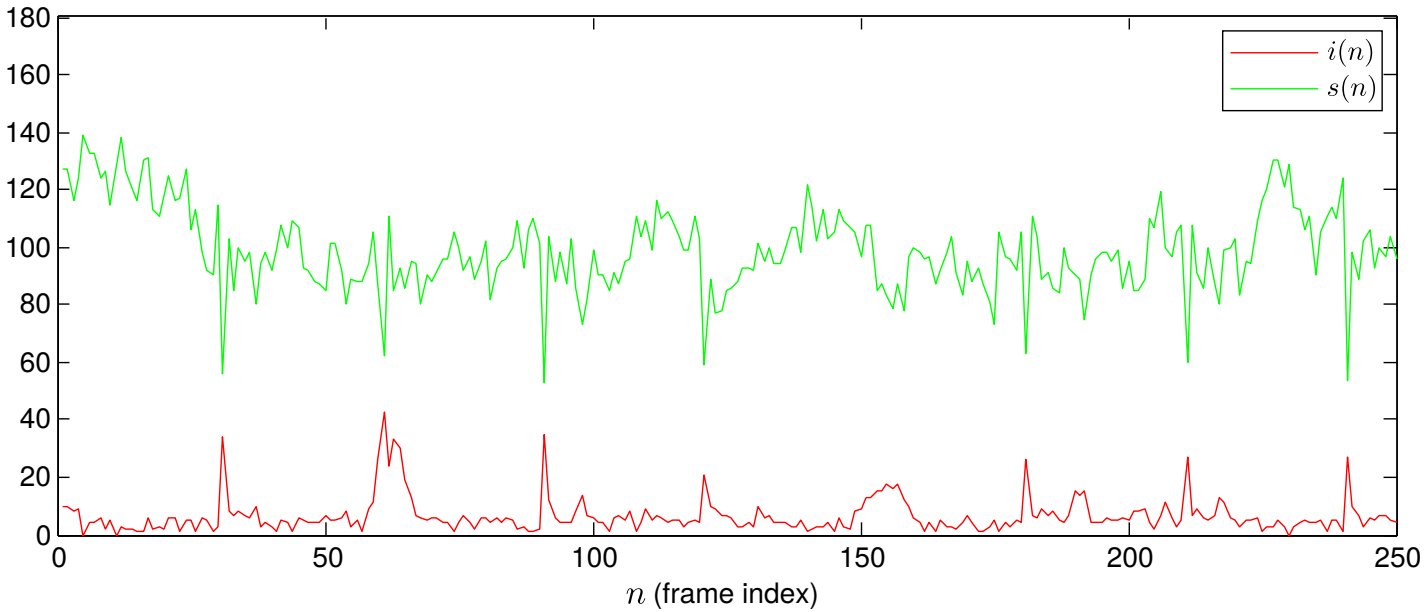


Peaks at multiples of G_2 correspond to I-frames in the 2nd encoding.

VPF Localization & Measurement

From the previous example:

- $i(n) \rightarrow$ number of I-MB at nth frame
- $s(n) \rightarrow$ number of S-MB at nth frame

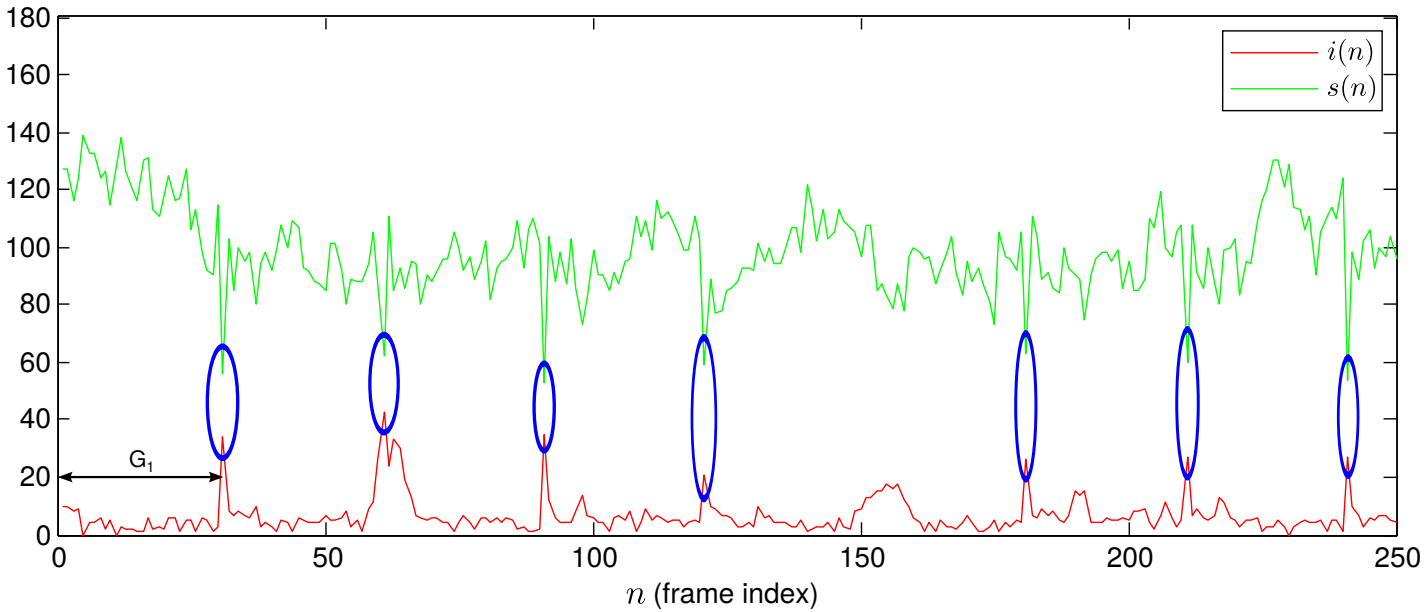


Where does the **VPF** take place?

VPF Localization & Measurement

From the previous example:

- $i(n) \rightarrow$ number of I-MB at nth frame
- $s(n) \rightarrow$ number of S-MB at nth frame

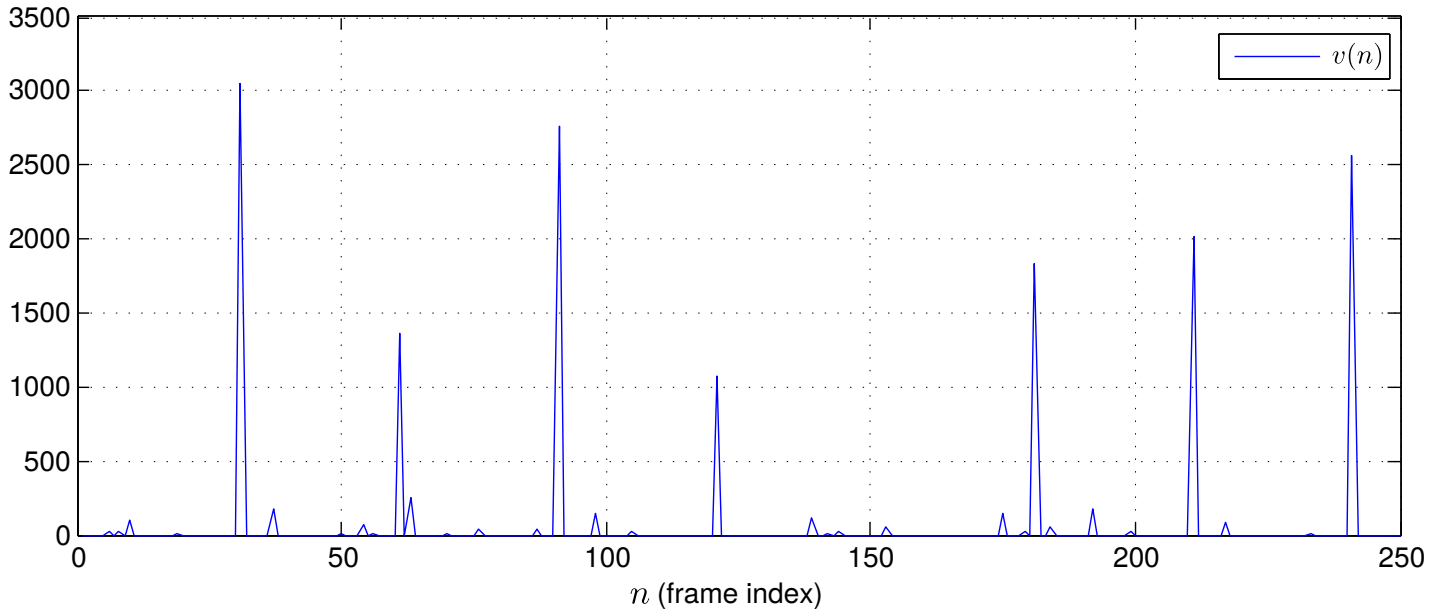


A set of frames $\mathcal{P}$ is defined where I-MB $\uparrow$ and S-MB $\downarrow$ simultaneously

VPF Localization & Measurement

From the previous example:

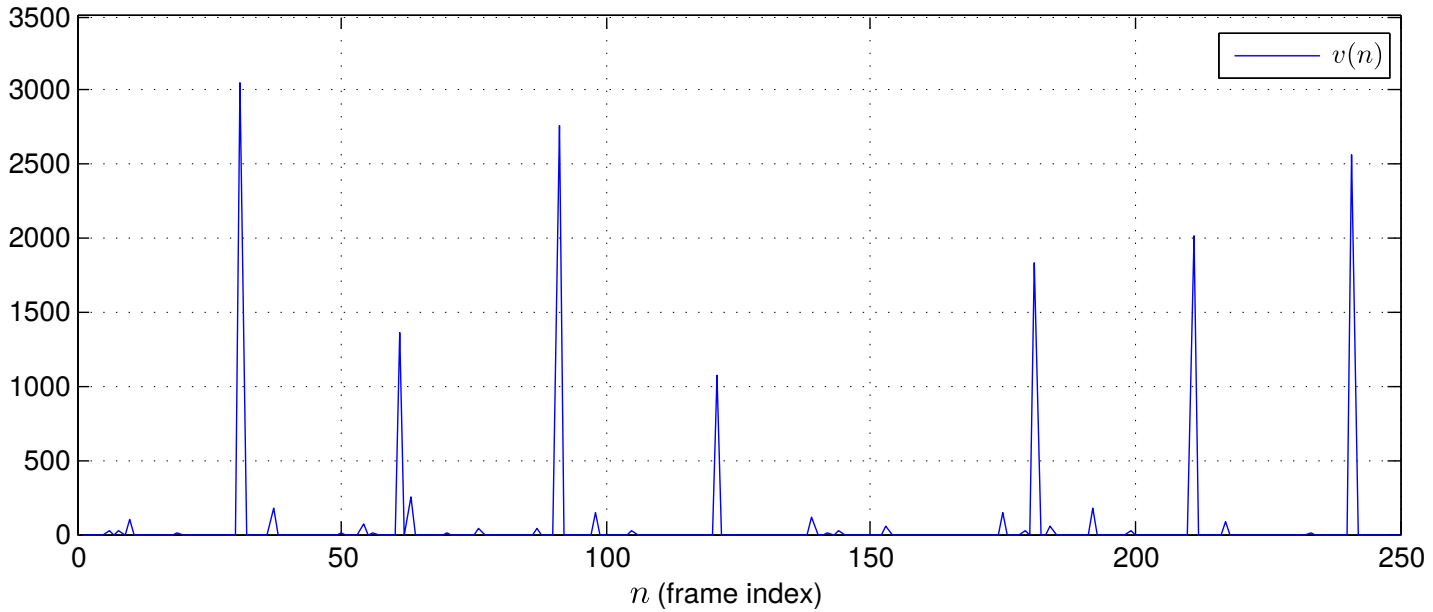
- $i(n) \rightarrow$ number of I-MB at nth frame
- $s(n) \rightarrow$ number of S-MB at nth frame



$$v(n) \triangleq \begin{cases} E(n), & \text{if } n \in \mathcal{P} \\ 0, & \text{otherwise} \end{cases} \longrightarrow \begin{aligned} E(n) \triangleq & |(i(n) - i(n-1))(s(n) - s(n-1))| \\ & + |(i(n+1) - i(n))(s(n+1) - s(n))| \end{aligned}$$

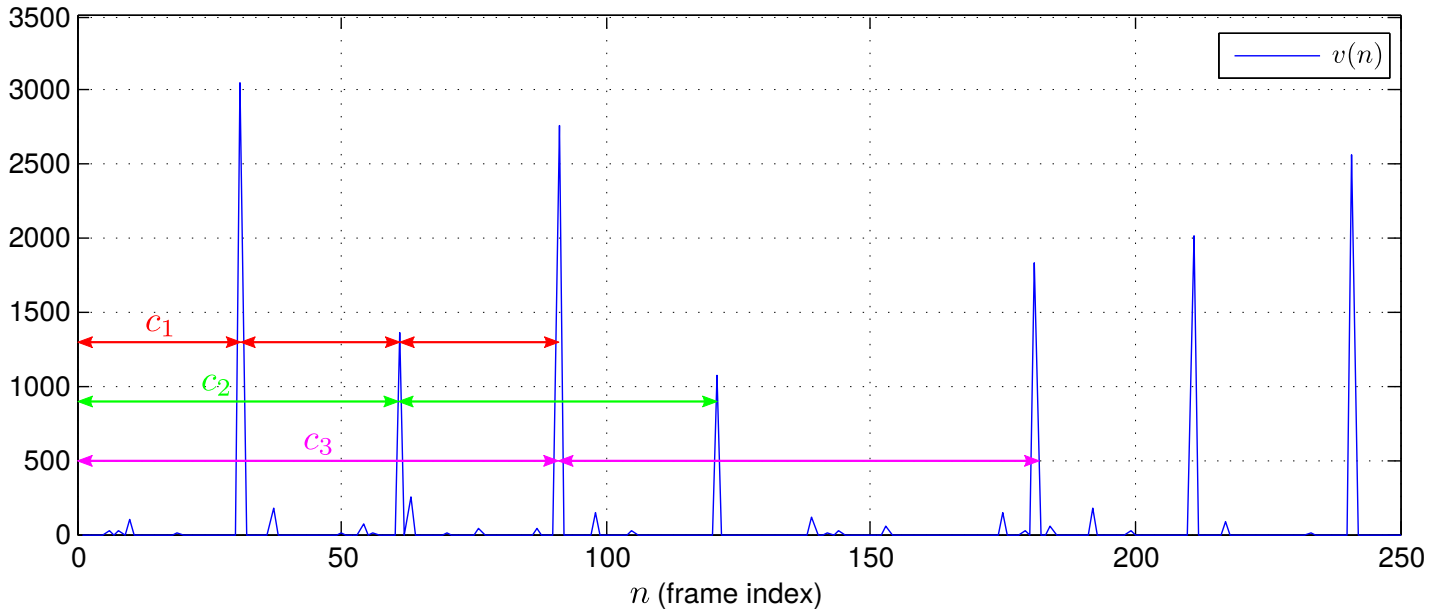
GOP Size Estimation

Analysis of $v(n)$:



GOP Size Estimation

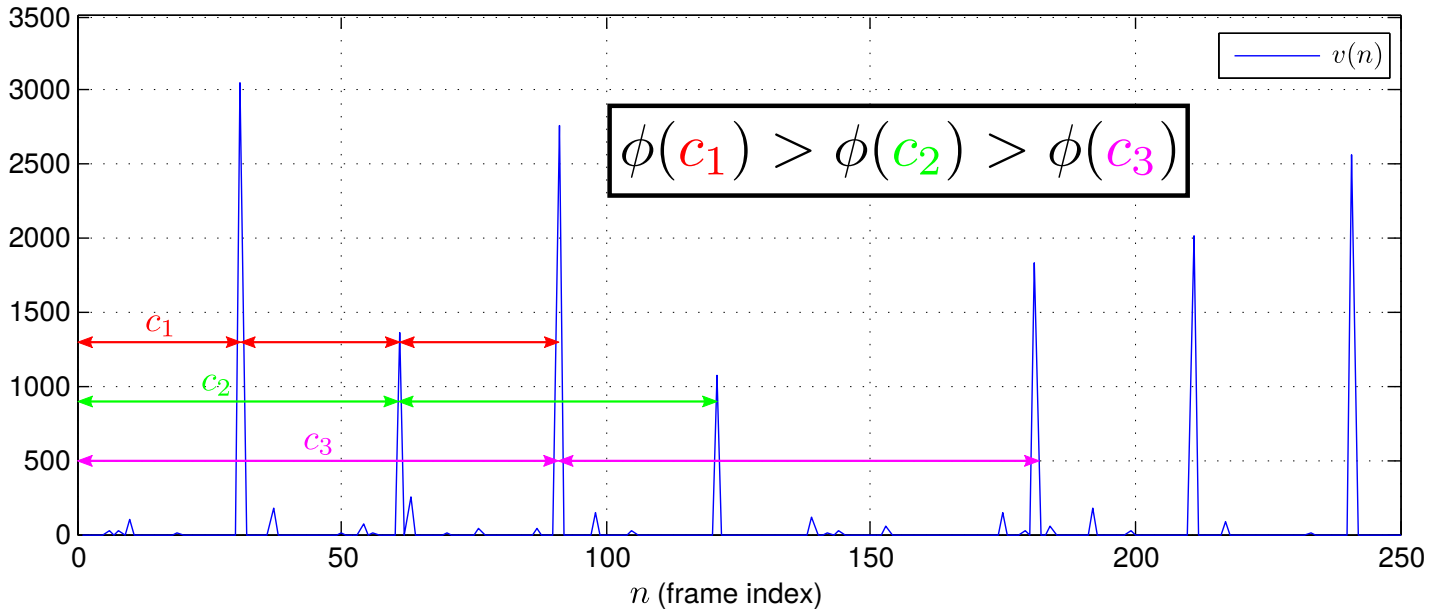
Analysis of $v(n)$:



1. **Set of candidate GOPs:** $\mathcal{C} = \{c \in \mathbb{N} : c = \mathrm{GCD}(n_1, n_2), \forall\ n_1, n_2 \in \mathcal{P}\}$

GOP Size Estimation

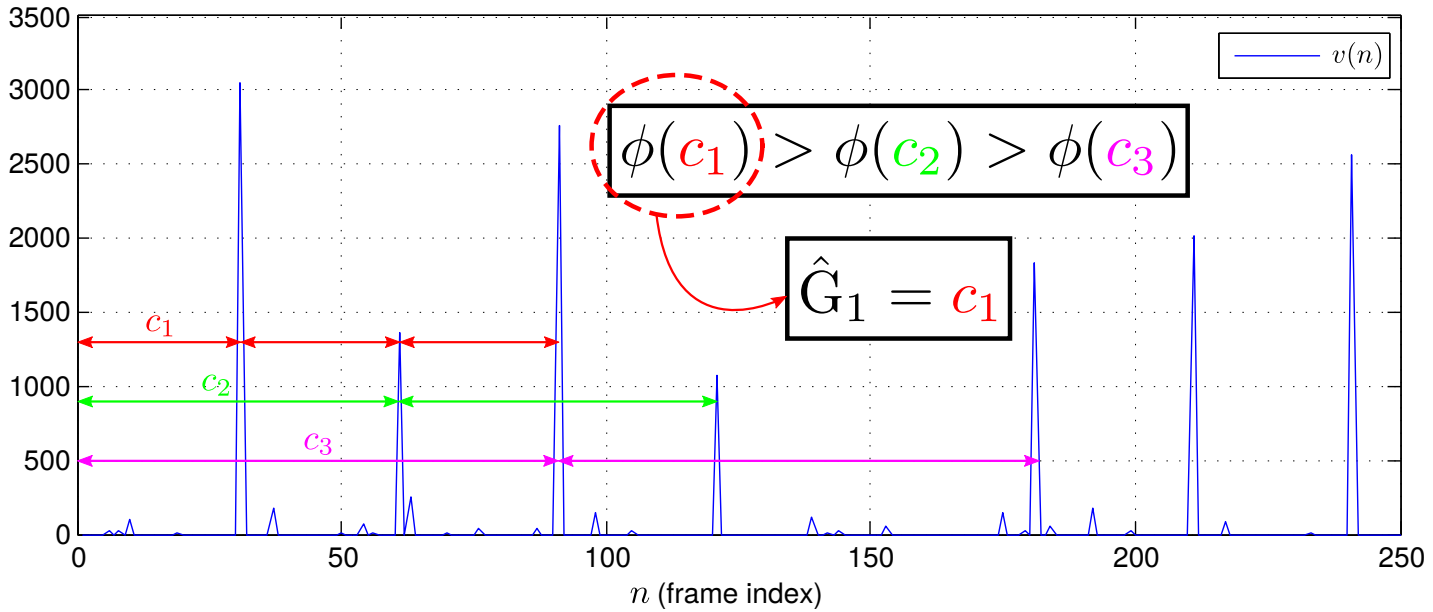
Analysis of $v(n)$:



1. **Set of candidate GOPs:** $\mathcal{C} = \{c \in \mathbb{N} : c = \text{GCD}(n_1, n_2), \forall\ n_1, n_2 \in \mathcal{P}\}$
2. **Fitness function:** $\phi(c)$ (penalizes less probable candidates)

GOP Size Estimation

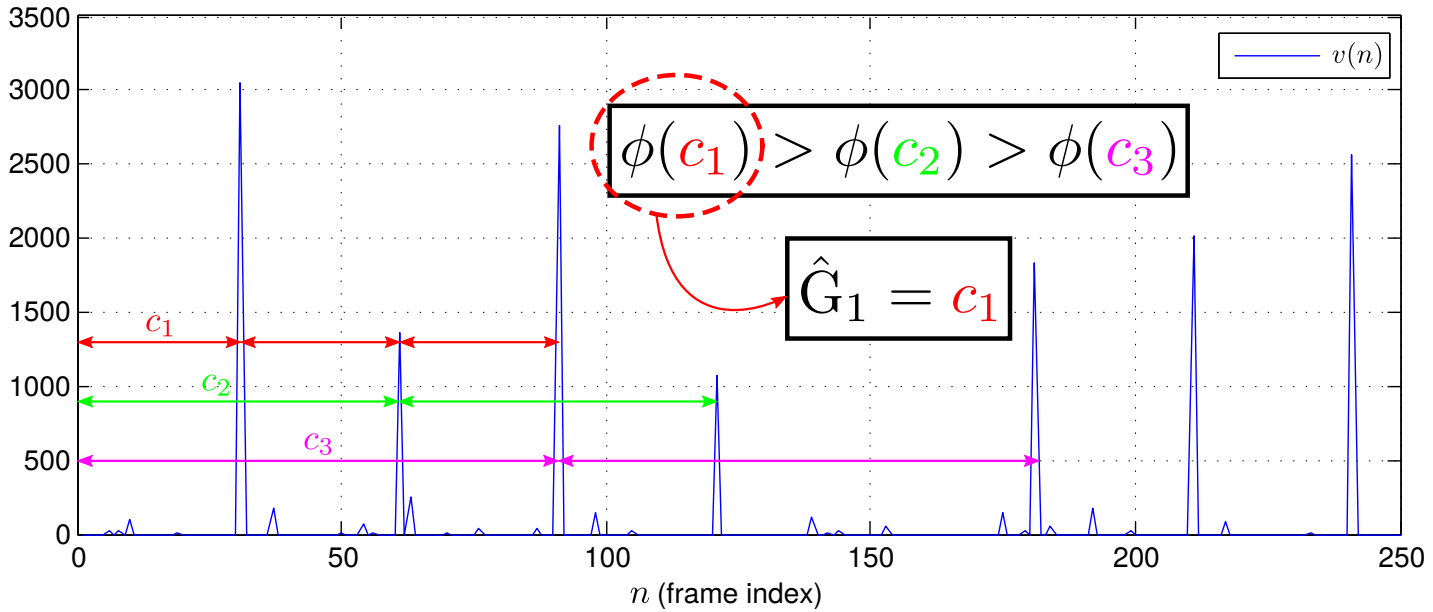
Analysis of $v(n)$:



1. **Set of candidate GOPs:** $\mathcal{C} = \{c \in \mathbb{N} : c = \text{GCD}(n_1, n_2), \forall\ n_1, n_2 \in \mathcal{P}\}$
2. **Fitness function:** $\phi(c)$ (penalizes less probable candidates)
3. **GOP size estimate:** $\hat{G}_1 = \arg\max_{c \in \mathcal{C}} \phi(c)$

GOP Size Estimation

Analysis of $v(n)$:



1. **Set of candidate GOPs:** $\mathcal{C} = \{c \in \mathbb{N} : c = \mathrm{GCD}(n_1, n_2), \forall\ n_1, n_2 \in \mathcal{P}\}$
2. **Fitness function:** $\phi(c)$ (penalizes less probable candidates)
3. **GOP size estimate:** $\hat{G}_1 = \arg\max_{c \in \mathcal{C}} \phi(c)$
4. **Test statistic for double encoding detection:** $\rho \triangleq \max_{c \in \mathcal{C}} \phi(c)$

Experimental Setup

Video Dataset

- 14 YUV video sequences from the Arizona State University
- **Resolution:** CIF (352×288)

Evaluation

1. **Double Encoding Detection:** 672 single vs 672 double encoded
2. **First GOP Size Estimation:** percentage of exact match of G_1

1st Encoding

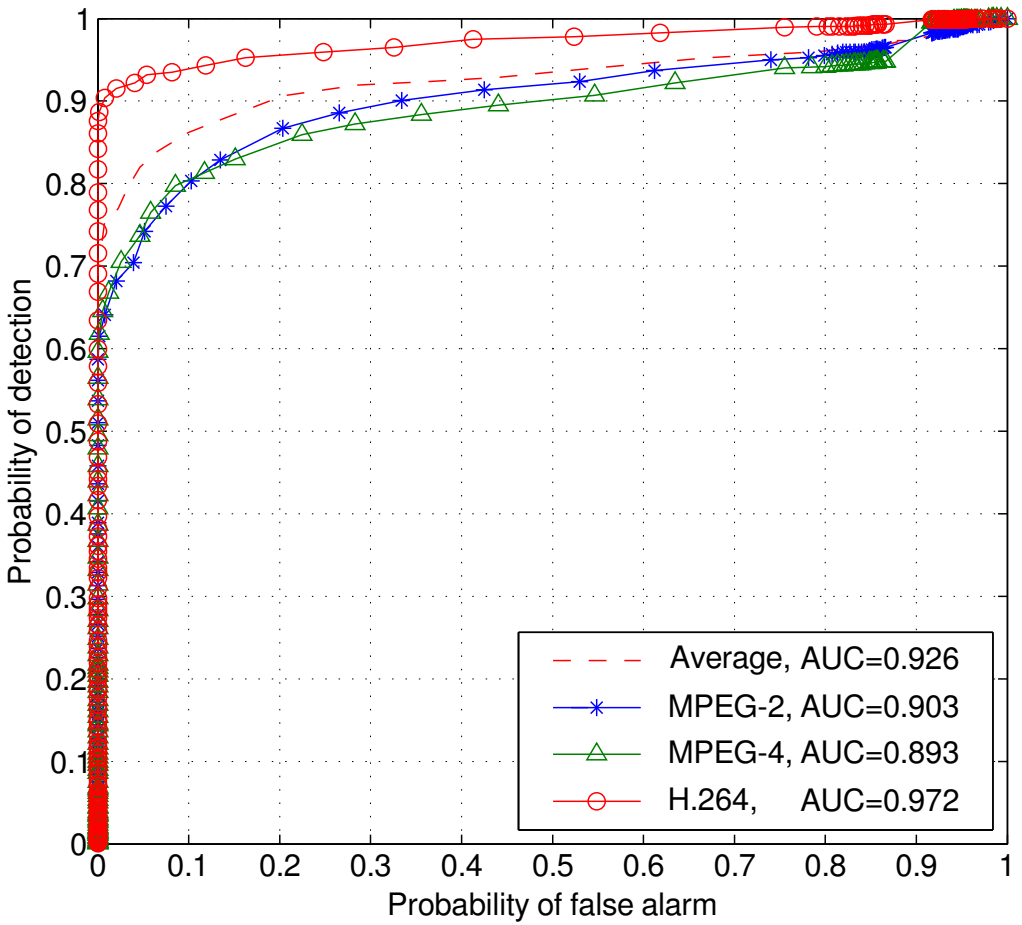
- **Encoder:** MPEG-2, MPEG-4, H.264
- **Bitrate:** 100, 300, 500, 700
- **GOP size:** 10, 15, 30, 40

2nd Encoding

- **Encoder:** MPEG-2, MPEG-4, H.264
- **Bitrate:** 100, 300, 500, 700
- **GOP size:** 9, 16, 33, 50

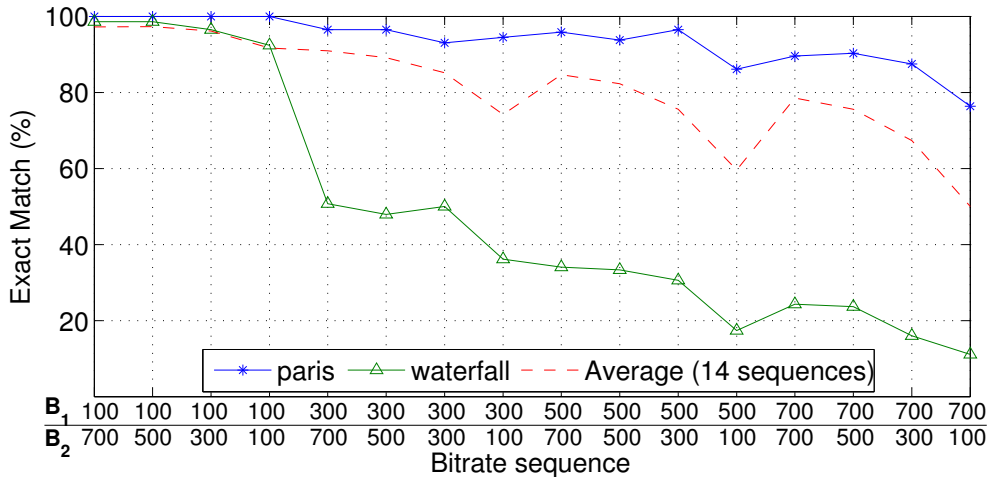
Experimental Results

Double Encoding Detection:



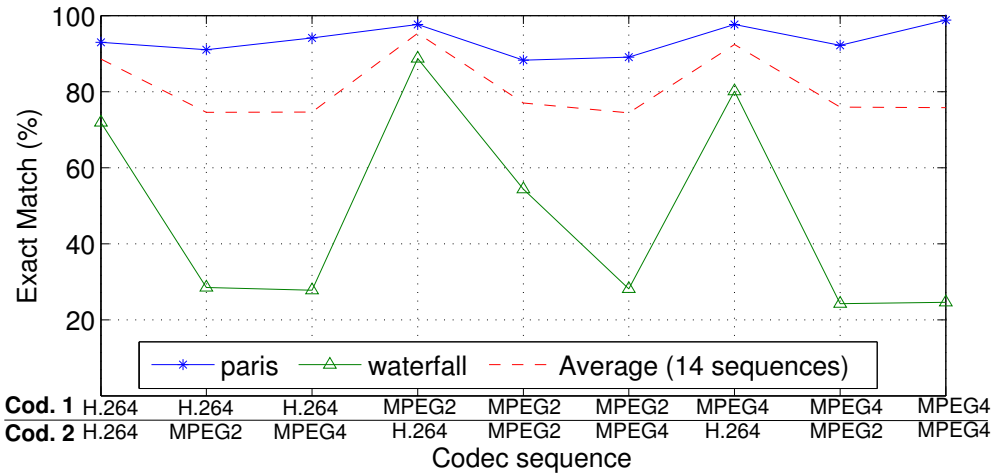
Experimental Results

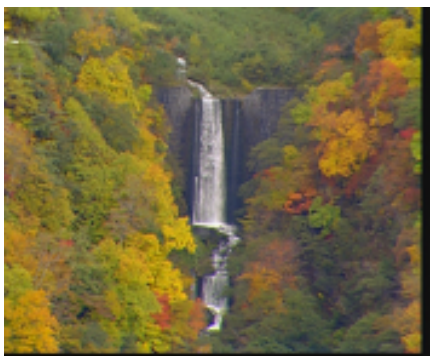
First GOP size estimation:





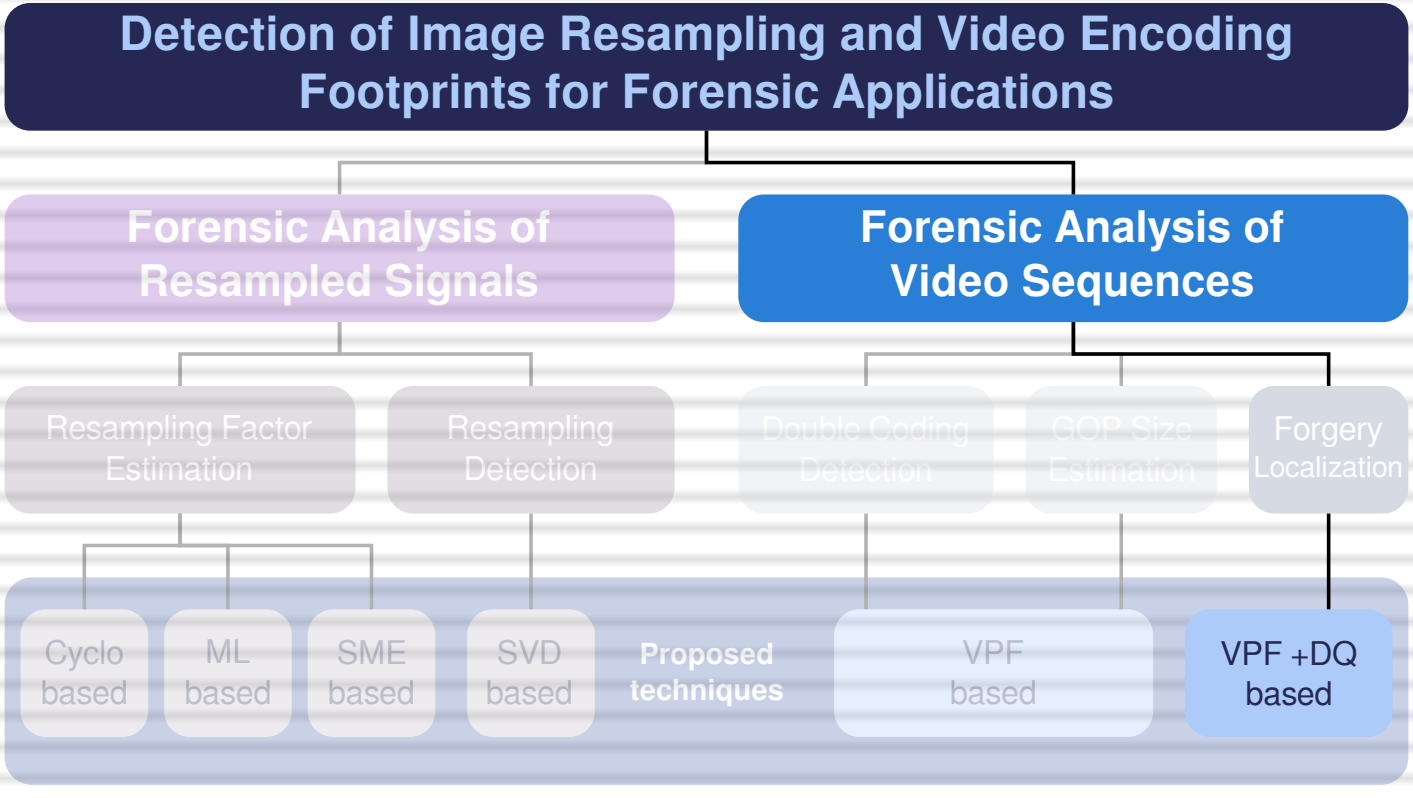
paris





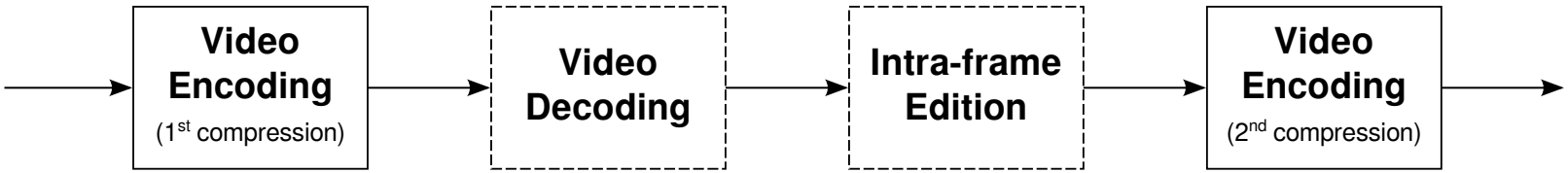
waterfall

3.3. **Proposed Techniques**: Method based on VPF+Double Quantization



Scenario Under Analysis

Intra-frame forgery processing chain:



1st Compression:

- **Fixed quantizer:** Q_1
- **GOP size:** G_1

2nd Compression:

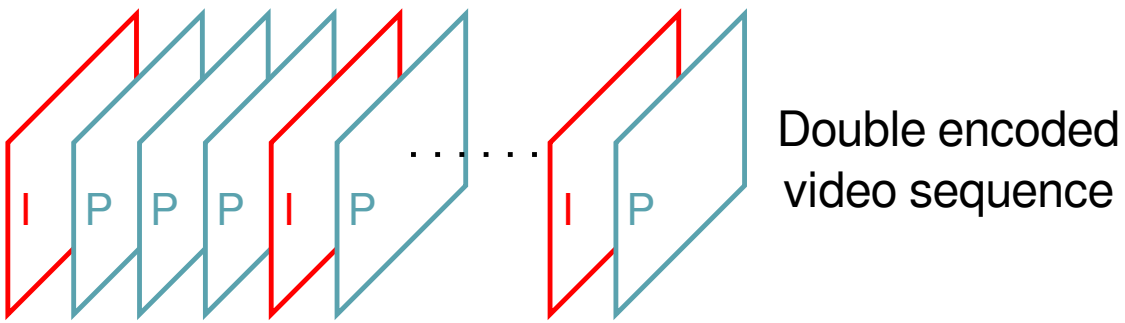
- **Fixed quantizer:** Q_2
- **GOP size:** G_2

Assumptions:

- **Encoders:** MPEG-2
- **GOP:** constant size with only I- and P-frames
- $G_1 \neq mG_2$ for any $m \in \mathbb{N}$, and $G_1, G_2 \neq 1$

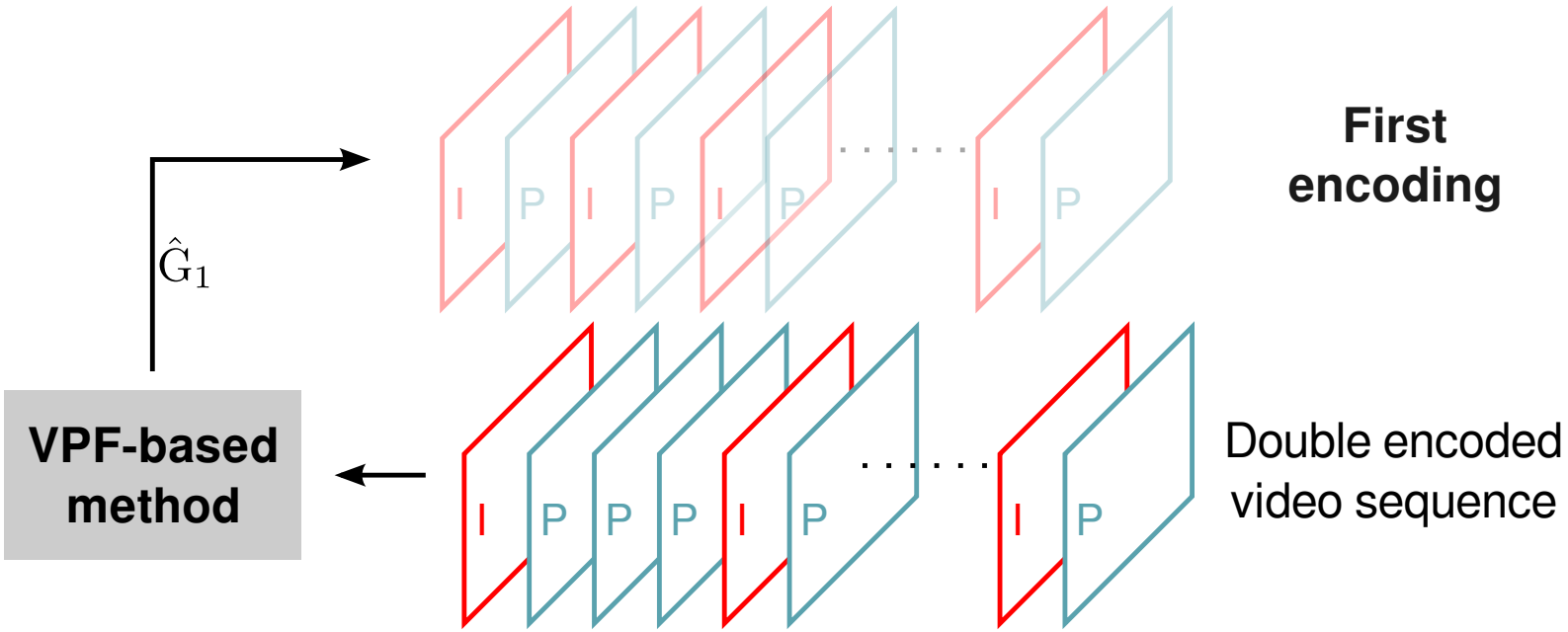
Intra-frame Forgery Localization

Main idea:



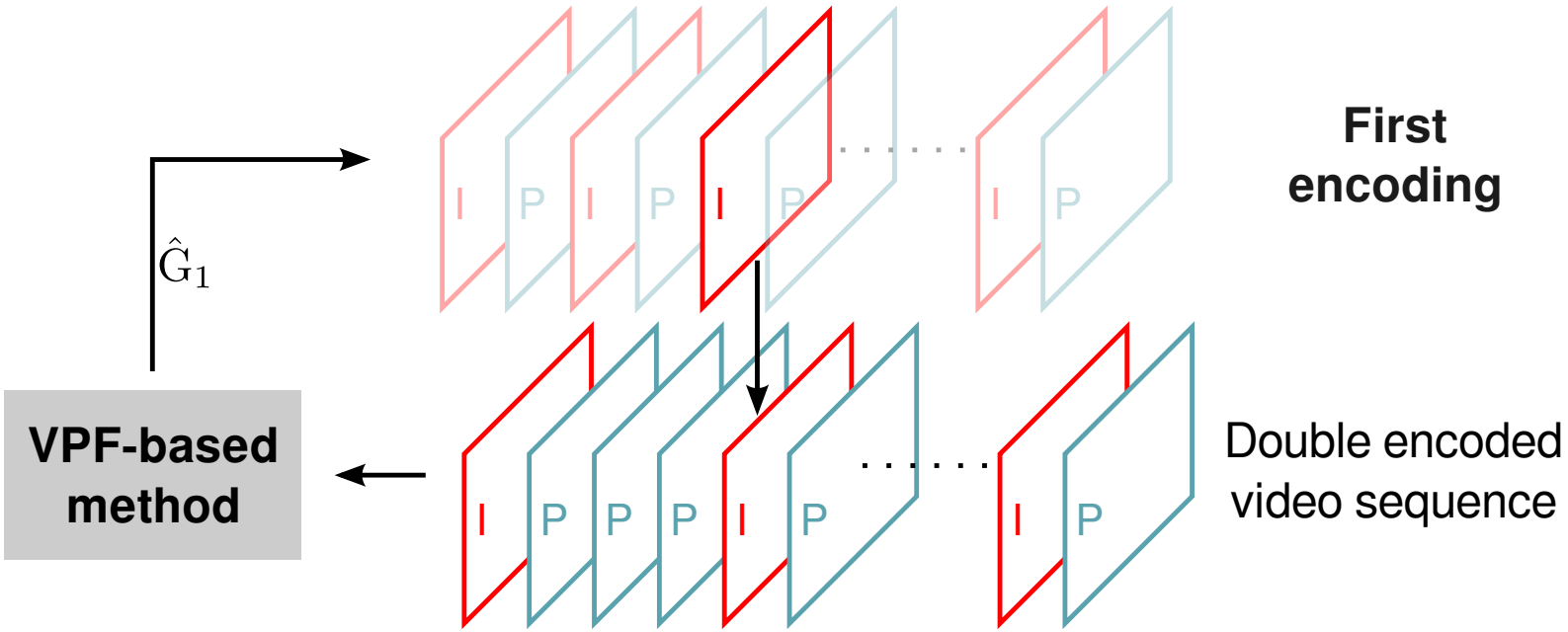
Intra-frame Forgery Localization

Main idea:



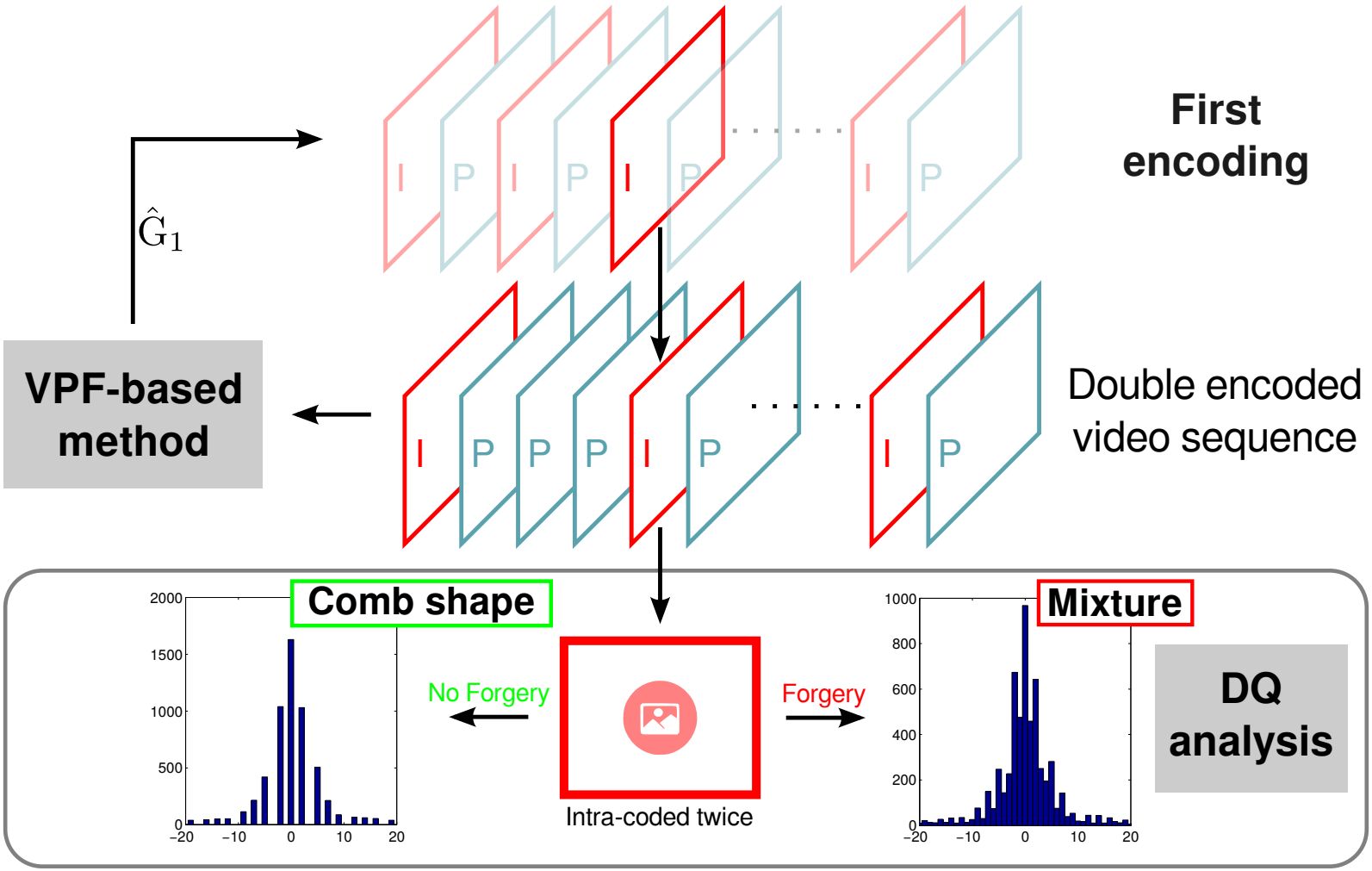
Intra-frame Forgery Localization

Main idea:



Intra-frame Forgery Localization

Main idea:



Double Quantization Analysis

Adaptation to MPEG-2

Bianchi et al. (2011): Bayesian inference method for JPEG images.

Hypothesis Test

- $\mathcal{H}_0$: 8×8 block is tampered (i.e., not showing DQ effect)
- $\mathcal{H}_1$: 8×8 block is original (i.e., DQ effect is present)

For each AC coefficient:

- $p(x|\mathcal{H}_0) = h(x)$
- $p(x|\mathcal{H}_1) = n(x)h(x), \quad$ with $x \neq 0$

For each 8×8 block:

$$p = \frac{1}{\prod_{i|x_i \neq 0} n_i(x_i) + 1}$$

Main step for computing the probability map:

Estimate the quantization matrix (Q_1) used by the first compression

Double Quantization Analysis

Adaptation to MPEG-2

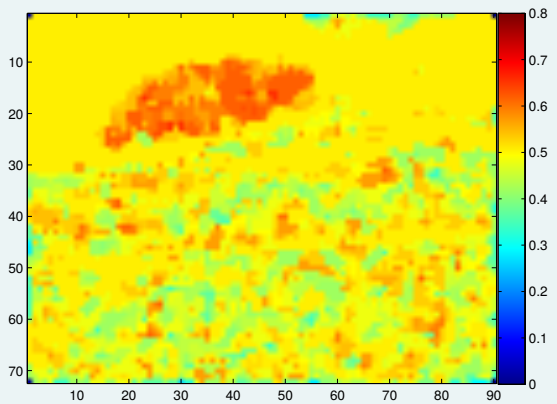
Bianchi et al. (2011): Bayesian inference method for JPEG images.

Hypothesis Test

- $\mathcal{H}_0$: 8×8 block is tampered (i.e., not showing DQ effect)
- $\mathcal{H}_1$: 8×8 block is original (i.e., DQ effect is present)

Example: probability map





Experimental Setup

Video Dataset

- 7 YUV video sequences from Xiph.org Video Test Media
- **Resoultion:** 576p (720×576).

1st Compression:

- $Q_1 \in \{6, 8, 10, 12\}$
- $G_1 = 12$

2nd Compression:

- $Q_2 \in \{2, 3, 4, 5\}$.
- $G_2 = 15$

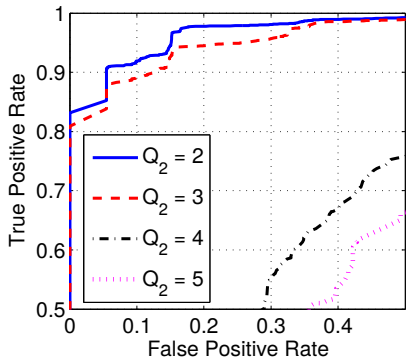
Intra-frame Forgery Procedure

1. First compression by Q_1.
2. A block of 200×200 pixels is replaced by its uncompressed version.
3. Second compression by Q_2.

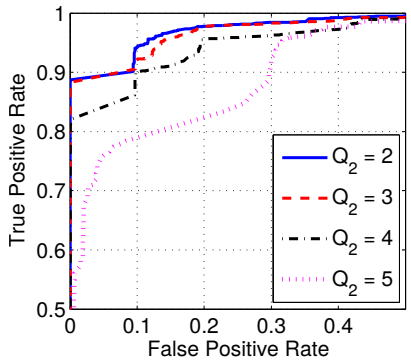
Experimental Results

ROC calculation:

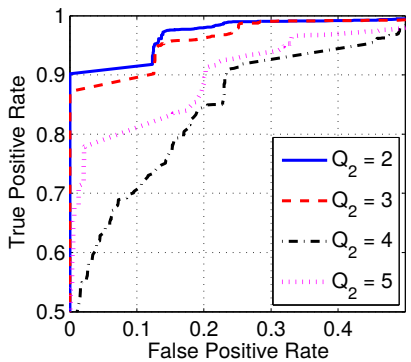
- The obtained probability map is thresholded
- Thresholded probability map is compared to the ground truth mask
- True positive and false positive rates are then calculated



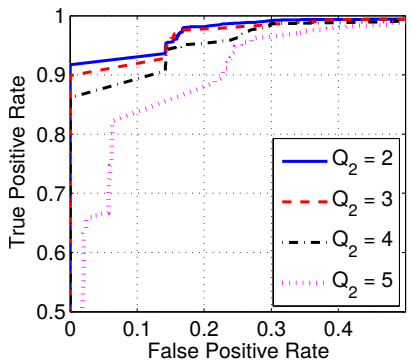
$Q_1 = 6$



$Q_1 = 8$



$Q_1 = 10$



$Q_1 = 12$

AUC Results:

Q_1 \ Q_2	2	3	4	5
6	0.98	0.97	0.68	0.63
8	0.98	0.98	0.96	0.93
10	0.98	0.98	0.91	0.94
12	0.98	0.98	0.97	0.94

4. Conclusions

Conclusions

Forensic analysis of resampled signals:

- Derivation of a theoretical framework for the estimation of parameters from the applied spatial transformation to an image.
- Resampling factor estimation following the ML criterion.
- Set-membership identification of resampled signals.
- Resampling detection as a subspace decomposition problem.

Conclusions

Forensic analysis of resampled signals:

- Derivation of a theoretical framework for the estimation of parameters from the applied spatial transformation to an image.
- Resampling factor estimation following the ML criterion.
- Set-membership identification of resampled signals.
- Resampling detection as a subspace decomposition problem.

Forensic analysis of video sequences:

- Discovery of a new digital footprint after double video encoding.
- GOP length estimation as part of the processing history of a video.
- Localization of intra-frame forgeries in MPEG-2.

Conclusions

Forensic analysis of resampled signals:

- Derivation of a theoretical framework for the estimation of parameters from the applied spatial transformation to an image.
- Resampling factor estimation following the ML criterion.
- Set-membership identification of resampled signals.
- Resampling detection as a subspace decomposition problem.

Forensic analysis of video sequences:

- Discovery of a new digital footprint after double video encoding.
- GOP length estimation as part of the processing history of a video.
- Localization of intra-frame forgeries in MPEG-2.

Publications:

- 8 international conference papers
- 1 patent application in active video forensics

Future Work

Forensic analysis of resampled signals:

- Modeling of the processing chain: resampling operation + JPEG compression.
- Study of the downsampling case.
- Evaluation of current techniques on non-linear interpolators.

Future Work

Forensic analysis of resampled signals:

- Modeling of the processing chain: resampling operation + JPEG compression.
- Study of the downsampling case.
- Evaluation of current techniques on non-linear interpolators.

Forensic analysis of video sequences:

- Tackle complex encoding profiles with B-frames or adaptive GOPs.
- Address intra-frame forgery localization with constant bitrate encoding.
- Evaluation of current techniques on realistic, hand-made, video forgeries.

Thanks for your attention!